

Cleavage of DNA  
with  
Methidiumpropyl-EDTA

Thesis by  
Robert P. Hertzberg

In Partial Fulfillment of the Requirements  
for the Degree of  
Doctor of Philosophy

California Institute of Technology  
Pasadena, California

1984

(submitted November 7, 1983)

To Denise  
and  
To My Parents

#### **ACKNOWLEDGEMENTS**

I thank my research advisor, Peter Dervan, for providing the innovative ideas which made this project possible. His enthusiasm, understanding, and friendship were a great support during my stay at Caltech.

I would also like to thank the friends I have made over the last four years for all the good times, particularly the members of the Dervan group for providing a friendly and stimulating environment in which to do research. I would especially like to thank Mike Van Dyke, Peter Schultz, Rick Ikeda, and John Taylor for their helpful scientific contributions. Sincere appreciation goes to Debbie Chester for expertly typing and coordinating this thesis. Financial support from the National Institutes of Health is gratefully acknowledged.

Finally, special thanks to my parents, for their encouragement and support, and to my wife Denise, for her love and understanding without which this work would have been impossible.

### ABSTRACT

Attachment of ethylenediaminetetraacetate (EDTA) to the DNA intercalator methidium creates an efficient DNA cleaving molecule, methidiumpropyl-EDTA (MPE). MPE·Fe(II) ( $10^{-7}$  M) single strand cleaves supercoiled pBR-322 plasmid DNA ( $10^{-5}$  M) in the presence of  $O_2$ , converting it to 56% open circular DNA. In the presence of 1 mM dithiothreitol (DTT) and  $O_2$ , MPE·Fe(II) ( $10^{-8}$  M) converts supercoiled pBR-322 DNA ( $10^{-5}$  M) to 97% open circular and 3% linear DNA. MPE·Mg(II) binds to sonicated calf thymus DNA with a binding affinity of  $1.2 \times 10^{-5} M^{-1}$  and binding site size of 1.9 base pairs, and unwinds supercoiled PM2 plasmid DNA with an unwinding angle of  $11^\circ \pm 3^\circ$ .

The reaction conditions for DNA cleavage and factors affecting the cleavage efficiency by MPE·Fe(II) have been determined. The cleavage is dependent on Fe(II) and  $O_2$ , inhibited by chelating agents, enhanced by reducing agents (ascorbate > DTT > NADH), inhibited by catalase, partially inhibited by radical scavengers, relatively unaffected by sodium concentration, and optimum at pH 7.4 (in Tris·HCl buffer). MPE·Fe(II) cleaves DNA in a relatively non-sequence specific manner, with significantly lower sequence specificity than the enzyme DNase I, and is a useful footprinting tool for the determination of small molecule binding sites on naturally occurring heterogeneous DNA.

The products from the cleavage reaction of MPE·Fe(II) with DNA have been characterized. The results demonstrate that each strand scission produces a free nucleotide base, a 5' phosphoryl group, and a mixture of 3' phosphoryl and 3' phosphoglycolic acid groups left on the polynucleotide chain. Very little malondialdehyde or base-propenals are

produced. These products are consistent with the intermediacy of hydroxyl radical in the strand scission reaction.

## Table of Contents

	Page
INTRODUCTION.....	1
DNA Cleaving Reagents.....	2
Reagent Design.....	12
RESULTS AND DISCUSSION.....	15
Synthesis.....	15
Biophysical Characterization of Methidiumpropyl- EDTA.....	15
Binding Affinity to Calf Thymus DNA.....	15
Unwinding Angle on Supercoiled DNA.....	25
Cleavage of Nucleic Acid by Methidiumpropyl-EDTA...	31
Factors Affecting the Cleavage	
Efficiency of DNA.....	31
Sequence Specificity of the DNA	
Cleavage Reaction.....	64
Cleavage of RNA.....	90
Products of the Cleavage Reaction of Methidiumpropyl-EDTA·Fe(II) with DNA.....	92
Base Release.....	92
Stoichiometry of Base Release.....	96
Analysis of Termini Produced by Methidiumpropyl-EDTA·Fe(II).....	101
Design and Approach to the Synthesis of Bis- Methidiumpropyl-EDTA.....	114
Conclusion .....	118
EXPERIMENTAL.....	120
REFERENCES.....	150
PROPOSITIONS.....	164

## INTRODUCTION

Many biological molecules which exhibit a high affinity for DNA are capable of inducing strand breakage of the double helix. Two major classes of such molecules are the nucleases and the antibiotics, both of which can display varying degrees of sequence specificity. The specific interactions between DNA and many of these agents which lead to recognition and strand cleavage are not known.

Nucleases are natural enzymes which hydrolyze phosphodiester bonds in nucleic acids. The non-specific nucleases, such as DNase I, are relatively indifferent with respect to nucleotide sequence and cleave all phosphodiester bonds in DNA almost equally.<sup>1</sup> These enzymes are useful for determining the locations and sizes of protein binding sites on heterogeneous DNA,<sup>2</sup> and for locating the sites of transcriptionally active genes.<sup>3</sup> In contrast, the restriction endonucleases produce double strand cleavage adjacent to four to six base pair recognition sequences.<sup>4</sup> These enzymes have been invaluable to molecular biologists with respect to DNA sequencing, gene isolation, chromosome analysis, and recombinant DNA techniques.

A number of naturally occurring small molecules with cytotoxic and antitumor antibiotic activity cause DNA strand breaks, which is believed to be related to their biological activity.<sup>5</sup> Most of these drugs degrade DNA through oxidative degradation of the deoxyribose. These agents are useful as probes to study the recognition of DNA by small molecules, and many are widely used as chemotherapeutic agents in man.

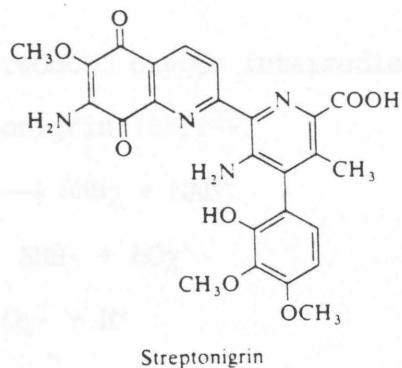
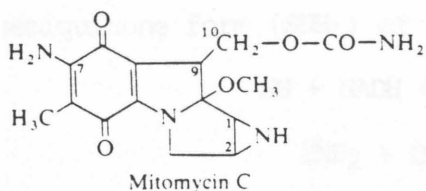
I describe here the synthesis of methidiumpropyl-EDTA (MPE), which contains the metal chelator, ethylenediaminetetraacetate (EDTA) tethered to the DNA intercalator, methidium. MPE·Fe(II) cleaves DNA efficiently in the presence of ferrous ion, oxygen, and reducing agents such as dithiothreitol (DTT).<sup>6,7</sup> MPE·Fe(II) cleaves DNA in a relatively non-sequence specific manner and with significantly lower sequence specificity than the enzyme DNase I, and is a useful footprinting tool for determining the locations, size and relative importance of small molecule binding sites on native DNA.<sup>8</sup>

I report here (1) the total synthesis of MPE, (2) DNA binding affinities and unwinding angles, (3) reaction conditions for DNA cleavage and factors affecting the cleavage efficiency by MPE·Fe(II) and (4) analyses of the DNA cleavage products.

#### **DNA Cleaving Reagents**

Most of the non-enzymatic reagents capable of producing strand breaks in DNA involve oxidative reactions with the deoxyribose moiety. These reactions are initiated by the activation of molecular oxygen near the site of the DNA helix. Agents capable of producing activated oxygen include quinones,<sup>9</sup> metal ions,<sup>10</sup> and  $\gamma$ -irradiation.<sup>11</sup> DNA cleaving reagents are often bifunctional molecules, incorporating one of these oxygen activation agents and a DNA binding moiety.

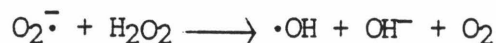
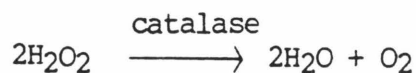
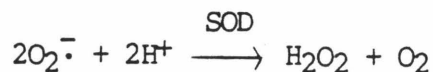
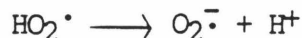
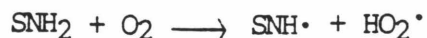
Streptonigrin and mitomycin are two examples of quinone-containing antibiotics capable of cleaving DNA. Both of these molecules



contain similar aminoquinone rings, and this feature is known to be essential for their biological activity.<sup>5</sup> Streptonigrin binds to DNA in vitro both reversibly and irreversibly,<sup>12</sup> but it does not bind via intercalation.<sup>13</sup> Its lethal action is directly correlated with its ability to degrade DNA.<sup>14</sup> It is thought that streptonigrin is reduced intracellularly to the hydroquinone form which can react with molecular oxygen, activating it for subsequent reaction with DNA. An electron source and oxygen were found to be required for streptonigrin to exert its greatest lethal effect in vivo,<sup>14</sup> and the esr spectrum of the semiquinone form has been observed in cultures of E.coli.<sup>15</sup>

More details concerning the cascade of reactions leading to oxygen activation and DNA strand scission by streptonigrin have been elucidated by studies with DNA in vitro. Strand breaks occur only in the presence of oxygen and a reducing agent.<sup>13,16</sup> The reaction is inhibited by free radical scavengers such as potassium iodide, and also by the enzymes catalase (which converts hydrogen peroxide to molecular oxygen and water) and superoxide dismutase (SOD, which converts superoxide,  $O_2^{\cdot-}$ , to hydrogen peroxide and oxygen). Cone et al. have proposed that the hydroxyl radical,  $\cdot OH$ , is the ultimate reactive species which initiates attack on DNA, and has put forward the following

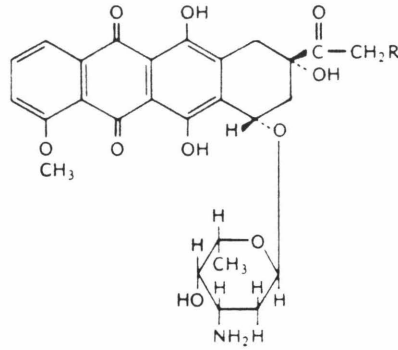
scheme to explain the involvement of reduced oxygen intermediates and the semiquinone form (SNH•) of streptonigrin (SN):<sup>13</sup>



The last reaction, known as the Haber-Weiss reaction, proceeds at a very slow rate in the absence of metal ions.<sup>17</sup> It is possible that divalent metal ions complex to streptonigrin and facilitate the generation of •OH by catalyzing this reaction.

Mitomycin will attack DNA to produce single-strand breaks in vitro in a reaction equivalent to that described for streptonigrin. The cleavage is dependent on molecular oxygen and reducing agents, and is inhibited by SOD, catalase, and free radical scavengers.<sup>18</sup> The property that sets mitomycin apart from streptonigrin is its ability to covalently bind to DNA through bifunctional alkylation, resulting in the cross-linking of complimentary strands on DNA.<sup>19</sup> This cross-linking reaction requires reduction of mitomycin to its hydroquinone derivative. The covalently bound reduced mitomycin is then poised to react with molecular oxygen to produce the semiquinone and a hydroperoxy radical, as described earlier.

Two other quinone-containing antitumor antibiotics which have been associated with DNA strand breaks are daunomycin and adriamycin.

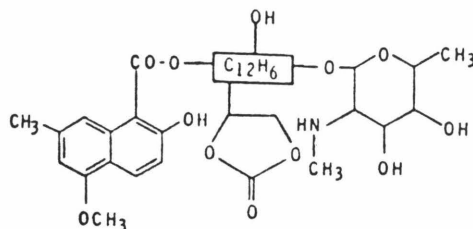


Daunomycin (R = H)  
Adriamycin (R = OH)

These drugs are DNA intercalators which cleave DNA in vitro with low efficiency and are dependent on potent reducing agents such as sodium borohydride.<sup>20</sup> Recently, Haseltine reported that NADPH cytochrome P-450 reductase could also reduce adriamycin to a semiquinone radical, resulting in DNA cleavage in a reaction mediated by molecular oxygen.<sup>21</sup> However this reaction probably is not important in vivo as evidenced by the fact that the quantity of adriamycin-induced DNA strand breaks in cultured cells is unaffected by low oxygen concentrations (< 4ppm oxygen).<sup>22</sup> It seems more likely that these anthracycline antibiotics induce the formation of strand breaks in vivo by distorting the helix in such a way as to provoke the action of a nuclease. This phenomenon has been demonstrated with other DNA intercalators such as ellipticine, actinomycin D, ethidium bromide, and lucanthone.<sup>23</sup>

In recent years a number of macromolecular (>10,000 dalton) antibiotics have been isolated which can cleave DNA. Among these are neocarzinostatin (NCS) and auroomycin, which are acidic polypeptides of molecular weight 10,700 and 12,500 respectively.<sup>24</sup> NCS contains a non-protein chromophore which possesses the full biological activity of

the holo-antibiotic.<sup>25</sup> This chromophore (molecular weight, 661) has not yet been fully characterized; a partial structure has been



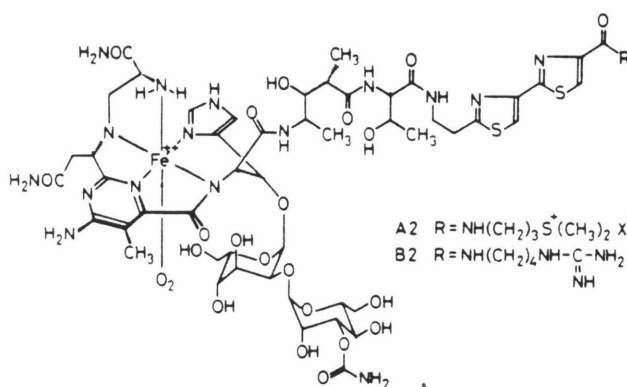
reported.<sup>26</sup> It is very labile in aqueous solution but is stabilized by binding to its apoprotein, from which it can be released for interaction with DNA.<sup>27</sup> The chromophore-free protein has no biological activity and apparently serves as a piggy-back molecule to stabilize and transport NCS-chromophore to its target.<sup>27a</sup>

The NCS-chromophore binds to DNA rather tightly ( $K_d = 0.25 \mu\text{M}$ ) with a binding site size of six nucleotides.<sup>24</sup> It is capable of unwinding supercoiled DNA, suggesting that intercalation is involved in the binding reaction.<sup>24,27c</sup> In the presence of reducing agents and molecular oxygen, NCS-chromophore produces strand breaks in DNA.<sup>24</sup> The inhibition of the reaction by free radical scavengers,<sup>28</sup> and the demonstration of ESR signals on drug activation<sup>29</sup> suggest that the mechanism of cleavage involves the generation of free radicals. The breaks occur primarily at thymidine and deoxyadenosine residues in DNA<sup>24,30</sup> and are accompanied by free base release.<sup>31</sup> The chemistry of DNA degradation by the NCS chromophore involves selective oxidation at the 5' carbon of nucleosides in DNA to produce a strand break and DNA fragments bearing a phosphate group on the 3'-end and a nucleoside-5'-aldehyde on the 5'-end.<sup>32</sup> It is thought that the highly

unsaturated  $C_{12}H_6$  unit of the NCS-chromophore, probably as a free radical species, is directly involved in the oxidation and can also form a covalent bond with the 5' carbon. Recently, adducts have been isolated which contain oligonucleotides covalently bound to chromophore,<sup>33</sup> supporting this view and implicating another mechanism by which NCS can cause damage to DNA.

The most well-studied group of antitumor antibiotics capable of cleaving DNA are the bleomycins. The bleomycins constitute a family of glycopeptide antibiotics which differ only in their terminal groups, and are active against several neoplasias in man.<sup>34</sup> They were discovered by Umezawa *et al.*<sup>35</sup>, who isolated them as copper complexes from culture media of *Streptomyces verticillus*. The therapeutic and cytotoxic activities of the drug probably result from degradation of DNA in bleomycin-treated cells.<sup>34</sup>

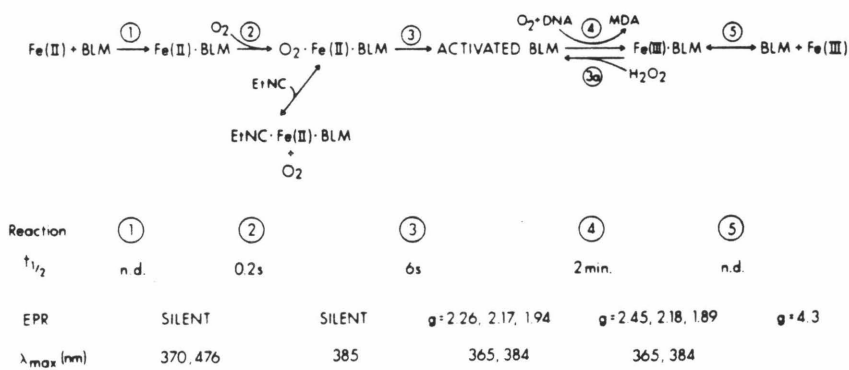
The structure of bleomycin (molecular weight 1419, for bleomycin A<sub>2</sub>) can be divided into two regions: the DNA binding portion containing the bithiazole moiety and terminal side chain, and the metal ion-chelating portion comprising most of the remainder of the molecule.



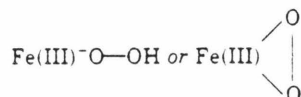
The proposed structure for bleomycin-Fe(II) complex

Whether the bithiazole intercalates between DNA bases or simply binds in the minor groove is disputed. Bleomycin shows some evidence of intercalation such as DNA unwinding and consistent electric dichroism measurements.<sup>36</sup> However NMR studies of the poly(dA-dT)·poly(dA-dT)-bleomycin A<sub>2</sub> complex are not consistent with an intercalative binding mode.<sup>37</sup> Recently an analogue of the DNA binding region has been analyzed by x-ray crystallography<sup>38</sup> and the structure found could be intercalated in DNA by computer graphics model-building. The binding constant of bleomycin to calf thymus DNA is  $5.7 \times 10^5 \text{ M}^{-1}$ , with a binding site size of 3.7 base pairs.<sup>39</sup>

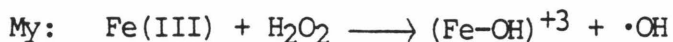
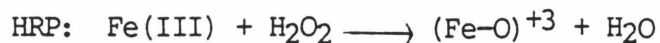
The other portion of the bleomycin molecule is capable of binding to metal ions. The crystal structure of an analogue of this moiety bound to Cu(II) indicates that the coordination geometry of the complex is square pyramidal, with the metal binding ligands shown in the figure. Horwitz and her coworkers<sup>40</sup> demonstrated convincingly that the Fe(II) complex is active in DNA strand scission. The reaction is dependent on O<sub>2</sub>, enhanced by reducing agents, and inhibited by iron chelators and non-ferrous metal ions. Peisach and coworkers have characterized steps leading to the activated bleomycin complex.<sup>41</sup>



Both oxygen activation of ferrous bleomycin and H<sub>2</sub>O<sub>2</sub> activation of ferric bleomycin give rise to the same activated complex. The production of DNA degradation products (MDA) coincides with the consumption of activated bleomycin. Also indicated is the reversible inhibition by the O<sub>2</sub> analogue, ethyl isocyanide (EtNC). The nature of the actual Fe species involved in DNA cleavage is still unknown, but EPR studies of the complex prepared with <sup>57</sup>Fe(II) and <sup>17</sup>O<sub>2</sub> demonstrate the presence of iron as Fe(III) and bound oxygen originating in dioxygen.<sup>41</sup> A plausible structure for activated bleomycin is a ferric-peroxo species:



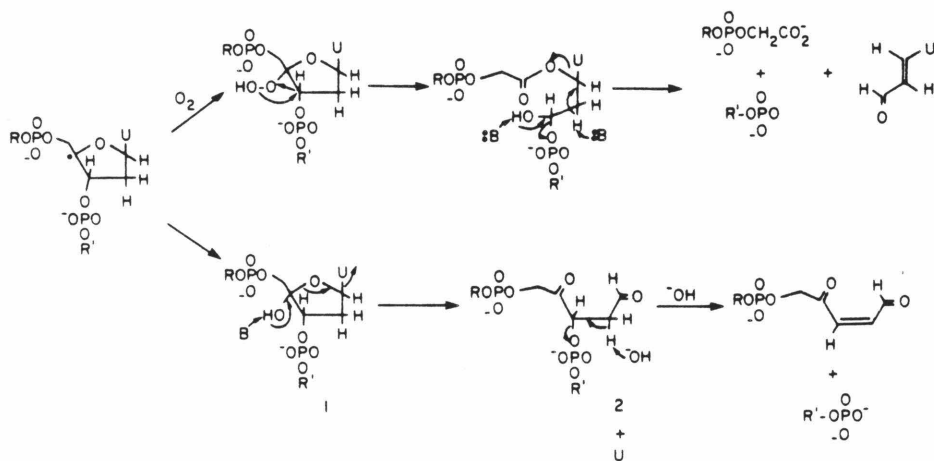
A subsequent step may be breakage of the O-O bond, although there is no direct evidence yet to support this. Analogous reactions occur with horseradish peroxidase (HRP) to form compound I<sup>42</sup>, or alternatively with metmyoglobin (My) to form •OH radical:<sup>43</sup>



Oxygen dependent cleavage of DNA by bleomycin occurs at specific base sequences on heterogeneous DNA. Strand scission is induced at the pyrimidine of a two base pair recognition site, 5'-GT-3' or 5'-GC-3'.<sup>30a,44</sup> The cleavage specificities of various different bleomycins are almost identical.<sup>45,46</sup> Therefore, the C-terminal substituent attached to the bithiazole ring is unimportant with respect

to base specific recognition and cleavage. Bleomycin does not degrade RNA,<sup>47</sup> or single-stranded DNA.<sup>45</sup>

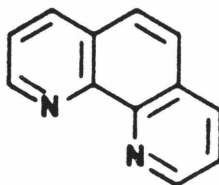
The products released when bleomycin cleaves DNA include free nucleotide bases and base propenals (base-CH=CH-CHO).<sup>48,49</sup> When the activated complex discussed earlier reacts with DNA anaerobically, only free base is released, and the phosphate backbone of the DNA remains intact but labile to alkali treatment.<sup>50</sup> Under aerobic conditions, both types of products are released and strand scission occurs. Therefore, there is a second oxygen requirement for the direct cleavage route. This route leads to DNA fragments bearing terminal 5'-phosphates and terminal 3'-phosphoglycolic acid residues.<sup>45,49</sup> The following mechanism has been proposed and is supported by tritium labelling experiments:<sup>51</sup>



Degradation is initiated by abstraction of the deoxyribose-C-4'-H followed by partitioning of the 4' radical center between hydroperoxide and hydroxyl formation. The 4'-hydroperoxide undergoes (C-3')-(C-4') bond breakage leading to the base propenals and DNA strand breakage. The 4'-hemiketal decomposes to release free base and structure 2, which is labile to alkali.

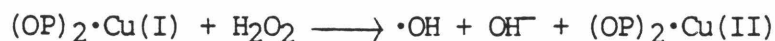
The total synthesis of bleomycin has recently been completed by two different groups.<sup>52,53</sup> These studies should lead to synthetic modifications that may help to define the relationship between metal coordination and oxygen activation, and between chemical structure and specific DNA recognition.

A chemical reagent which is capable of DNA cleavage is the metal chelator 1,10-phenanthroline. The cleavage reaction occurs with the



1,10-phenanthroline

2:1 phenanthroline-cuprous complex  $[(OP)_2 \cdot Cu(I)]$  and is dependent on molecular oxygen.<sup>54</sup> The reaction is blocked by catalase, and is greatly enhanced by thiols and  $H_2O_2$ .<sup>55</sup> Hydroxyl radicals have been suggested as the reactive species in the degradation of DNA. It is thought that the metal complex binds to DNA, and Fenton-type chemistry takes place near the site of the helix:



Evidence for DNA binding comes from the fact that cleavage is inhibited by intercalators.<sup>55a</sup> Double-stranded DNA is a much better substrate than single-strand DNA, suggesting intercalation as the DNA binding mode. Studies concerning the sequence-specificity of the strand-scission have indicated that Cu-phenanthroline cleavage is virtually identical to that of micrococcal nuclease.<sup>56</sup> Both of these agents recognize conformational perturbations in the helix resulting in an uneven pattern of cleavage.

The only known method of introducing DNA strand breaks in a totally sequence-neutral manner is the random generation of hydroxyl radicals. This is achieved by  $\gamma$ -irradiation, which decomposes water to the following products:<sup>57</sup>

$\cdot\text{OH}$ ,  $e_{\text{aq}}^-$  (trapped as  $\text{O}_2\cdot^-$ ),  $\text{H}\cdot$  (trapped as  $\cdot\text{O}_2\text{H}$ ),  $\text{H}_2$ ,  $\text{H}_2\text{O}_2$ ,  $\text{H}_3\text{O}^+$ . Of these,  $\cdot\text{OH}$ ,  $e_{\text{aq}}^-$ , and  $\text{H}\cdot$  are the short lived species expected to react with DNA. Solvated electrons ( $e_{\text{aq}}^-$ ) and H atoms are scavenged by  $\text{O}_2$  and the base moieties, but an appreciable part (10-20%) of the  $\cdot\text{OH}$  radicals react with the deoxyribose moiety on DNA by hydrogen abstraction.<sup>58</sup> This leads to deoxyribose fragmentation, base release, and strand scission.<sup>58a,59</sup> The end groups which remain on the DNA fragments are 5'-phosphates, and a mixture of 3'-phosphates and 3'-phosphoglycolic acid residues.<sup>60</sup> To date, no scheme which satisfactorily explains all of the reaction products and DNA end groups associated with  $\gamma$ -irradiation induced cleavage has been proposed.

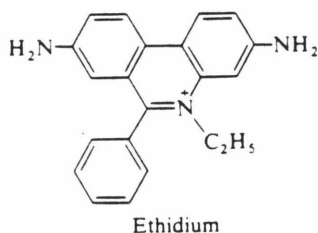
### Reagent Design

All of the DNA cleaving molecules described above are bifunctional, incorporating a DNA binding moiety and an oxygen

activation reagent. Inspired by these naturally occurring molecules, we designed a simple new reagent capable of causing efficient strand scission of DNA. We chose to use a chelated ferrous ion as our oxygen activation reagent, and tethered it to the well-characterized DNA intercalator methidium.

Among chelating agents with a high affinity for ferrous ion, ethylenediaminetetraacetic acid (EDTA) has many of the desired properties for use as a DNA cleavage reagent. EDTA forms a stable, water-soluble complex with Fe(II),<sup>61,62</sup> and EDTA·Fe(II) is known to produce ·OH radicals in aqueous solution.<sup>63</sup>

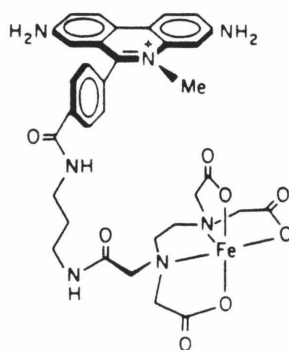
DNA intercalators are flat aromatic molecules which insert between adjacent base pairs of nucleic acids.<sup>64</sup> These molecules can be used to deliver a desired chemical functionality uniquely to the site of the helix. Ethidium bromide<sup>65</sup> is an intercalator which has been used as



a probe of nucleic acid structure and function, and was chosen as the DNA binding portion of the bifunctional cleaving reagent.

The final aspect of the reagent design was the selection of an appropriate tether to covalently link methidium to EDTA. Studies involving bleomycin indicated that the 4'-H on the deoxyribose is the initial site of attack by oxygen radicals.<sup>51</sup> Since the geometry and groove specificity of ethidium is known,<sup>65,66</sup> we were able to construct

molecular models of methidium-EDTA compounds bound to DNA. It was determined that a short hydrocarbon tether, the propyl group, afforded the appropriate length and flexibility to facilitate the positioning of EDTA·Fe(II) group over the 4'-H of the deoxyribose. We undertook the synthesis of methidiumpropyl-EDTA (MPE),<sup>6</sup> shown here as the Fe(II) complex.



MPE · Fe(II)

## RESULTS AND DISCUSSION

**Synthesis.** MPE was synthesized by two different methods (Fig. 1). Paracarboxymethidium (1) is a known compound readily available in six steps from 2-aminobiphenyl.<sup>67</sup> In method A, the imidazole<sup>68</sup> of paracarboxymethidium was allowed to react with an excess of 1,3-diaminopropane in dry DMSO affording methidiumpropylamine (2). Condensation of 2 with excess EDTA in dry DMF at 120°C yielded MPE (3). In method B, 2 was condensed with the imidazole of triethyl ester 4, available in two steps from EDTA,<sup>69</sup> affording MPE-triethyl ester (5). Hydrolysis of 5 with aqueous lithium hydroxide yielded MPE, identical in all respects to that produced by method A.

EDTA-propane (6) was synthesized as a control reagent in order to compare its DNA cleavage efficiency to that of MPE. MPE and 6 contain identical chelating moieties, and differ only in the fact that MPE contains the DNA binder methidium. The imidazole of 4 was condensed with propylamine in dry DMF, followed by hydrolysis with aqueous lithium hydroxide affording 6 (Fig. 1).

### Biophysical Characterization of MPE

**Binding Affinity to Calf Thymus DNA.** The binding of MPE to DNA can be monitored by absorption spectroscopy because, like ethidium bromide, a metachromatic shift results when MPE binds to nucleic acid. The visible absorption spectrum of MPE unbound and bound to sonicated calf thymus DNA is shown in Fig. 2. The  $\lambda_{\max}$  of MPE in the free state is 488 nm, while the  $\lambda_{\max}$  of MPE in the presence of excess DNA is 529 nm. This metachromatic shift is identical for the metal complexes MPE•Ni(II) and MPE•Mg(II). The binding affinities were determined by

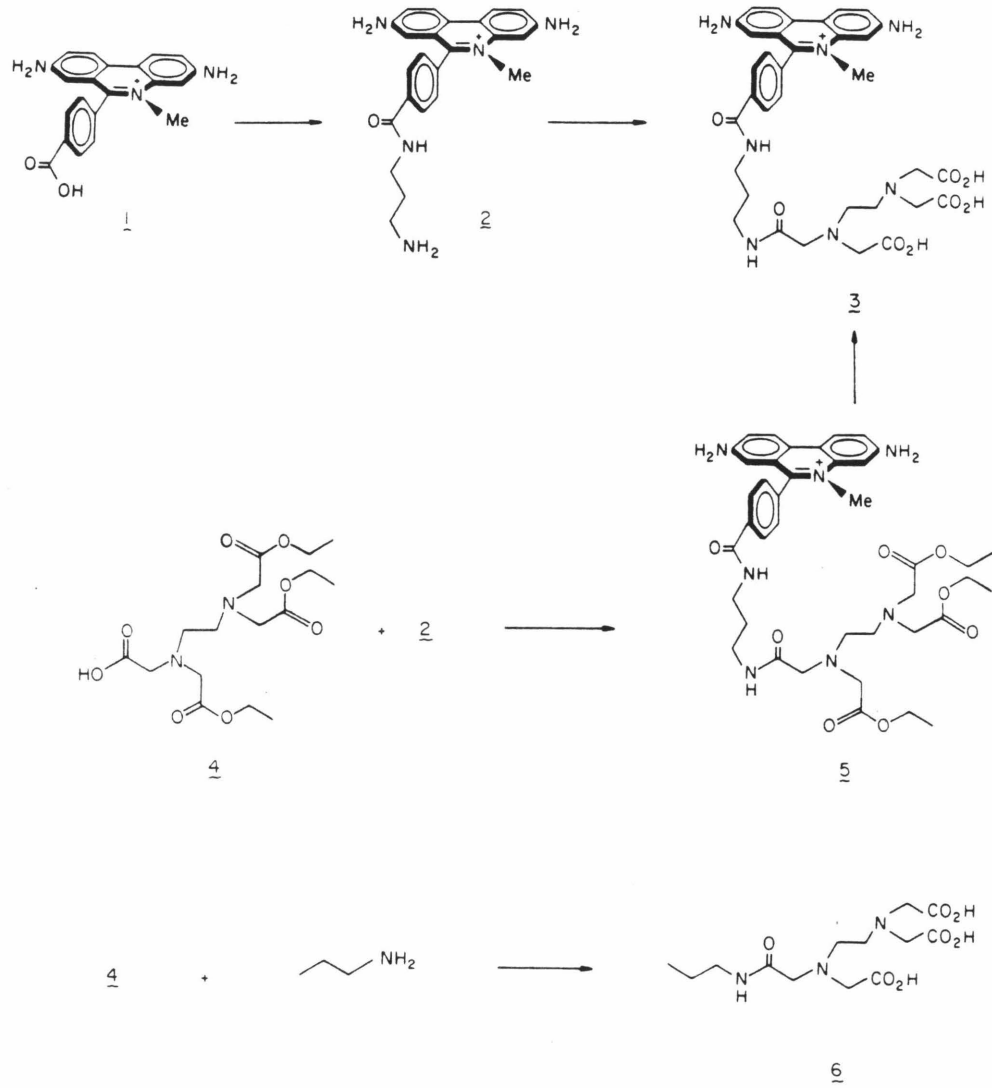


Figure 1

absorbance titrations at 488 nm, the wavelength where the extinction coefficients of bound and free drug differ most. The data are presented in Scatchard form<sup>70</sup> and a comparison of the experimentally observed plots to theoretical plots generated by the binding equations of McGhee and von Hippel<sup>71</sup> allows an estimation of the binding affinity and binding site size (Fig. 3, Table 1) (for binding equations, see page 52).

Table I

Molecule	Binding Affinity ( $M^{-1}$ )	Binding Site Size (bp)
MPE	$2.4 \times 10^4$	2.0
MPE·Ni(II)	$1.5 \times 10^5$	2.1
MPE·Mg(II)	$1.2 \times 10^5$	1.9
Ethidium bromide	$8.0 \times 10^5$	2.3

Comparison of the binding affinities and binding site sizes of MPE and ethidium bromide to sonicated calf thymus DNA. Experimental details are described in the legend to Figure 3. The buffer was 10 mM Tris·HCl, 50 mM NaCl, pH 7.4. In addition, 1 mM EDTA was included in the metal free MPE titration experiments.

The binding constants for MPE·Ni(II) and MPE·Mg(II) are very similar, while metal-free MPE binds with 5-6 times lower affinity. This is not unexpected due to the effect of electrostatic interactions. Divalent metal complexes of MPE have a net zero charge, while metal free MPE has a net negative charge. Since these experiments were carried out at relatively low salt concentrations ( $[Na^+] = 0.050 M$ ), the electrostatic repulsion between metal-free MPE and the DNA phosphates

**Figure 2**

Comparison of the visible spectra of MPE unbound and bound to 4 mM sonicated calf thymus DNA. The buffer was 10 mM Tris·HCl, 50 mM NaCl, pH 7.4. The extinction coefficient at 488 nm for free MPE is  $5994 \text{ M}^{-1} \text{ cm}^{-1}$ ; and of bound MPE is  $2685 \text{ M}^{-1} \text{ cm}^{-1}$ .

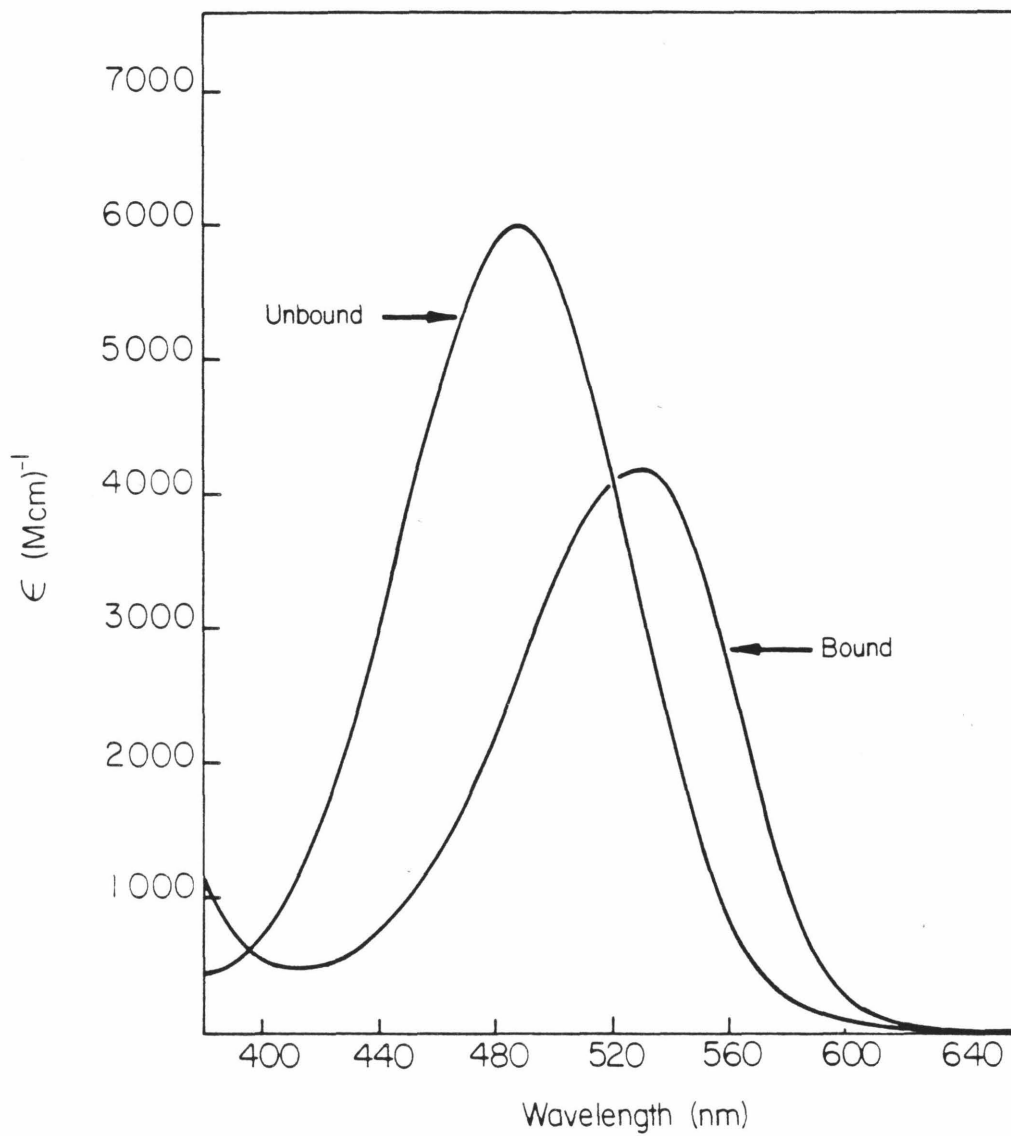
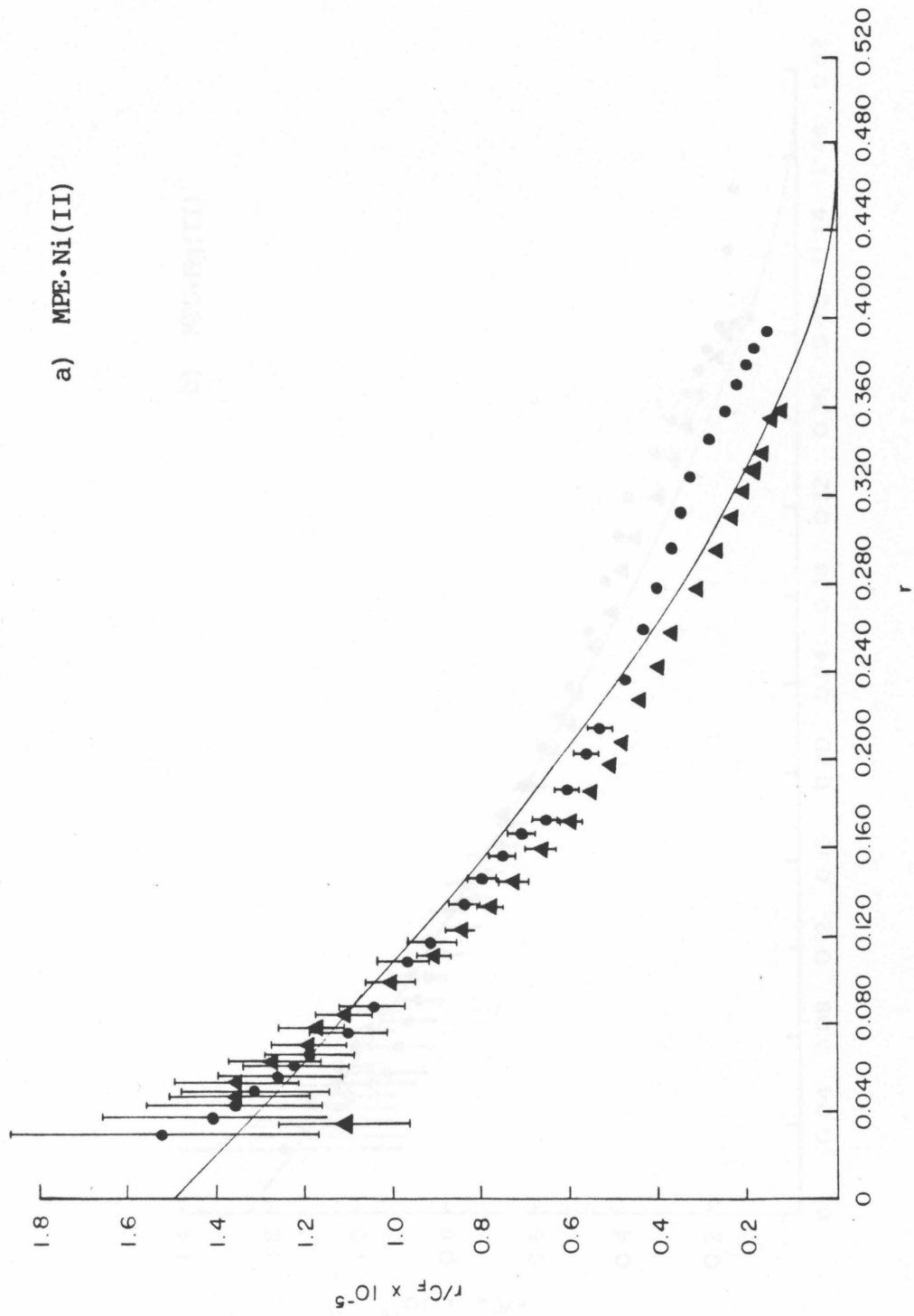


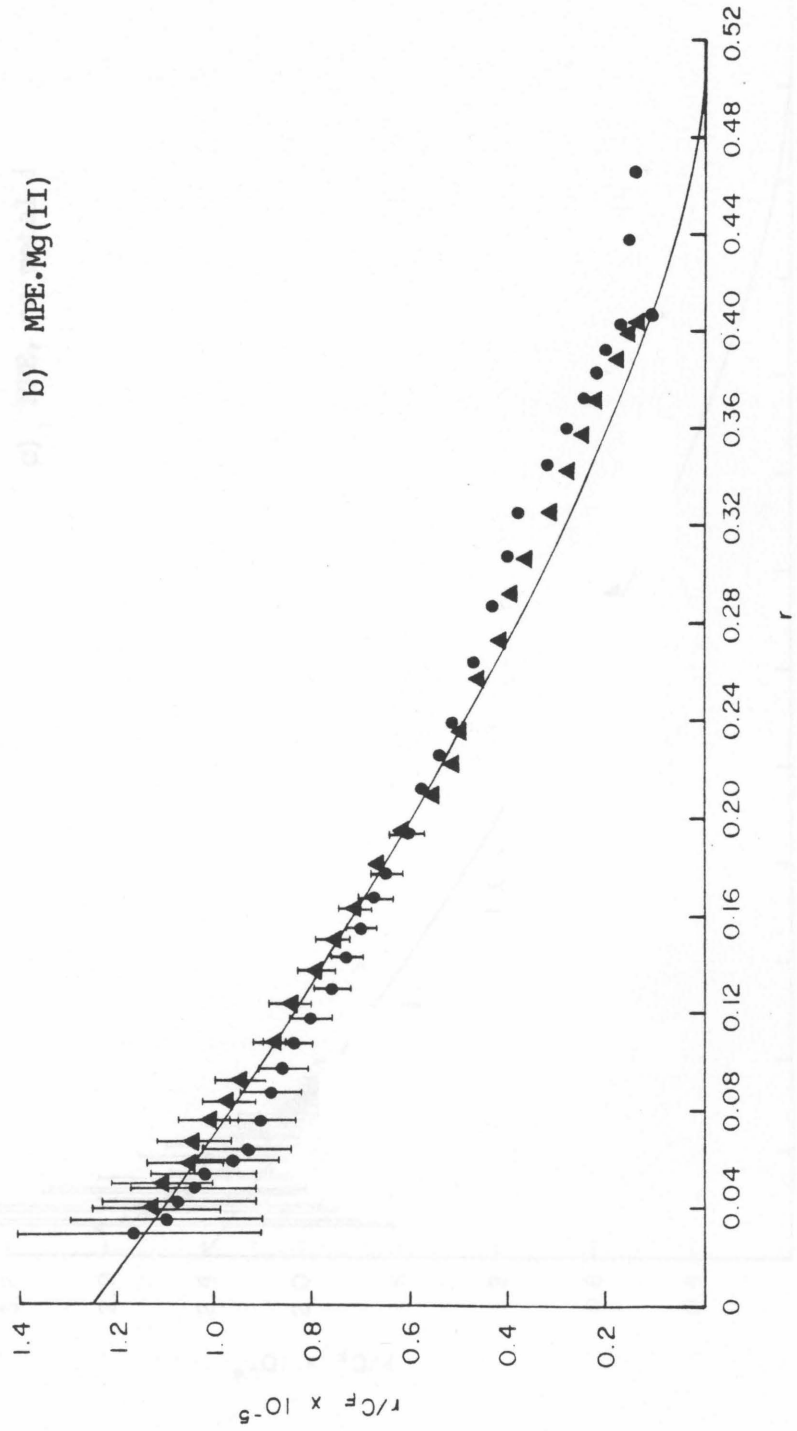
### Figure 3

Scatchard plots determined by spectrophotometric titrations. For each experiment the results of titrations at two different DNA concentrations are shown. (a) MPE·Ni(II) was added to  $9.6 \times 10^{-6}$  M bp ( $\bullet$ ), or  $1.9 \times 10^{-5}$  M bp ( $\blacktriangle$ ) calf thymus DNA; (b) MPE·Mg(II) was added to  $7.7 \times 10^{-6}$  M bp ( $\bullet$ ), or  $1.5 \times 10^{-5}$  M bp ( $\blacktriangle$ ) calf thymus DNA; (c) MPE was added to  $7.4 \times 10^{-6}$  M bp ( $\bullet$ ), or  $1.4 \times 10^{-5}$  M bp ( $\blacktriangle$ ) calf thymus DNA in the presence of 1 mM EDTA; (d) Ethidium bromide was added to  $7.4 \times 10^{-6}$  M bp ( $\bullet$ ), or  $1.5 \times 10^{-5}$  M bp ( $\blacktriangle$ ) calf thymus DNA. The binding density, concentration of bound drug per bp ( $r$ ), is plotted against the ratio  $r/C_F$ , where  $C_F$  is the concentration of free drug. Solid lines are theoretical plots generated by the binding equation of McGhee and von Hippel<sup>71</sup> for the binding affinity ( $K$ ) and binding site size ( $n$ ) indicated in Table I. The binding is assumed to be noncooperative ( $\omega = 1$ ).

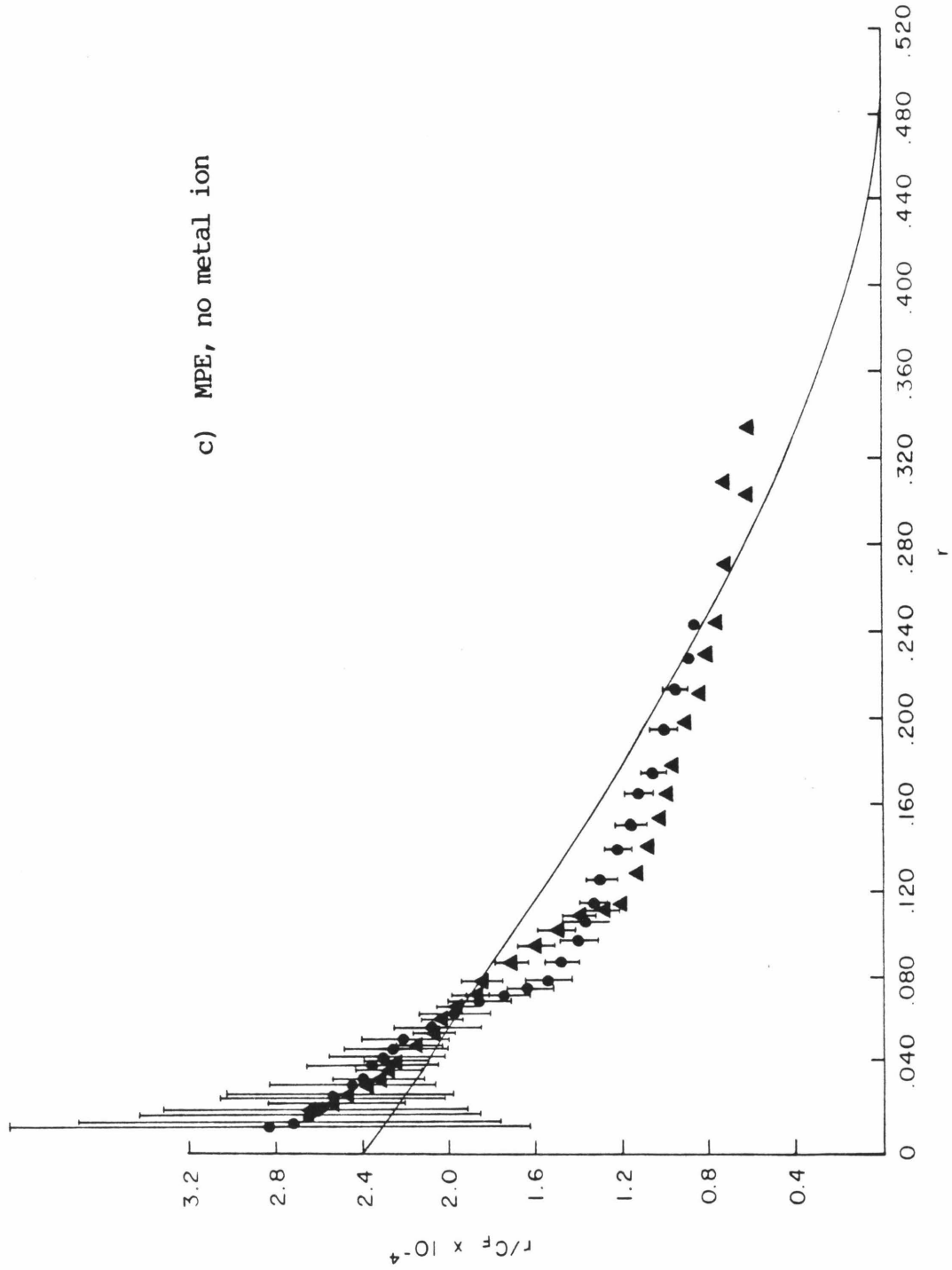
a) MPE-Ni(II)

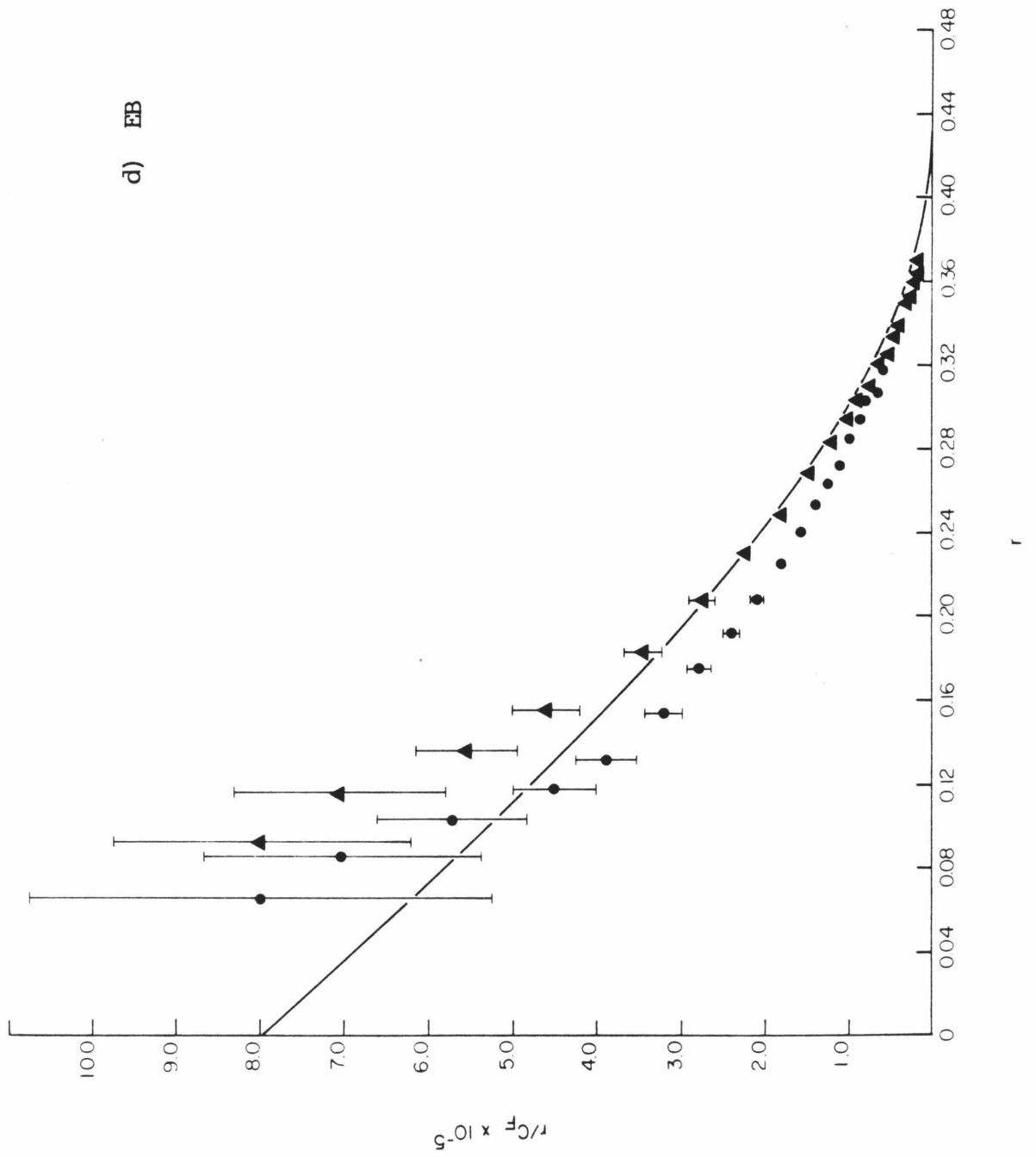


b) MPE-Mg(II)



c) MPE, no metal ion





lowers its binding affinity. Ethidium bromide has a net positive charge and binds to DNA stronger than MPE·Ni(II) or MPE·Mg(II) due to electrostatic attraction. Binding affinity titrations using MPE·Fe(II) were not possible because of problems associated with drug degradation and precipitation. However, since Fe(II) is a divalent metal we may assume that the binding constant for MPE·Fe(II) to DNA is on the order of  $10^5$ .

The binding site size for all four molecules in Table I was estimated to be approximately 2 bp. This is in accordance with the neighbor exclusion model which applies to intercalators.<sup>72</sup> This model states that each space between base pairs forms a potential binding site, but binding sites immediately adjacent to a site already filled are forbidden. This principle is generally thought to hold true for ethidium, which is known to intercalate between base pairs on DNA.<sup>65,66</sup> The question arises whether MPE is also a DNA intercalator. Probably the most critical test for intercalative binding to DNA arises from the expected unwinding of the double helix, and so we undertook a determination of the unwinding angle of MPE on double-helical DNA.

**Unwinding Angle on Supercoiled DNA.** Supercoiled DNA molecules are covalently closed circular double helices which are topologically bonded. The topology of the closed circle is defined by the number of twists in the helix and the number of supercoils in the circle. When a drug binds to and unwinds supercoiled DNA, the number of twists in the helix changes. Since the topology is bonded, the number of supercoils must also change. This change in superhelicity can be determined by agarose gel electrophoresis, which can resolve topoisomers differing by

one turn.

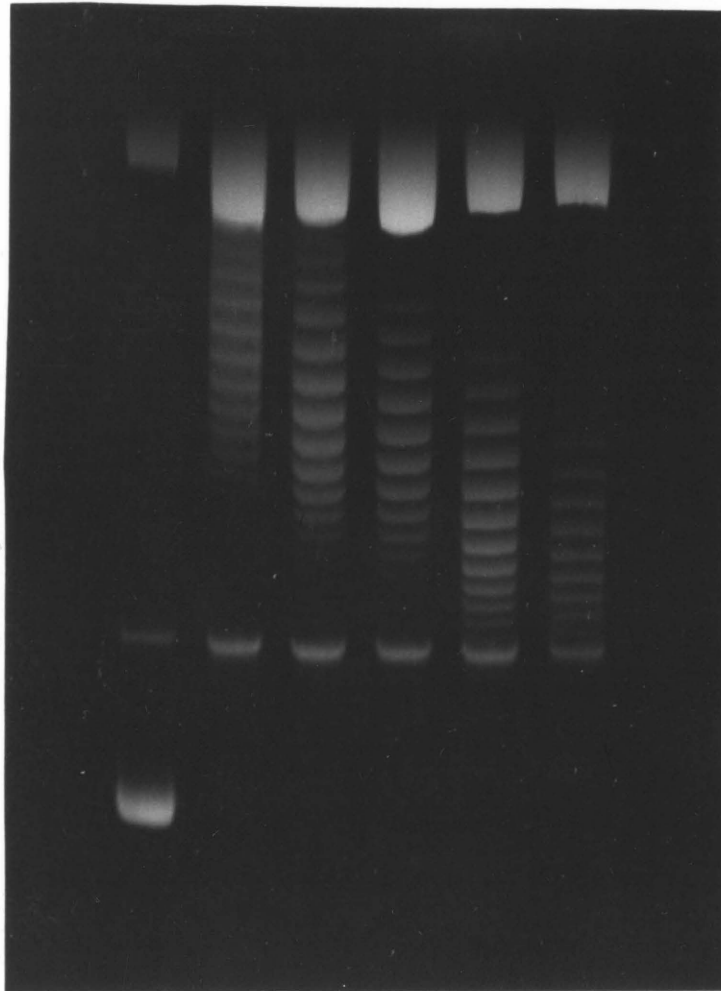
In determining the unwinding angle of MPE we used superhelical PM2 plasmid DNA. The method is called electrophoretic band counting<sup>73</sup> and involves relaxing supercoiled molecules in the presence of various amounts of MPE with topoisomerase I. The result is a complex between drug and covalently closed relaxed circular DNA. The drug is then removed with cation exchange resin and the DNA becomes superhelical, with the degree of superhelicity dependent on the number of drug molecules and the unwinding angle. The samples are analyzed by agarose gel electrophoresis, and the band positions are determined by scanning densitometry.

Figure 4 shows an unwinding angle gel with MPE and PM2 DNA. Since the action of topoisomerase I requires 10 mM magnesium, the chelation state of the MPE was MPE·Mg(II). As the concentration of MPE was increased, the DNA moved faster on the gel indicating an increase in superhelicity. A plot of the relative linking number versus number of MPE molecules (Fig. 5) gives rise to an apparent unwinding angle of  $11^{\circ} \pm 3^{\circ}$  per MPE·Mg(II) molecule. The unwinding angle was calculated by multiplying the slope of Figure 5 (number of turns per MPE·Mg(II) molecule) by  $360^{\circ}$ .<sup>73</sup> This number is valid if all of the added drug molecules are bound and intercalated. Since the binding constant and DNA concentration are known, the relative amounts of bound and free drug can be calculated from the McGhee-von Hippel equations.<sup>71</sup> This calculation yields a ratio bound to free drug of 54; that is essentially all of the MPE is bound to DNA. It is unknown what percentage of these bound species are intercalated and what percentages are outside bound.

**Figure 4**

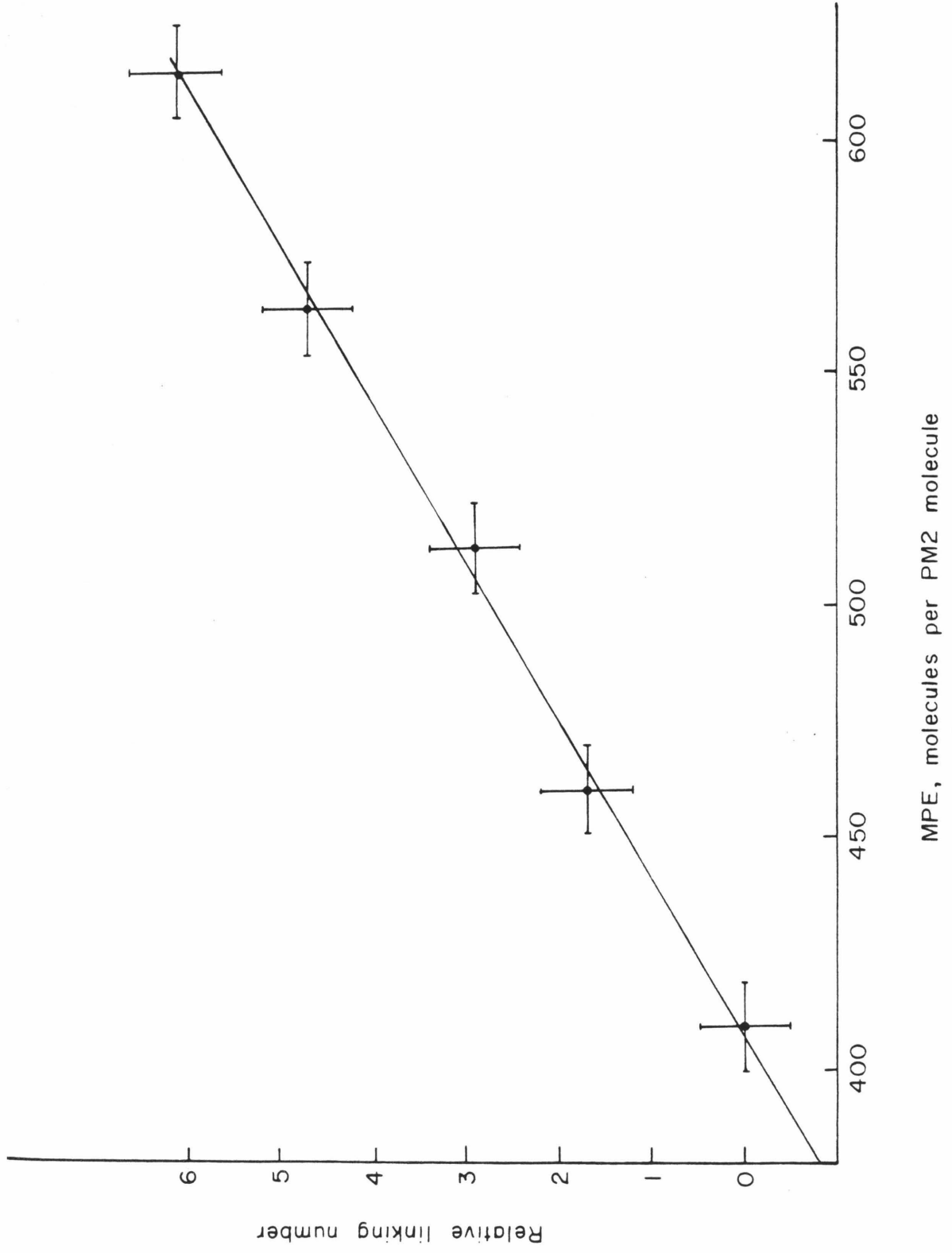
Agarose gel of PM2 DNA relaxed with Topoisomerase I and increasing amounts of MPE·Mg(II).  $5 \times 10^{-4}$  M (bp) PM2 DNA was combined with: lane (A) no drug or enzyme; (B) 409 molecules of MPE·Mg(II) per PM2 molecule ( $r = 0.040$ ); (C) 460 ( $r = 0.045$ ); (D) 511 ( $r = 0.050$ ); (E) 563 ( $r = 0.055$ ); (F) 614 ( $r = 0.060$ ) molecules of MPE·Mg(II) per PM2 molecule and Topoisomerase I. After the reaction the samples were worked up and electrophoresed as described in the Experimental Section.

A B C D E F



**Figure 5**

Unwinding angle plot for MPE·Mg(II) and PM2 DNA. The gel in Figure 4 was scanned with a densitometer and the band positions determined. The least squares slope calculated from these points corresponds to  $11^\circ \pm 3^\circ$  unwinding per added MPE·Mg(II) molecule.

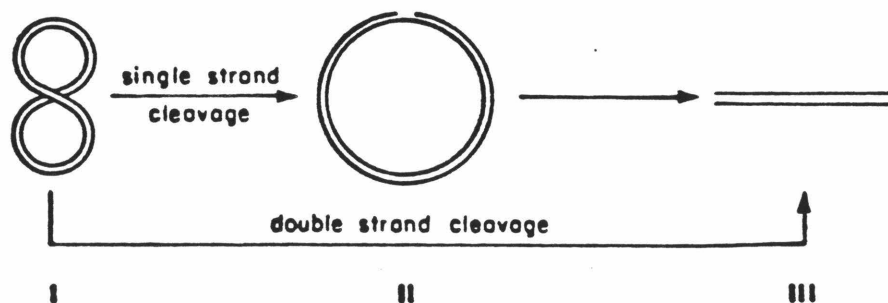


Bresloff and Crothers<sup>65a</sup> found that for ethidium bromide, 80% is intercalated; the unwinding angle for each intercalated ethidium is  $26^{\circ}$ <sup>74</sup> or  $28.9^{\circ}$ .<sup>73b</sup>

This unwinding angle for MPE·Mg(II) of  $11^{\circ}$  can be interpreted in two ways. If every MPE molecule is bound to DNA in the same manner, then it binds with a geometry different to that of ethidium bromide. It has been noted experimentally, and demonstrated theoretically, that for DNA at least two major intercalation geometries exist: one which unwinds  $26^{\circ}$  and another which unwinds  $18^{\circ}$ .<sup>75</sup> Alternatively, if MPE binds to DNA in more than one mode, then it is possible that 42% of the molecules intercalate identically to ethidium (and unwind  $26^{\circ}$ ) while others bind differently and do not unwind the helix.

#### Cleavage of Nucleic Acid by MPE

**Factors Affecting the Cleavage Efficiency of DNA.** The cleavage efficiency of DNA was assayed by monitoring the conversion of supercoiled (form I) pBR-322 plasmid DNA<sup>76</sup> to open circular (form II) and linear forms (form III) by non-denaturing agarose gel electrophoresis.<sup>77</sup> The introduction of one single-strand break converts form I to form II. The introduction of a second single-strand break within 16 base pairs of an existing break converts form II to form III.<sup>78</sup>



The cleavage efficiency of MPE·Fe(II) is compared to that of EDTA·Fe(II), EDTA-propene·Fe(II) [E-C<sub>3</sub>·Fe(II)], and bleomycin·Fe(II) [BLM·Fe(II)] in Table II.

Table II

Reagent	conc. M	% Form			sa
		I	II	III	
EDTA·Fe(II)	10 <sup>-4</sup>	94	6	0	0.06
E-C <sub>3</sub> ·Fe(II)	10 <sup>-4</sup>	92	8	0	0.08
Fe(II)	10 <sup>-4</sup>	92	8	0	0.08
MPE·Fe(II)	10 <sup>-8</sup>	81	19	0	0.21
MPE·Fe(II)	10 <sup>-7</sup>	44	56	0	0.81
MPE·Fe(II)	10 <sup>-6</sup>	3	96	1	3.17
MPE	10 <sup>-6</sup>	93	7	0	0.07
BLM·Fe(II)	10 <sup>-8</sup>	30	57	13	
BLM·Fe(II)	10 <sup>-7</sup>	0	67	33	
BLM·Fe(II)	10 <sup>-6</sup>	0	12	88	
BLM	10 <sup>-6</sup>	72	24	4	

Form I pBR-322 DNA (10<sup>-5</sup> M bp), reagent, and buffer (10 mM Tris·HCl, 50 mM NaCl, pH 7.4) were allowed to react at 22°C for 60 min. Forms I-III were analyzed with agarose gel electrophoresis and quantitated after ethidium bromide staining by densitometry. (a) Mean number of single-strand scissions per DNA molecule, calculated as described in the Experimental Section. These values cannot be calculated for bleomycin because of a non-random accumulation of single-strand breaks.

EDTA·Fe(II) at  $10^{-4}$  M concentrations will cleave plasmid DNA, but with low efficiency. The results with free Fe(II) or E-C<sub>3</sub>·Fe(II) are the same, and addition of ethidium bromide to these reagents does not promote the cleavage reaction. We find that MPE·Fe(II) cleaves plasmid DNA efficiently at three orders of magnitude lower concentration ( $10^{-7}$  M) (Table II). The addition of Fe(II) is required; MPE alone is inactive. This is analogous to bleomycin, where it has been demonstrated that the Fe(II) complex is required for DNA strand scission.<sup>40</sup>

Table II shows that the conversion of form I to form II by MPE·Fe(II) and bleomycin·Fe(II) is achieved with comparable efficiencies. However, bleomycin·Fe(II) is more efficient at double-strand breaks to produce form III (linear) DNA. In general, bleomycin produces more linear molecules than would be expected from a random accumulation of single-strand breaks.<sup>79</sup> This is most likely a result of its base sequence specificity,<sup>30a,44</sup> which results in the preferential cleavage of certain regions on the plasmid.<sup>79</sup> In contrast, cleavage by MPE·Fe(II) follows statistical predictions for the production of forms I, II, and III, indicating a random accumulation of single-strand breaks.

**Inhibition by Chelating Agents.** If Fe(II) is absolutely necessary for MPE activity, then chelating agents should inhibit strand scission by virtue of their ability to bind to Fe(II) and sequester it from MPE (Table III).

Table III

Inhibitor	conc. M	% Form			S
		I	II	III	
None	--	13	87	0	2.0
EDTA	10 <sup>-2</sup>	86	14	0	0.15
EDTA	5 x 10 <sup>-2</sup>	94	6	0	0.06
Des	10 <sup>-2</sup>	97	3	0	0.03
Des	5 x 10 <sup>-2</sup>	100	0	0	0.0

Form I pBR-322 (10<sup>-5</sup> M bp), MPE (10<sup>-5</sup> M), inhibitor, and buffer (40 mM Tris·HCl, 5 mM NaOAc, pH 7.8) were combined and then Fe(II) (10<sup>-5</sup> M) was added. The reaction was at 22°C for 60 min; analysis was as described in the legend to Table I.

Both desferrioxamine (Des), a potent iron chelating agent,<sup>80</sup> and EDTA were effective at inhibition. Since MPE contains the EDTA moiety and would be expected to have a high affinity for Fe(II), an excess of exogeneous chelating agent is necessary for inhibition. Des has a higher iron affinity than EDTA and is a more potent inhibitor. This indicates that metal ions, and particularly Fe(II), are central to the DNA cleavage activity associated with MPE.

**Enhancement by Reducing Agents.** The activation of molecular oxygen by Fe(II) involves reduction of the O<sub>2</sub> and oxidation of the Fe(II).<sup>10</sup> The DNA cleaving reagents which degrade DNA through oxygen activation are dependent on a source of electrons to carry out this

reduction. Ferrous ion can act as this source, but once the Fe(II) has been oxidized to Fe(III) the electron source has been depleted and the oxygen activation ends. Therefore, the addition of another electron source is necessary for most efficient DNA cleavage. With the metal-dependent DNA cleaving reagents bleomycin and 1,10-phenanthroline, reducing agents such as thiols and ascorbate have been found to greatly enhance cleavage efficiencies.<sup>40,55</sup> We quantitated the effect of three reducing agents (dithiothreitol (DTT), sodium ascorbate, and NADH) on the MPE•Fe(II) strand scission reaction (Table IV, Figs. 6-8).

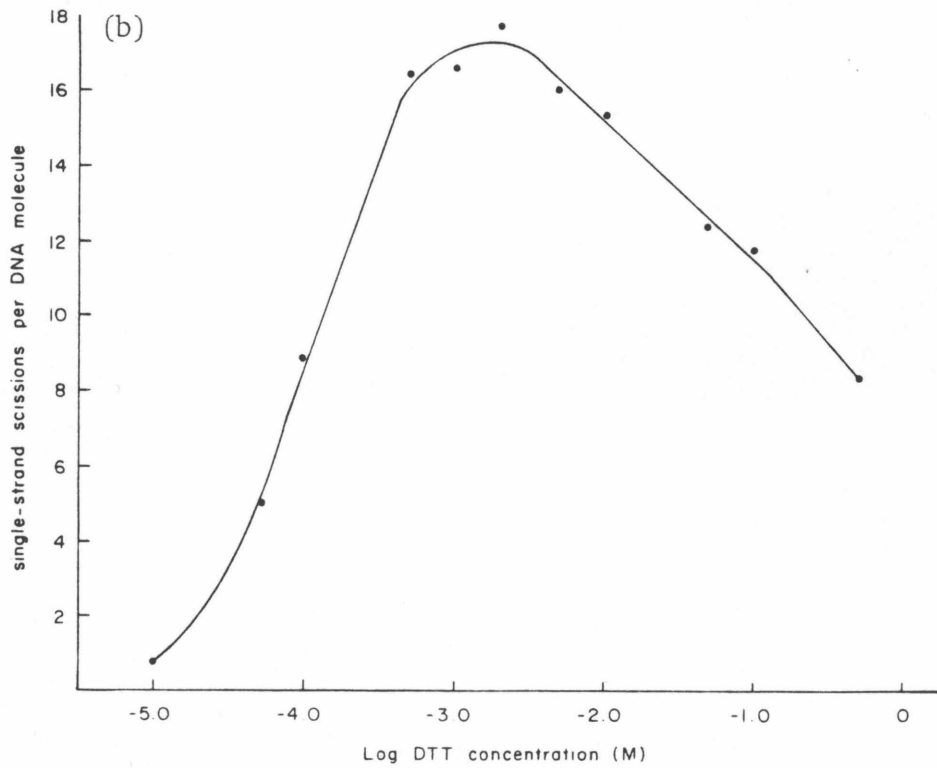
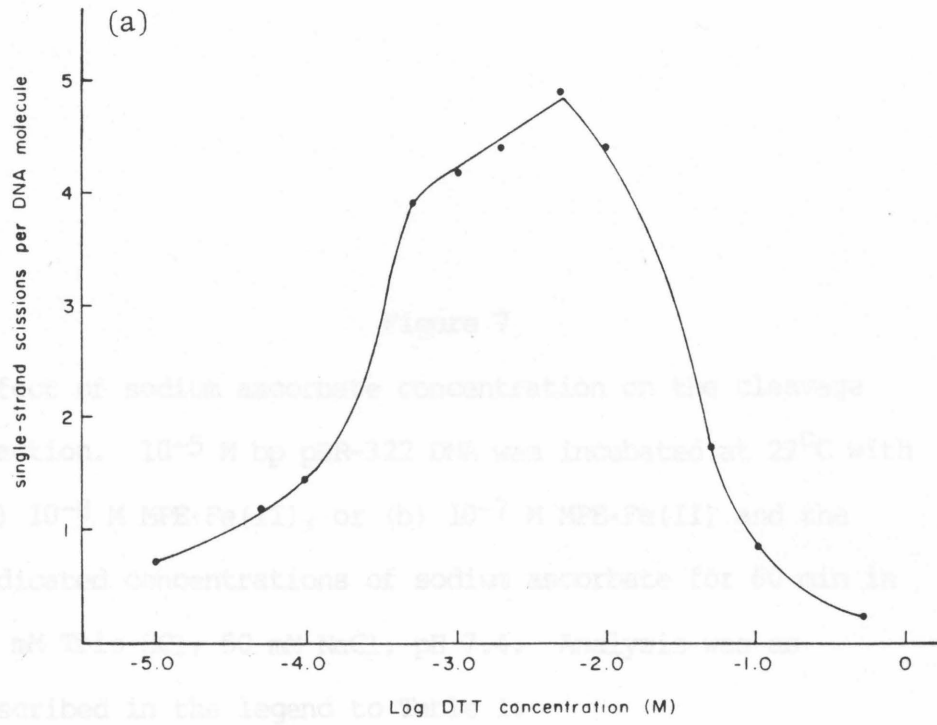
These reducing agents enhance the cleavage reaction at concentrations as low as  $10^{-5}$  M, and effect their maximum enhancements in the 1 to 5 mM range. At concentrations higher than these, the cleavage falls off. Comparison of the three reducing agents reveals that sodium ascorbate is most efficient, followed by DTT and then NADH. Controls using either EDTA•Fe(II) or EDTA-propane•Fe(II) in the presence of these reducing agents show very little strand scission. The concentration of chelated Fe(II) used in these controls was  $10^{-6}$  M, 10-100 times higher than that used in the MPE cleavage experiments. Only with sodium ascorbate did any strand scission take place, and even then only 0.87 nicks per DNA plasmid occurred, compared to 5.3 nicks per plasmid for  $10^{-8}$  M MPE•Fe(II)/sodium ascorbate (Table IV).

Table IV

conc. M MPE·Fe(II)	Reducing Agent	conc. M	% Form			S		
			I	II	III			
10 <sup>-7</sup>	DTT	10 <sup>-5</sup>	48	52	0	0.73		
		5 x 10 <sup>-5</sup>	0	95	5	5.0		
		10 <sup>-4</sup>	0	86	14	8.8		
		5 x 10 <sup>-4</sup>	0	59	41	16.5		
		10 <sup>-3</sup>	0	58	42	16.6		
		2 x 10 <sup>-3</sup>	0	54	46	17.7		
		5 x 10 <sup>-3</sup>	0	60	40	16.1		
		10 <sup>-2</sup>	0	63	37	15.4		
		5 x 10 <sup>-2</sup>	0	74	26	12.5		
		10 <sup>-1</sup>	0	77	23	11.8		
10 <sup>-8</sup>	DTT	5 x 10 <sup>-1</sup>	0	87	13	8.4		
		10 <sup>-5</sup>	48	52	0	0.73		
		5 x 10 <sup>-5</sup>	31	69	0	1.2		
		10 <sup>-4</sup>	24	76	0	1.4		
		5 x 10 <sup>-4</sup>	0	97	3	3.9		
		10 <sup>-3</sup>	0	97	3	4.2		
		2 x 10 <sup>-3</sup>	0	96	4	4.4		
		5 x 10 <sup>-3</sup>	0	95	5	4.9		
		10 <sup>-2</sup>	0	96	4	4.4		
		5 x 10 <sup>-2</sup>	81	19	0	0.21		
10 <sup>-7</sup>	Ascorbate	10 <sup>-5</sup>	0	76	24	12		
		5 x 10 <sup>-5</sup>	0	49	51	19		
		10 <sup>-4</sup>	0	37	63	23		
		5 x 10 <sup>-4</sup>	0	23	77	27		
		10 <sup>-3</sup>	0	15	85	31		
		5 x 10 <sup>-3</sup>	0	9	91	34		
		10 <sup>-2</sup>	0	13	87	32		
		5 x 10 <sup>-2</sup>	0	89	11	7.9		
		10 <sup>-8</sup>	Ascorbate	10 <sup>-5</sup>	8	92	0	2.5
				5 x 10 <sup>-5</sup>	3	97	0	3.5
10 <sup>-4</sup>	0			97	3	4.2		
5 x 10 <sup>-4</sup>	0			96	4	4.9		
10 <sup>-3</sup>	0			95	5	5.3		
5 x 10 <sup>-3</sup>	0			93	7	6.2		
10 <sup>-2</sup>	0			95	5	5.3		
5 x 10 <sup>-2</sup>	62			38	0	0.48		
10 <sup>-7</sup>	NADH			10 <sup>-6</sup>	33	67	0	1.1
				10 <sup>-5</sup>	20	80	0	1.6
		10 <sup>-4</sup>	14	86	0	2.0		
		10 <sup>-3</sup>	0	95	5	5.3		
		10 <sup>-8</sup>	NADH	10 <sup>-6</sup>	79	21	0	0.23
10 <sup>-5</sup>	69			31	0	0.37		
10 <sup>-4</sup>	53			47	0	0.63		
10 <sup>-3</sup>	31			69	0	1.2		
10 <sup>-6</sup> EDTA·Fe(II)	DTT			10 <sup>-3</sup>	96	4	0	0.04
10 <sup>-6</sup> EDTA·Fe(II)	Ascorbate	10 <sup>-3</sup>	42	58	0	0.87		
10 <sup>-5</sup> EDTA·Fe(II)	NADH	10 <sup>-3</sup>	95	5	0	0.05		
10 <sup>-6</sup> E-C3·Fe(II)	DTT	10 <sup>-3</sup>	95	5	0	0.05		
10 <sup>-6</sup> E-C3·Fe(II)	Ascorbate	10 <sup>-3</sup>	44	56	0	0.82		
10 <sup>-5</sup> E-C3·Fe(II)	NADH	10 <sup>-3</sup>	95	5	0	0.05		

**Figure 6**

Effect of DTT concentration on the cleavage reaction.  $10^{-5}$  M bp pBR-322 DNA was incubated at  $22^{\circ}\text{C}$  with (a)  $10^{-8}$  M MPE $\cdot$ Fe(II), or (b)  $10^{-7}$  M MPE $\cdot$ Fe(II) and the indicated concentrations of DTT for 60 min in 10 mM Tris $\cdot$ HCl, 50 mM NaCl, pH 7.4. Analysis was as described in the legend to Table I.



**Figure 7**

Effect of sodium ascorbate concentration on the cleavage reaction.  $10^{-5}$  M bp pBR-322 DNA was incubated at  $22^{\circ}\text{C}$  with (a)  $10^{-8}$  M MPE·Fe(II), or (b)  $10^{-7}$  M MPE·Fe(II) and the indicated concentrations of sodium ascorbate for 60 min in 10 mM Tris·HCl, 50 mM NaCl, pH 7.4. Analysis was as described in the legend to Table I.

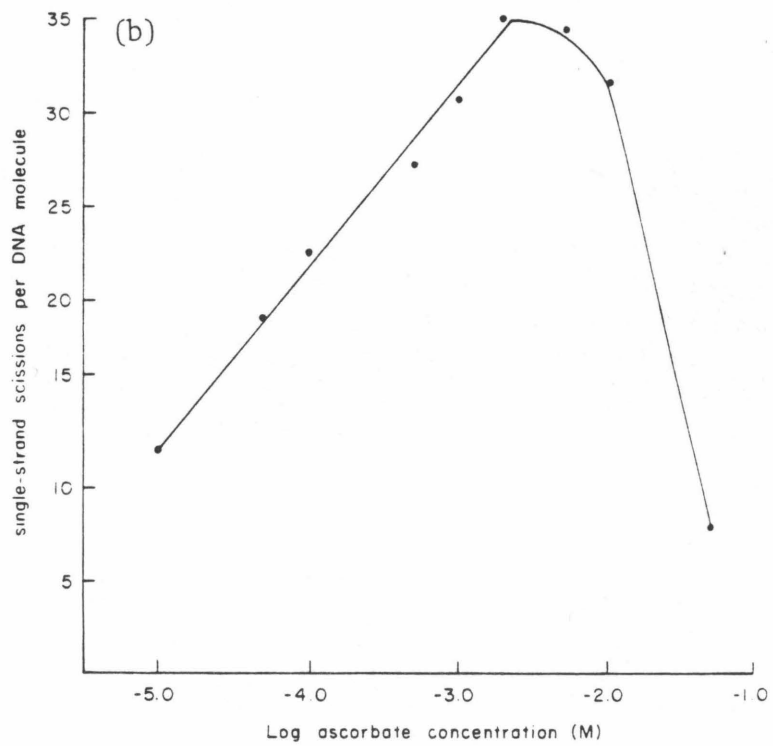
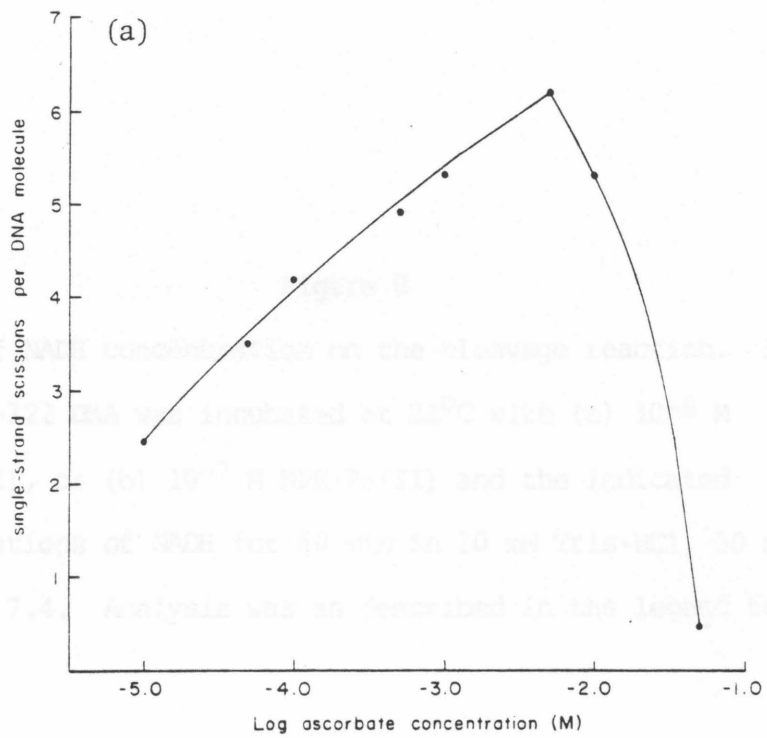
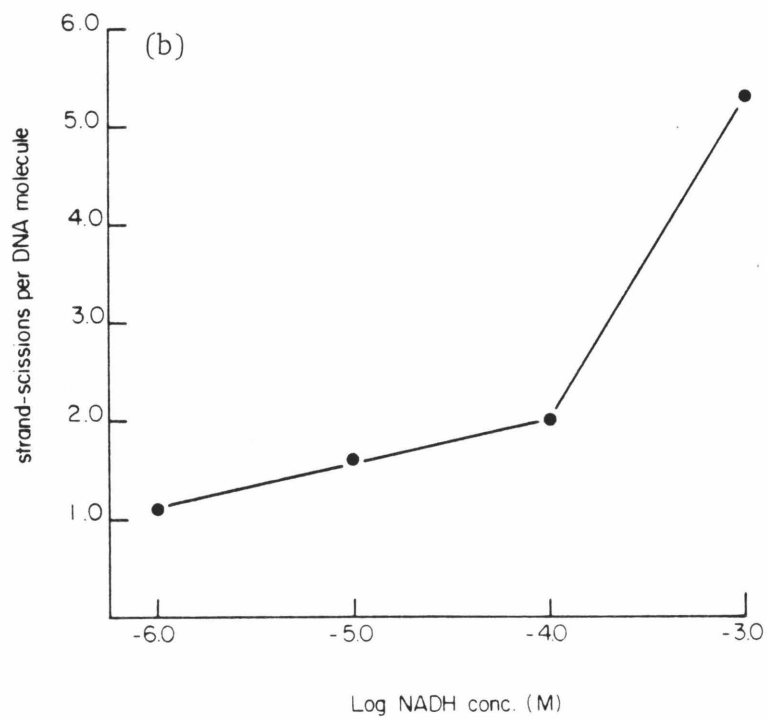
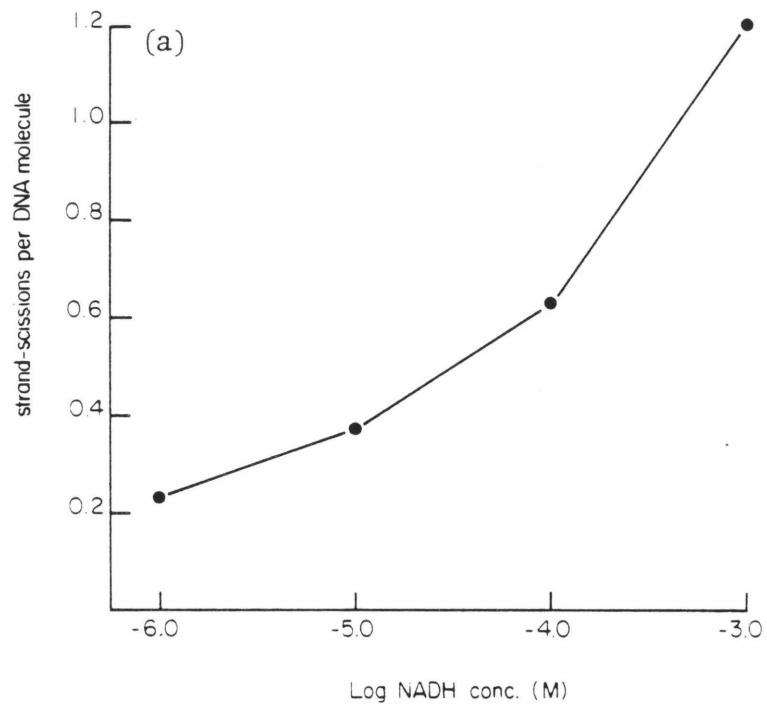


**Figure 8**

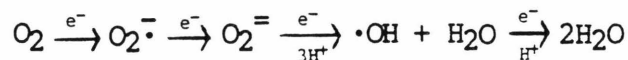
Effect of NADH concentration on the cleavage reaction.  $10^{-5}$  M bp pBR-322 DNA was incubated at  $22^{\circ}\text{C}$  with (a)  $10^{-8}$  M MPE•Fe(II), or (b)  $10^{-7}$  M MPE•Fe(II) and the indicated concentrations of NADH for 60 min in 10 mM Tris•HCl, 50 mM NaCl, pH 7.4. Analysis was as described in the legend to Table I.



The ability of reducing agents to enhance the MPE•Fe(II) cleavage reaction presumably results from regeneration of Fe(II) from Fe(III) to produce a continuous source of active metal ion. This can occur over and over as the reducing equivalents are transferred to molecular oxygen, mediated by Fe. This proposal then predicts that the action of MPE•Fe(II) is catalytic. This prediction is confirmed by an examination of the turnover number (single-strand scissions per MPE•Fe(II) molecule). The turnover number for  $10^{-8}$  M MPE•Fe(II)/ascorbate is 1.42, and for  $10^{-8}$  M MPE•Fe(II)/DTT is 1.12. Thus, there are more single-strand scissions than MPE•Fe(II) molecules under these conditions, indicating recycling of the Fe(II).

Examination of figures 6 and 7 reveals that at high concentrations of DTT or ascorbate, the cleavage of DNA by MPE•Fe(II) is inhibited. Both of these reagents are hydroxyl radical scavengers,<sup>81,82</sup> and this may account for the reduction in strand-scission. This raises the issue of the ultimate reactive species which initiates attack on DNA. The importance of an electron source and metal ions has been shown. Given the precedents discussed earlier involving DNA cleaving reagents, some form of activated oxygen would seem to be a likely candidate.

**Importance of O<sub>2</sub> and Oxygen Radicals.** Dioxygen is formally capable of undergoing a four-electron reduction to H<sub>2</sub>O. Although this process is thermodynamically favorable, molecular oxygen contains two unpaired electrons in the ground state and direct reaction with a singlet reductant molecule to give singlet products is spin forbidden. Therefore, oxidation reactions involving oxygen are likely to proceed by one-electron steps and to involve free radical intermediates:<sup>83</sup>



The intermediacy of these species in the DNA cleavage reaction by MPE•Fe(II) was examined (Table V).

Table V

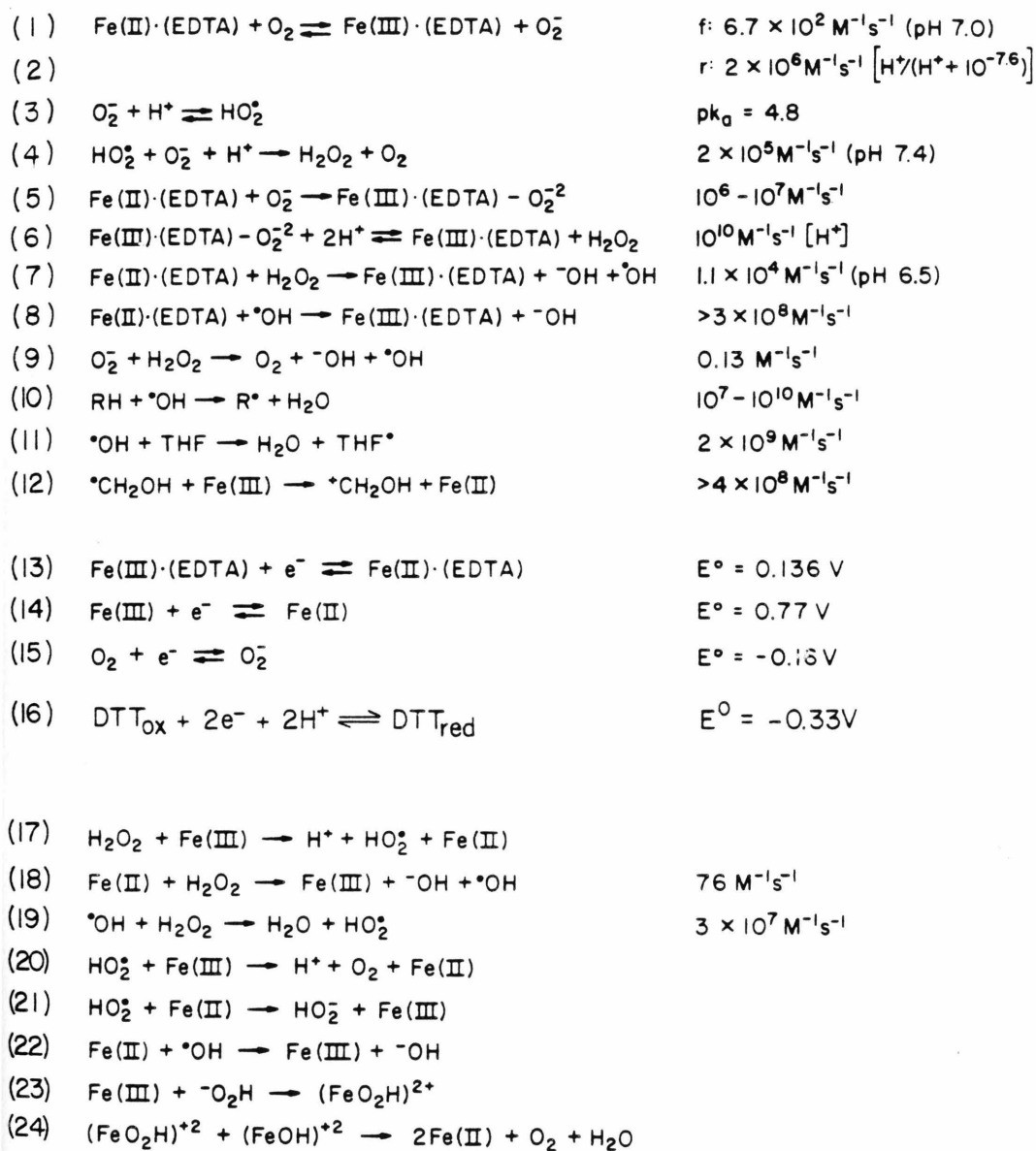
O <sub>2</sub>	Inhibitor	conc. M	% Form			
			I	II	III	S
+	none	--	13	87	0	2.0
-	none	--	97	3	0	0.03
+	SOD <sup>a</sup>	100 <sup>b</sup>	72	28	0	0.33
+	Catalase	100 <sup>b</sup>	96	4	0	0.04
+	DMSO	1.0	36	64	0	1.0
+	DTT	1.0	34	66	0	1.1
+	Sodium Formate	1.0	38	62	0	0.98

Form I pBR-322 DNA (10<sup>-5</sup> M bp), MPE (10<sup>-5</sup> M), inhibitor and buffer (40 mM Tris•HCl, 5 mM NaOAc, pH 7.8) were combined and then Fe(10<sup>-5</sup> M) was added. The reaction was at 22°C for 60 min. Anaerobic reaction was performed as described in the Experimental Section. a) SOD is superoxide dismutase. b) Concentration in µg/ml.

Molecular oxygen is an absolute requirement; MPE•Fe(II) is unable to promote strand-scission in its absence. The addition of the enzyme catalase inhibits the cleavage reaction. The radical scavengers DMSO, DTT, or sodium formate and the enzyme superoxide dismutase (SOD) are all only partially competent at inhibition; cleavage occurs in their presence, but at a decreased level.

These results can be explained by examining the reactions in Scheme I. Molecular oxygen can oxidize EDTA•Fe(II) to EDTA•Fe(III),

Scheme I89



forming superoxide ( $O_2^{\cdot-}$ ). This reaction (1 and 2, Scheme I) is reversible; superoxide can act as a reducing agent for Fe(III). Superoxide can also dismutate to  $H_2O_2$  and  $O_2$  (reaction 4), or act as an oxidizing agent for EDTA·Fe(II), producing  $H_2O_2$  and EDTA·Fe(III) (reactions 5 and 6). The complete protection of DNA from MPE·Fe(II) cleavage by catalase strongly suggests that  $H_2O_2$  (produced by reactions 4 and 6) is involved in the cleavage of DNA, and manifests its activity by being converted to  $\cdot OH$  in the Fenton reaction (reaction 7). Catalase is an enzyme which converts  $H_2O_2$  to  $H_2O$  and  $O_2$ , thereby preventing the Fenton reaction. The Haber-Weiss reaction (reaction 9) is slow, and is unlikely to be source of  $\cdot OH$ .

SOD is an enzyme which catalyzes the conversion of superoxide to  $H_2O_2$  and  $O_2$ . The rate of this reaction increases from  $2 \times 10^5 M^{-1} s^{-1}$  to  $2 \times 10^9 M^{-1} s^{-1}$  upon SOD catalysis.<sup>84</sup> Strand-scission induced by MPE·Fe(II) is inhibited by SOD because the enzyme removes a source of reducing power, thereby decreasing the amount of reduced ferrous ion available for the Fenton reaction. Reducing agents recycle the Fe(III) produced in reactions 1, 6 and 7 to generate active ferrous ion. When DTT or ascorbate is present, the reducing power of superoxide is not needed and SOD has no effect on the cleavage efficiency.

The production of free  $\cdot OH$  as the primary species which initiates cleavage predicts that high concentrations of  $\cdot OH$  scavengers would inhibit the reaction.  $\cdot OH$  scavengers are known to protect DNA against damage by this species generated free in solution.<sup>85</sup> However, only partial inhibition occurs with MPE·Fe(II) (Table V), which means that either another active species can attack the DNA, or else  $\cdot OH$

formed by  $\text{MPE}\cdot\text{Fe(II)}$  is closely associated with the DNA and cannot be scavenged before it reacts with the deoxyribose rings.

A possibility for another active species is an iron-bound oxygen such as  $(\text{Fe-O})^{+3}$ , formed by splitting the O-O bond of  $\text{EDTA}\cdot\text{Fe(III)}-\text{O}_2^{-2}$  (product of reaction 5). This reaction is analogous to that by which  $\text{H}_2\text{O}_2$  reacts with peroxidase to form compound I.<sup>42</sup> However in that system, and in others which are thought to proceed via iron-bound oxygen such as catalase<sup>42,86</sup> and cytochrome P-450,<sup>87</sup> the iron is surrounded by a porphyrin. The formal assignment of compound I is an oxy-cation of  $\text{Fe(V)}$ , but Mossbauer and spectral evidence contribute to the widely held view that compound I is an  $\text{Fe(IV)}$  species, with the additional oxidizing equivalent residing on the porphyrin in the form of a  $\pi$ -cation radical.<sup>88</sup> Since the metal ligand on MPE is not a porphyrin, it seems unlikely that an iron bound oxygen intermediate is involved, although the possibility cannot be ruled out.

$\text{MPE}\cdot\text{Fe(III)}$  is relatively inefficient at strand-scission unless a reducing agent is added. We have found that  $\text{H}_2\text{O}_2$  can enhance the cleavage of DNA by  $\text{MPE}\cdot\text{Fe(III)}$  (Table VI).

Table VI

Reagent	Reagent conc. M	Cofactor	Cofactor conc. M	% Form			S
				I	II	III	
MPE•Fe(III)	10 <sup>-7</sup>	H <sub>2</sub> O <sub>2</sub>	0	75	25	0	0.29
			10 <sup>-6</sup>	40	60	0	0.91
			10 <sup>-5</sup>	17	83	0	1.8
			10 <sup>-4</sup>	18	82	0	1.7
			10 <sup>-3</sup>	27	73	0	1.3
MPE•Fe(III)	10 <sup>-8</sup>	H <sub>2</sub> O <sub>2</sub>	0	92	9	0	0.09
			10 <sup>-6</sup>	81	19	0	0.21
			10 <sup>-5</sup>	74	26	0	0.30
			10 <sup>-4</sup>	73	27	0	0.31
			10 <sup>-3</sup>	76	24	0	0.27
EDTA•Fe(III)	10 <sup>-6</sup>	H <sub>2</sub> O <sub>2</sub>	10 <sup>-3</sup>	96	4	0	0.04
E-C <sub>3</sub> •Fe(III)	10 <sup>-6</sup>	H <sub>2</sub> O <sub>2</sub>	10 <sup>-3</sup>	97	3	0	0.03
MPE•Fe(III)	10 <sup>-7</sup>	PhIO <sup>a</sup>	10 <sup>-5</sup>	67	33	0	0.40
MPE•Fe(III)	10 <sup>-8</sup>	PhIO <sup>a</sup>	10 <sup>-5</sup>	86	14	0	0.15

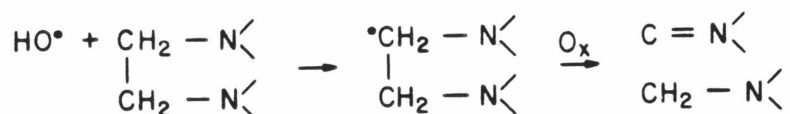
Form I pBR-322 (10<sup>-5</sup> M bp); MPE•Fe(III), EDTA•Fe(III), or E-C<sub>3</sub>•Fe(III); and buffer (40 mM Tris•HCl, 5 mM NaOAc, pH 7.8) were combined and then H<sub>2</sub>O<sub>2</sub> or PhIO was added. The reaction was at 22°C for 60 mins. a) PhIO is Iodosylbenzene.

There are two possibilities for the activation of oxygen in the MPE•Fe(III)/H<sub>2</sub>O<sub>2</sub> system. One is the formation of MPE•Fe(III)-O<sub>2</sub><sup>-2</sup> (Scheme I, reverse of reaction 6), followed by O-O bond splitting to give iron bound oxygen as discussed earlier. Alternatively, H<sub>2</sub>O<sub>2</sub> could act as a reducing agent for Fe(III) (reaction 17), and the resulting Fe(II) would react with another molecule of hydrogen peroxide in a Fenton reaction to produce •OH. Walling and coworkers<sup>90</sup> have studied the decomposition of H<sub>2</sub>O<sub>2</sub> catalyzed by EDTA•Fe(III), and their results are consistent with an •OH radical chain mechanism.

Groves has studied ferric ion mediated hydroxylation of organic compounds using iodosylbenzene (PhIO) as the oxidant.<sup>91</sup> Using Fe(III)-porphyrins as catalysts, PhIO will hydroxylate unactivated C-H bonds. The most reasonable interpretation is that an Fe(V)-oxo (or

Fe(IV)O + porphyrin cation radical) intermediate is the hydroxylating species. We have found that PhIO is relatively inefficient as an activating agent for MPE•Fe(III) (Table VI), although there was a slight enhancement compared to MPE•Fe(III) alone. This is not surprising since the ligand on MPE is not a porphyrin, and the formation of Fe(V)O is unlikely.

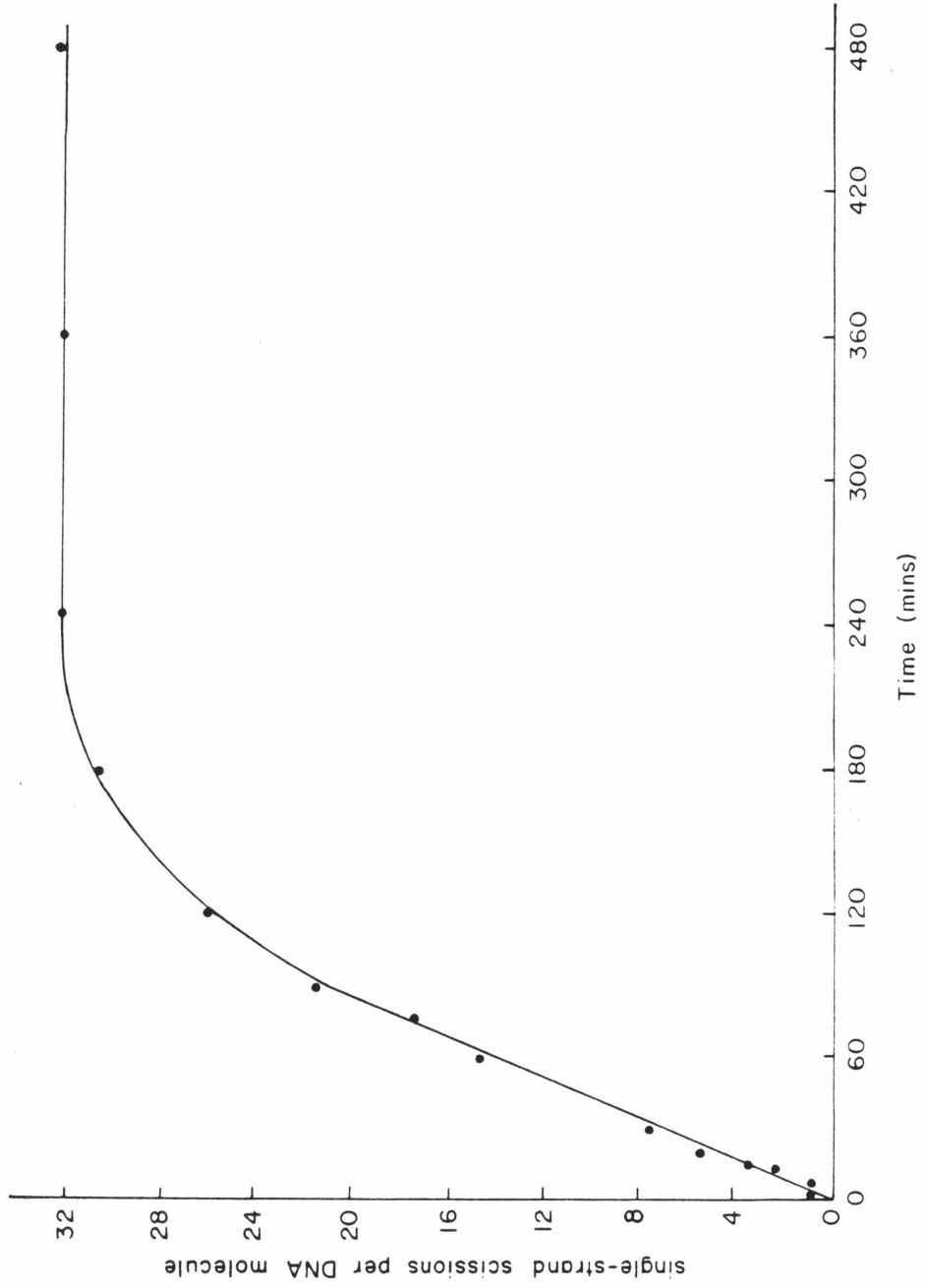
**Time Course.** MPE•Fe(II)/DTT was allowed to react with supercoiled pBR-322 and the reaction was stopped at various intervals in order to examine the rate of strand scission (Figure 9). Cleavage increases linearly with time up to about 200 mins, and then the drug becomes inactive. Addition of more DTT at either 60 min or 120 min fails to reactivate the MPE•Fe(II), indicating that DTT is not the limiting factor. The localized production of hydroxyl radicals may be responsible for degradation of the EDTA moiety on MPE, resulting in drug inactivation.



The rate constant for this reaction has been determined,  $2.76 \times 10^9 \text{ M}^{-1} \text{ s}^{-1}$ ,<sup>89b</sup> and should be competitive with abstraction of a hydrogen atom from deoxyribose.

**Figure 9**

Time course of the cleavage reaction.  $10^{-5}$  M pBR-322 DNA was incubated at  $22^{\circ}\text{C}$  with  $10^{-7}$  M MPE·Fe(II) and  $10^{-3}$  M DTT in 10 mM Tris·HCl, 50 mM NaCl, pH 7.4. At the indicated times, aliquots were removed and terminated with 50 mM desferrioxamine (Ciba-Geigy) followed by freezing in dry ice. Analysis was as described in the legend to Table I.



**Effect of DNA Concentration.** McGhee and von Hippel have developed a theoretical model for the binding of molecules to DNA.<sup>71</sup> One consequence of their model is that at low DNA concentrations, less drug will be bound to the DNA. The amount of bound drug is also dependent on the binding constant and binding site size of the drug, all of which are related by the following equation:

$$\frac{r}{L_F} = K(1 - nr) \left[ \frac{1 - nr}{1 - (n-1)r} \right]^{n-1}$$

where  $r$  is the bound drug to DNA base pair ratio (binding density),  $L_F$  is the concentration of free drug,  $n$  is the binding site size, and  $K$  is the binding constant. This equation was used to calculate bound drug at three different DNA concentrations, assuming  $K$  and  $n$  to be the same for MPE•Fe(II) as they are for MPE•Ni(II) ( $1.5 \times 10^5 \text{ M}^{-1}$  and 2.1 bp, respectively). The cleavage efficiency at these DNA concentrations was determined (Table VII).

Table VII

MPE•Fe(II) conc. M	DNA conc. M	MPE•Fe(II) per DNA bp	% Form			S
			I	II	III	
10 <sup>-9</sup>	10 <sup>-5</sup>	10 <sup>-4</sup>	42	58	0	0.87
10 <sup>-8</sup>	10 <sup>-4</sup>	10 <sup>-4</sup>	40	60	0	0.92
10 <sup>-7</sup>	10 <sup>-3</sup>	10 <sup>-4</sup>	45	55	0	0.80
10 <sup>-8</sup>	10 <sup>-5</sup>	10 <sup>-3</sup>	0	94	6	5.7
10 <sup>-7</sup>	10 <sup>-4</sup>	10 <sup>-3</sup>	0	95	5	5.2
10 <sup>-6</sup>	10 <sup>-3</sup>	10 <sup>-3</sup>	0	96	4	4.6

Form I pBR-322, MPE•Fe(II), DIT ( $5 \times 10^{-3} \text{ M}$ ) and buffer (10 mM Tris•HCl, 50 mM NaCl, pH7.4) were allowed to react for 60 mins at 22°C.

Table VII illustrates that at constant drug to bp ratios, the strand scission is relatively independent of DNA concentration. Therefore it is probable that all of the MPE·Fe(II) is bound to the plasmid throughout this DNA concentration range. However, the von Hippel-McGhee equation predicts that only 60% of the MPE·Fe(II) will be bound at  $10^{-5}$  M (bp) DNA, while > 99% will be bound at  $10^{-3}$  M (bp) DNA. Most likely the binding constant of MPE·Fe(II) to supercoiled DNA is higher than  $1.5 \times 10^5 \text{ M}^{-1}$ , and all of the drug is bound even at  $10^{-5}$  M (bp) DNA.

**Effect of pH and Salt Concentration.** MPE·Fe(II) was allowed to react with supercoiled DNA in the presence of 1 mM DTT at various pH values from pH 4 to pH 10 (Table VIII, Fig. 10). The buffer used was a combination of phosphate, citrate, and borate which has buffering capacity in the pH 4-10 range. While the optimum pH was 8.0, efficient cleavage occurred between pH 7 and pH 10. At pH values below 6.0, very little cleavage took place. One possible reason for decreased cleavage at low pH levels is a competition between hydrogen ions and Fe for the carboxylate ligands on MPE.

The pH effect was further characterized in the physiological range of pH 7-8.6, using Tris buffer (Table IX). The optimum pH was found to be 7.4, although efficient cleavage occurred throughout this range.

Table VIII

MPE·Fe(II) conc. M	pH	% Form			
		I	II	III	S
10 <sup>-7</sup>	4.0	95	5	0	0.05
	5.0	80	20	0	0.22
	6.0	48	52	0	0.74
	7.0	5	95	0	3.0
	8.0	0	93	7	6.4
	9.0	0	94	6	5.6
	10.0	5	95	0	3.0
10 <sup>-8</sup>	4.0	94	6	0	0.06
	5.0	94	6	0	0.06
	6.0	88	12	0	0.13
	7.0	71	29	0	0.34
	8.0	59	41	0	0.53
	9.0	62	38	0	0.48
	10.0	66	34	0	0.41

Form I pBR-322 ( $10^{-5}$  M bp), MPE·Fe(II), DIT ( $10^{-3}$  M), and buffer (20 mM citrate, 20 mM phosphate, 10 mM borate at the indicated pH) were allowed to react for 60 mins at 22°C.

Table IX

pH	% Form			S
	I	II	III	
7.0	0	96	4	4.6
7.2	0	96	4	4.7
7.4	0	95	5	5.0
7.6	0	96	4	4.5
7.8	0	98	2	3.3
8.0	0	98	2	3.3
8.2	1	98	1	3.3
8.4	1	98	1	3.3
8.6	2	98	0	3.3

Form I pBR-322 ( $10^{-5}$  M bp), MPE·Fe(II) ( $10^{-8}$  M), DTT ( $10^{-3}$  M) and buffer (10 mM Tris·HCl, 50 mM NaCl, at the indicated pH) were allowed to react for 60 mins at 22°C.

The concentration of sodium ions was found to have little effect on the MPE·Fe(II)/DTT cleavage of DNA (Table X, Figure 11). Strand-scission was almost constant in the 5 mM to 250 mM range, falling off at higher sodium ion concentrations. At 1 M sodium, cleavage efficiency was one-third that found for the optimum (5 mM  $[Na^+]$ ). The cleavage was also lower at zero sodium ion concentration.

**Figure 10**

Effect of pH on the cleavage reaction.  $10^{-5}$  M bp pBR-322 DNA was incubated at  $22^{\circ}\text{C}$  with (a)  $10^{-8}$  M MPE·Fe(II), or (b)  $10^{-7}$  M MPE·Fe(II) and  $10^{-3}$  M DTT for 60 min. The buffer used was 20 mM citrate, 20 mM phosphate, 10 mM borate at the indicated pH. Analysis was as described in the legend to Table I.

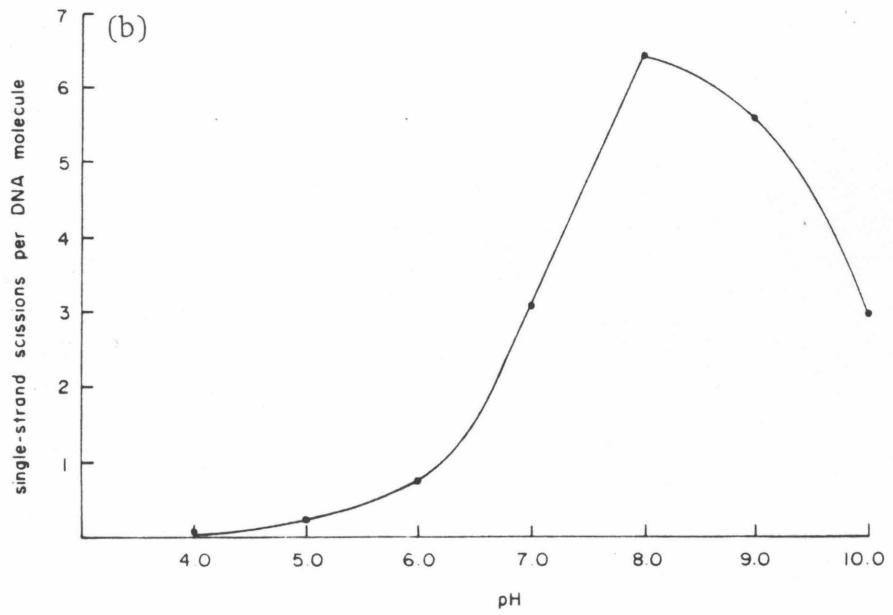
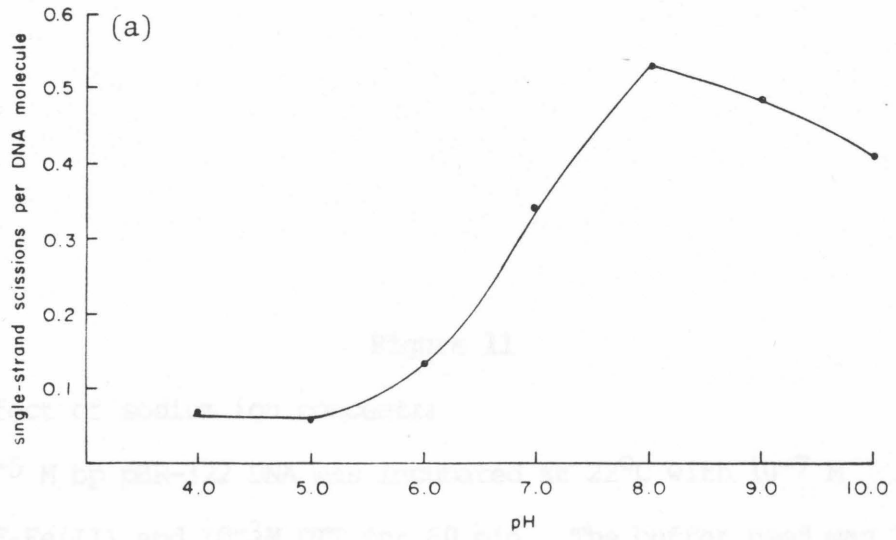


**Figure 11**

Effect of sodium ion concentration on the cleavage reaction.  $10^{-5}$  M bp pBR-322 DNA was incubated at  $22^{\circ}\text{C}$  with  $10^{-7}$  M MPE·Fe(II) and  $10^{-3}$  M DTT for 60 min. The buffer used was 10 mM Tris·HCl, pH 7.4, and the indicated concentration of NaCl. Analysis was as described in the legend to Table I.

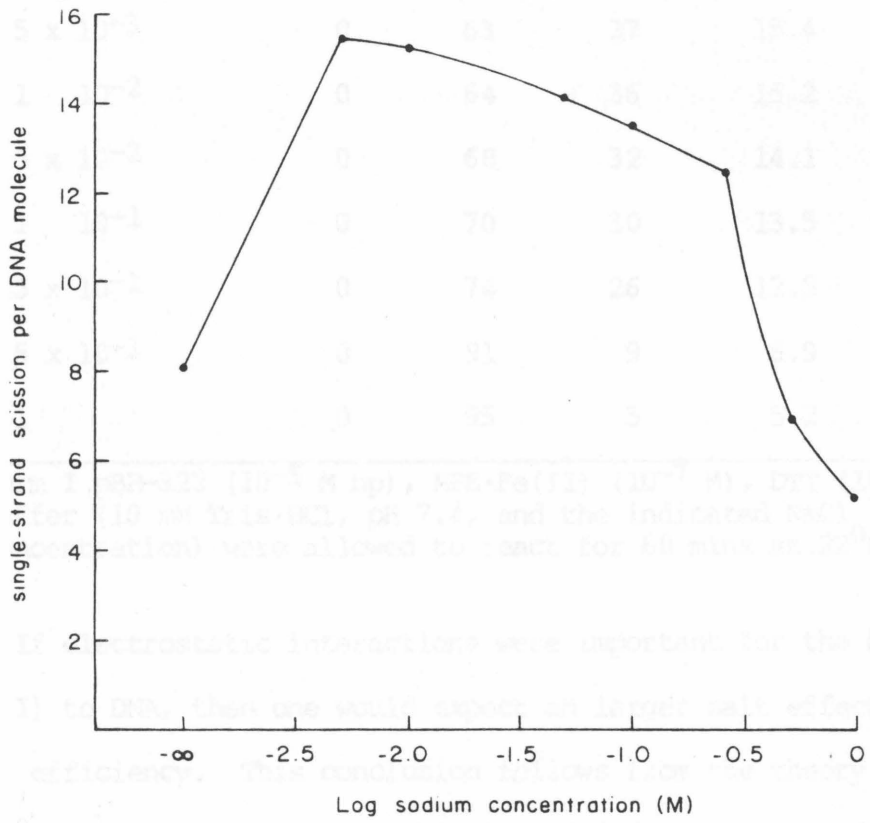


Table X

NaCl conc. M	% Form			
	I	II	III	S
0	0	88	12	8.1
5 x 10 <sup>-3</sup>	0	63	37	15.4
1 10 <sup>-2</sup>	0	64	36	15.2
5 x 10 <sup>-2</sup>	0	68	32	14.1
1 10 <sup>-1</sup>	0	70	30	13.5
2.5 x 10 <sup>-1</sup>	0	74	26	12.5
5 x 10 <sup>-1</sup>	0	91	9	6.9
1	0	95	5	5.2

Form I pBR-322 (10<sup>-5</sup> M bp), MPE·Fe(II) (10<sup>-7</sup> M), DTT (10<sup>-3</sup> M) and buffer (10 mM Tris·HCl, pH 7.4, and the indicated NaCl concentration) were allowed to react for 60 mins at 22°C.

If electrostatic interactions were important for the binding of MPE·Fe(II) to DNA, then one would expect an larger salt effect on the cleavage efficiency. This conclusion follows from the theory of Record,<sup>92</sup> who has noted that the binding affinity of a ligand  $1 M^+$  (monovalent cation concentration) is related to the number of ion-pair interactions ( $n$ ), and a charge density interaction ( $\psi$ ):

$$K = K_1 [M^+]^{-n\psi}$$

$K_1$  is the binding affinity at  $1 M^+$  and  $K$  is the binding affinity at another salt concentration. If we assume that cleavage efficiency is

directly related to binding affinity (all other things being equal) then  $K_{.005}/K_1$  is 15.4/5.2 or about 3 (Table X). In other words, the binding affinity at 5 mM salt is only three times that at 1 M salt, giving rise to a value of only 0.2 for  $n\psi$ . This is expected since  $MPE \cdot Fe(II)$  has zero net charge (+1 for ethidium moiety, +2 for ferrous ion, -3 for EDTA moiety), while  $MPE \cdot Fe(III)$  has one net positive charge. Since recycling between  $Fe(II)$  and  $Fe(III)$  occurs when DTT is present, the average net charge of the drug would be expected to be between zero and one (and probably closer to zero), consistent with the value found for  $n\psi$  of 0.2. This analysis is further complicated by the fact that the  $Na^+$  competes with Fe for the carboxylate ligands on MPE. Therefore it is difficult to precisely quantitate the electrostatic interaction between  $MPE \cdot Fe$  and DNA, but we can conclude that it is not very large.

**Effect of Other Metals.** Although metal free MPE is capable of cleaving DNA in the presence of DTT (possibly due to trace metal contaminants), the addition of  $Fe(II)$  or  $Fe(III)$  greatly enhances the reaction. We examined the ability of other metals to enhance the cleavage reaction by MPE (Table XI). Of the metals tested,  $Cu(II)$  and  $Mn(II)$  had little effect, while  $Co(II)$ ,  $Mg(II)$ ,  $Ni(II)$ , and  $Zn(II)$  inhibited strand scission when present in stoichiometric amounts.

Table XI

Added Metal	% Form			S
	I	II	III	
None	51	49	0	0.68
Fe(II)	0	58	42	16.6
Fe(III)	0	54	46	17.5
Cu(II)	64	36	0	0.45
Mn(II)	65	35	0	0.43
Co(II)	92	8	0	0.08
Mg(II)	87	13	0	0.14
Ni(II)	87	13	0	0.14
Zn(II)	82	18	0	0.19

Form I pBR-322 ( $10^{-5}$  M bp), MPE ( $10^{-7}$  M), metal ion ( $10^{-7}$  M), DTT ( $10^{-3}$  M), and buffer (10 mM Tris·HCl, 50 mM NaCl, pH 7.4) were allowed to react for 60 mins at 22°C.

These results further point to the importance of iron in the cleavage reaction by MPE. One may have expected that some other metal ions, particularly Cu, would also have been competent at activating oxygen and promoting strand scission. Cu-phenanthroline cleaves DNA in the presence of thiols, and the formation of hydroxyl radicals by Fenton-type reactions with Cu(I) have been suggested to be responsible.<sup>54,55</sup> In the case of bleomycin it has been reported that the Cu(II) complex does not efficiently promote strand-scission, even in the presence of reducing agents capable of forming Cu(I)·BLM *in situ*.<sup>40</sup>

Most recent results, however, have indicated that  $\text{Cu(I)} \cdot \text{BLM}$  can cleave DNA, if the Cu is not added in excessive quantities.<sup>93</sup> With regard to MPE, Table XI shows that some cleavage does occur in the presence of  $\text{Cu(II)}$  or  $\text{Mn(II)}$  and DTT, but only at levels equal to or less than if no metal was added. Trace iron is probably responsible for these levels of DNA breakage. The inability of Cu and Mn to enhance cleavage may be a reflection of an inappropriate redox potential when these metals are chelated to MPE.

**Alkali-Lability of MPE-Fe(II) treated DNA.** In addition to direct strand breakage, many agents which cause damage to DNA induce lesions in the sugar moiety which lead to breakage under alkaline conditions; these are referred to as alkali-labile sites. The  $\cdot\text{OH}$  radicals produced by ionizing radiation have been reported to produce alkali-labile sites.<sup>58a,59</sup> We investigated the possibility that MPE-Fe(II) also induces these lesions in DNA (Table XII).

pBR-322 was cleaved with MPE-Fe(II), treated with sodium hydroxide or piperidine, and then analyzed by agarose gel electrophoresis. This post-reaction treatment resulted in denaturation of the DNA; form I (supercoiled) DNA went to denatured form I, and form II (open-circular, nicked) DNA went to single-stranded open circular and single-stranded linear molecules. After the treatment with base, the solution was neutralized. The form I DNA quickly renatured, while the other fragments remained single-stranded. When analyzed by gel electrophoresis, these single-stranded fragments do not stain well with ethidium bromide. Therefore, scission was quantitated by comparing the amount of form I DNA remaining relative to an adjacent control lane, containing unreacted starting material.

Table XII

Post-reaction Treatment	% Form I Remaining	S
none	46	0.78
30 mM NaOH, 65°C, 30 min	48	0.73
1 M Piperidine, 90°C, 30 min	42	0.87
30 mM NaCl, 65°C, 30 min	45	0.80

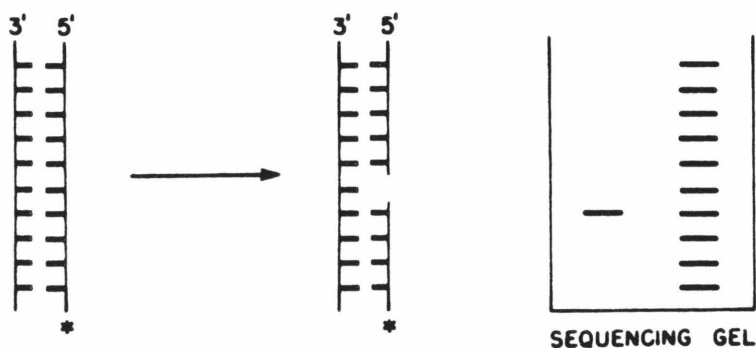
Form I pBR-322 ( $10^{-5}$  M bp), MPE·Fe(II) ( $10^{-7}$  M) and buffer (10 mM Tris·HCl, 50 mM NaCl, pH 7.4) were allowed to react for 60 mins at 22°C (total volume 40  $\mu$ L). The reaction was divided into 4 equal portions and each was treated as noted. The solutions were neutralized with 0.5 M HCl, and then electrophoresed on agarose as described. A control lane containing 10  $\mu$ L of form I pBR-322 ( $10^{-5}$  M) was run as a standard (taken as 100%) to calculate the percent form I remaining in each experiment.

The results indicate that there are no sites produced which are labile to 30 mM NaOH (pH 12.5) or 1 M piperidine. These conditions are strong enough to catalyze the cleavage of depurinated DNA and other alkali-labile bonds.<sup>94</sup> The absence of these lesions has implications on the organic reaction mechanism of MPE·Fe(II) induced cleavage, which will be discussed later in the section on cleavage products.

**Sequence Specificity of the DNA Cleavage Reaction.** The DNA binding portion of MPE, methidium, is an intercalator of low overall base composition specificity.<sup>65c,d,95</sup> However, a preference for binding to (3'-5')pyrimidine-purine sequences compared to (3'-5')purine-pyrimidine sequences in deoxyribonucleotides has been established for ethidium,<sup>96</sup> as well as a preference for certain conformations of double-helical DNA.<sup>97</sup> We wondered if the cleavage of DNA by MPE·Fe(II) occurs preferentially at specific base sequences or

DNA conformations.

In order to answer this question, linear DNA restriction fragments labeled with  $^{32}\text{P}$  at the 3'-ends were used as substrates for strand-scission by  $\text{MPE}\cdot\text{Fe}(\text{II})$ . The DNA fragments from this reaction were frozen, lyophilized, denatured in formamide at  $90^\circ\text{C}$ , and electrophoresed on a high resolution denaturing polyacrylamide gel capable of resolving DNA fragments differing in length by one



nucleotide. Each specifically located strand-scission gives rise to one uniquely-sized radioactive DNA fragment, which appears as a single band on an autoradiogram of the gel. Random strand-scission results in a set of radioactive DNA fragments which differ from one another by one base pair. These appear as a uniform ladder of bands on the autoradiogram.

The  $\text{MPE}\cdot\text{Fe}(\text{II})$  cleavage reaction results in a uniform pattern of bands, indicating relatively non-sequence specific cleavage (Figure 12). On certain DNA fragments, the pattern observed is not as completely uniform as that shown in Figure 12. We have concluded that  $\text{MPE}\cdot\text{Fe}(\text{II})$

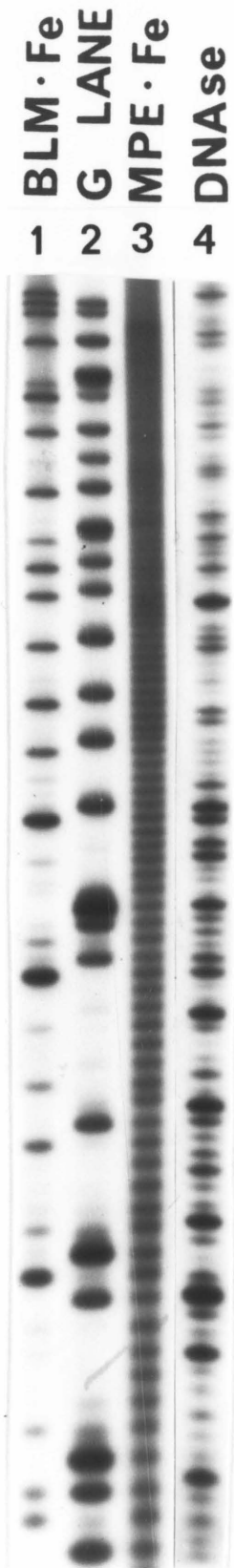
has a slight base sequence bias against regions rich in AT base pairs. This bias will be evident in subsequent gels (Figures 14, 17 and 18).

Figure 12 also shows the pattern of bands produced by the antibiotic bleomycin·Fe(II). Bleomycin has a two base pair recognition site, and cleaves DNA at 5'-GT-3' or 5'-GC-3' base sequences.<sup>30a,44</sup> For comparison, a lane illustrating the cleavage specificity of DNase I is also included. DNase I is a nuclease which is relatively non-specific; however it is known to be sensitive to DNA structure.<sup>98</sup> Although it does cleave at every base pair, the ladder is far from uniform as certain sites are preferred over others. Finally, Figure 12 illustrates the cleavage specificity of a reagent with a one base pair recognition site, dimethyl sulfate. This reagent alkylates guanine, rendering the site labile to cleavage by piperidine in what is referred to as the Maxam-Gilbert G reaction.<sup>99</sup>

These experiments address the question of base sequence specificity, but ethidium has also been postulated to exhibit a preference for certain conformations of double helical DNA.<sup>97</sup> Yielding and coworkers<sup>100</sup> studied this phenomenon using an ethidium analog, monoazido ethidium, which covalently binds to DNA upon photoactivation. They found that at low drug concentrations (drug to nucleotide ratios ranging from 1:100 to 1:8000), covalent attachment of monoazido ethidium to PBR-322 plasmids resulted in a blockage of specific restriction sites. All of the sites had the same base sequence [d(GGCG)], and they concluded that selective drug binding was dictated by long range conformational parameters.

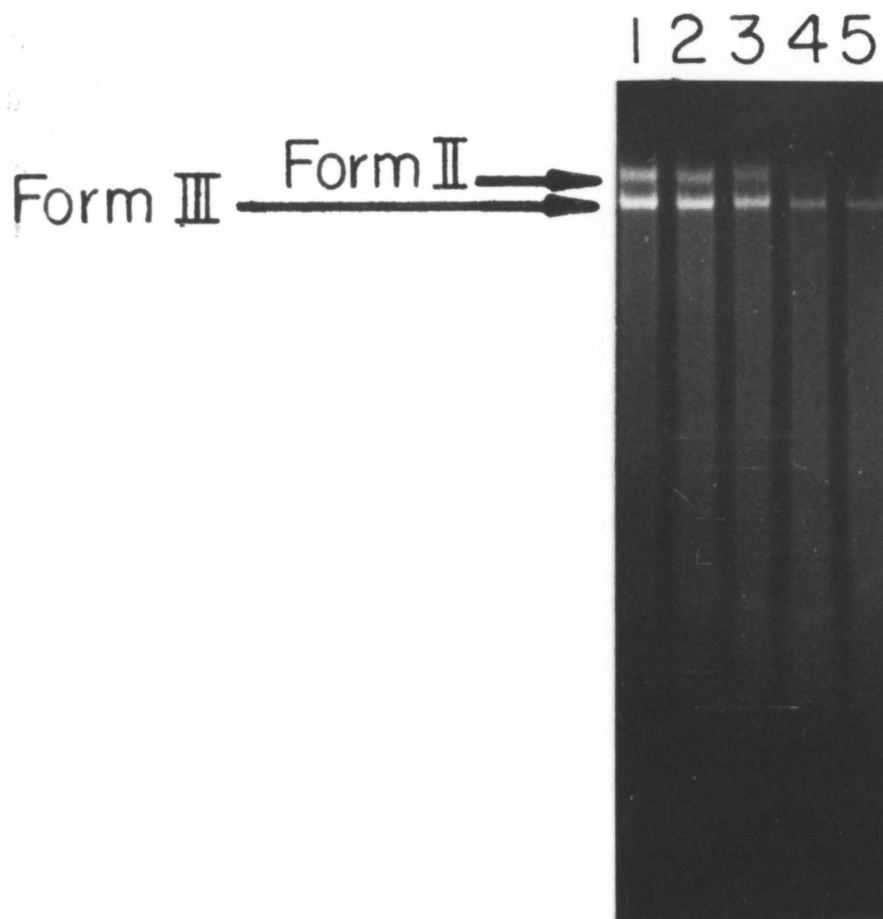
**Figure 12**

Examples of different cleavage specificities. 3'-end labeled DNA fragments ( $\geq 10^4$  cpm) and sonicated calf thymus DNA (total DNA concentration was 100  $\mu$ M bp) were incubated with: lane 1, 100  $\mu$ M bleomycin $\cdot$ Fe(II); lane 2, Maxam-Gilbert G reaction<sup>99</sup>; lane 3, 10  $\mu$ M MPE $\cdot$ Fe(II) and 1 mM DTT; lane 4, 5  $\mu$ g/ml DNase I. The buffer was 10 mM Tris $\cdot$ HCl, 50 mM NaCl, pH 7.4. Polyacrylamide gel electrophoresis and autoradiography are described in the Experimental Section.



**Figure 13**

$10^{-5}$  M bp pBR-322 was incubated for 60 min at  $22^{\circ}\text{C}$  with  $10^{-7}$  M MPE·Fe(II) and: Lane 1, 0.5 mM sodium ascorbate (asc); 2, 1 mM asc; 3, 2 mM asc; 4, 5 mM asc; 5, 10 mM asc.

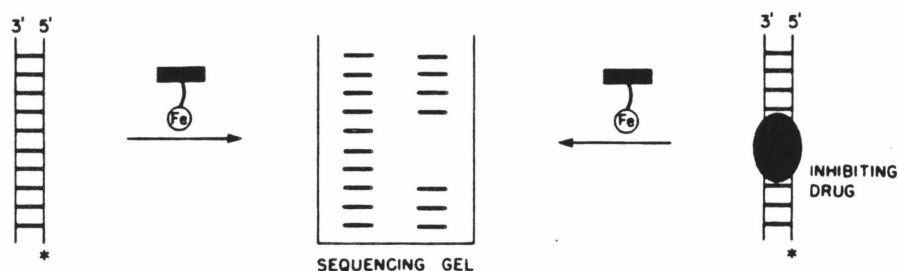


If there are regions on pBR-322 plasmid DNA that are targets for selective binding of monoazido ethidium, then one might expect that they might also preferentially bind MPE. These conformational hot-spots would be cleaved more often than the rest of the plasmid, giving rise to patterns on a gel. However we find that MPE·Fe(II)/ascorbate induced cleavage of whole pBR-322 plasmids results in a completely uniform streak on a gel, with no evidence of specific bands or patterns (Figure 13). The drug to nucleotide ratio was 1:200, within the range used in the monoazido ethidium experiments. The lack of any patterns found with MPE·Fe(II) is probably because the degree of conformational specificity is too low to be picked up on an agarose gel. The photoaffinity labeling technique of Yielding is more sensitive, and can detect high affinity ethidium sites at very low binding densities. Alternatively, Yielding's experiment is detecting specificity in the photoactivated covalent bond formation reaction, not in the non-covalent ethidium binding, and our results are more indicative of the true conformational specificity.

**MPE·Fe(II) Footprinting.**<sup>101</sup> Many small molecules, such as drugs useful in antibiotic, antiviral, and antitumor chemotherapy bind double helical nucleic acid in a sequence specific fashion at sites typically two to four base pairs in size.<sup>5</sup> Small molecules such as bleomycin chemically modify DNA, which allows identification of specific binding sites on heterogeneous DNA from DNA cleavage patterns on Maxam-Gilbert sequencing gels.<sup>30a,44</sup> However, many DNA binding molecules do not modify nucleic acids and our understanding of their sequence preferences has been limited to comparison of binding isotherms

obtained by spectrophotometric analyses of drug binding to homopolymer and copolymer nucleic acids.<sup>5</sup>

In the case of protein-DNA binding specificity, one useful method for determining the locations and sizes of binding sites on DNA is DNase I footprinting, which combines DNase I cleavage of protein-protected DNA fragments and Maxam-Gilbert sequencing gel methods.<sup>2</sup> This technique relies on the relatively low specificity of DNase I in a partial digestion and the ability of DNA-bound protein to prevent cleavage of the DNA backbone between the base pairs it covers. The protein-protected DNA sequence is expressed as a gap in the sequencing ladder seen in the autoradiogram of a Maxam-Gilbert gel, revealing the position and extent of the protein binding site.

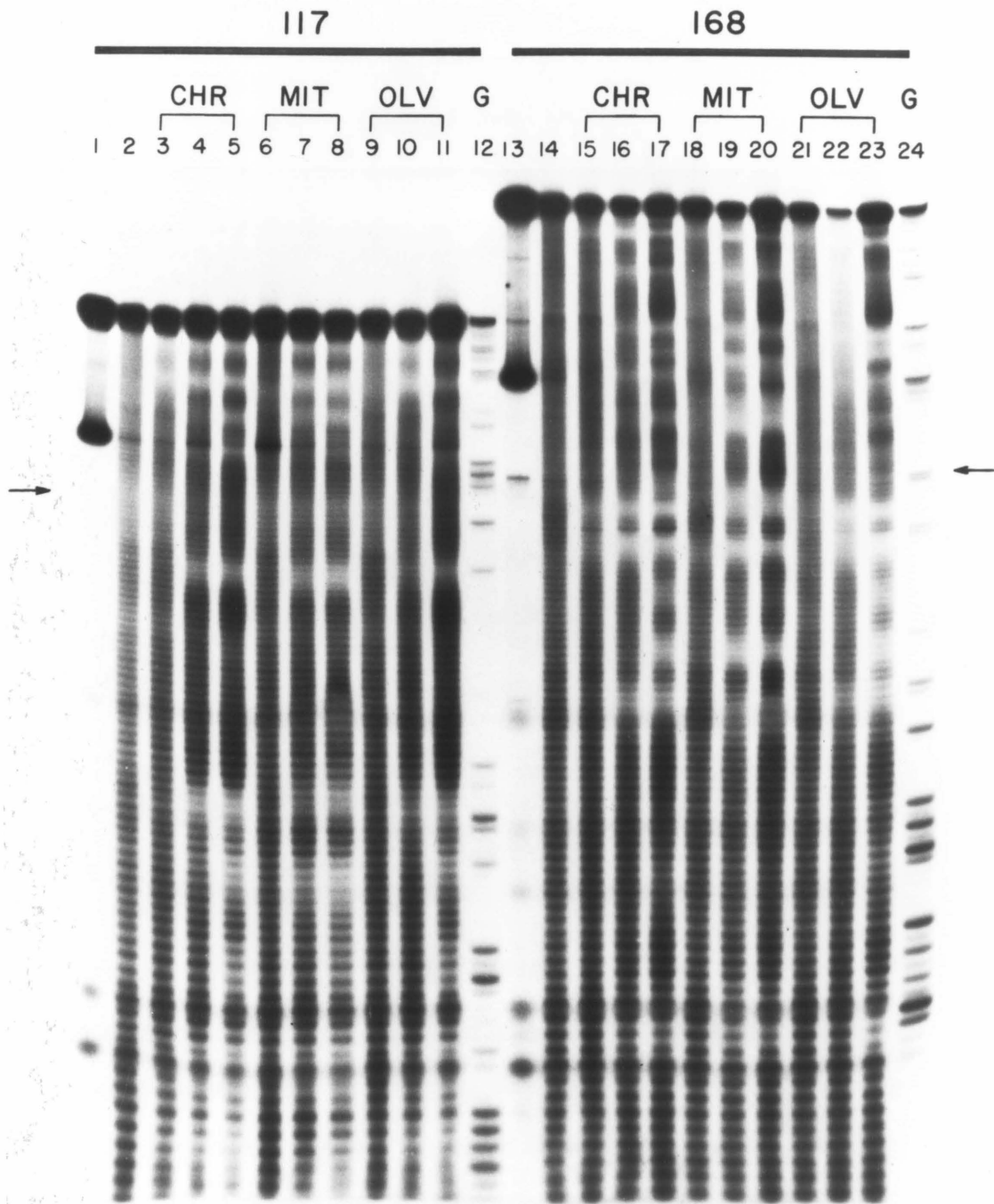


MPE·Fe(II) is a DNA cleaving reagent with lower sequence specificity than DNase I (Figure 12). In effect, MPE·Fe(II) is a small synthetic scissor for DNA and, because of its size, might be a useful tool for probing the locations and size of binding sites of drugs on naturally occurring DNA. Van Dyke and Dervan have used MPE·Fe(II) as a footprinting tool to determine the binding sites of actinomycin, netropsin, distamycin, chromomycin, mithramycin, and olivomycin on some



**Figure 14**

Autoradiogram of DNA cleavage inhibition patterns for chromomycin, mithramycin, and olivomycin on 117 and 168 base pair fragments of pBR-322, taken from Van Dyke and Dervan.<sup>8c</sup> Lanes 1-11 (117 bp fragment) and 13-23 (168 bp fragment) have a 10  $\mu$ l final volume, each containing 10 mM Tris·HCl (pH 7.4), 50 mM NaCl, 1.1 mM NH<sub>4</sub>OAc, 0.18 mM EDTA, 4 mM DTT, 100  $\mu$ M bp DNA (end-labeled fragment and calf thymus carrier), and 10  $\mu$ M MPE·Fe(II). Lanes 12 and 24 are the Maxam-Gilbert G reactions on the 117 and 168 bp fragments, respectively. Lanes 1 and 13 are intact buffered DNA. Lanes 2 and 14 are the MPE·Fe(II) cleavage controls. Lanes 3-5 and 15-17 contain 6.3, 25, and 100  $\mu$ M chromomycin (chr.) respectively. Lanes 6-8 and 18-20 contain 6.3, 25, and 100  $\mu$ M mithramycin (mit.), respectively. Lanes 9-11 and 21-23 contain 6.3, 25, and 100  $\mu$ M olivomycin (olv.), respectively. Each reaction containing chr., mit., or olv. contains a two-fold molar excess of Mg(II).



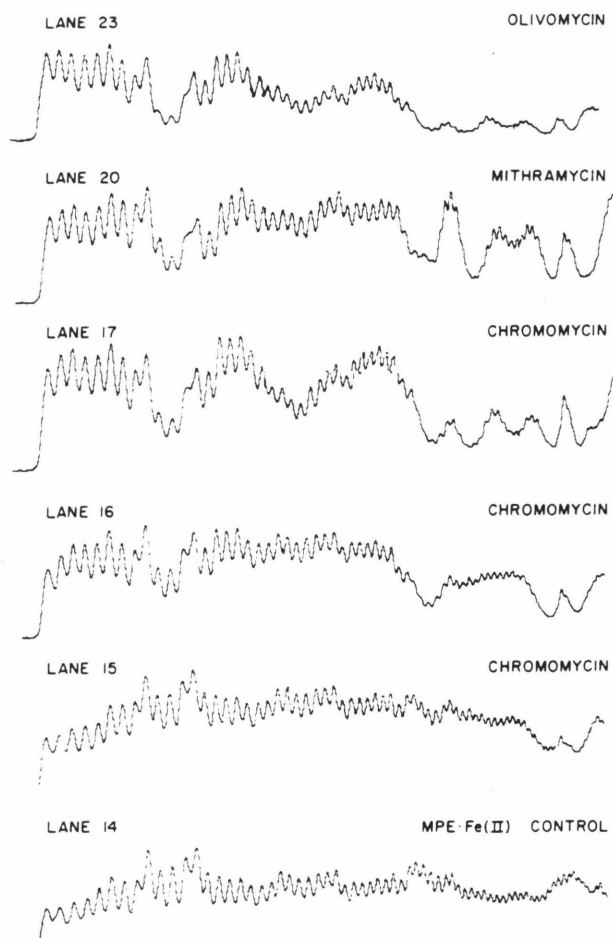


**Figure 15**

Densitometer scans of DNA cleavage inhibition patterns, taken from Van Dyke and Dervan.<sup>8c</sup> Left to right corresponds to the bottom of the gel autoradiogram to the arrow shown in Figure 14. Valleys are drug-protected regions from MPE•Fe(II) cleavage.

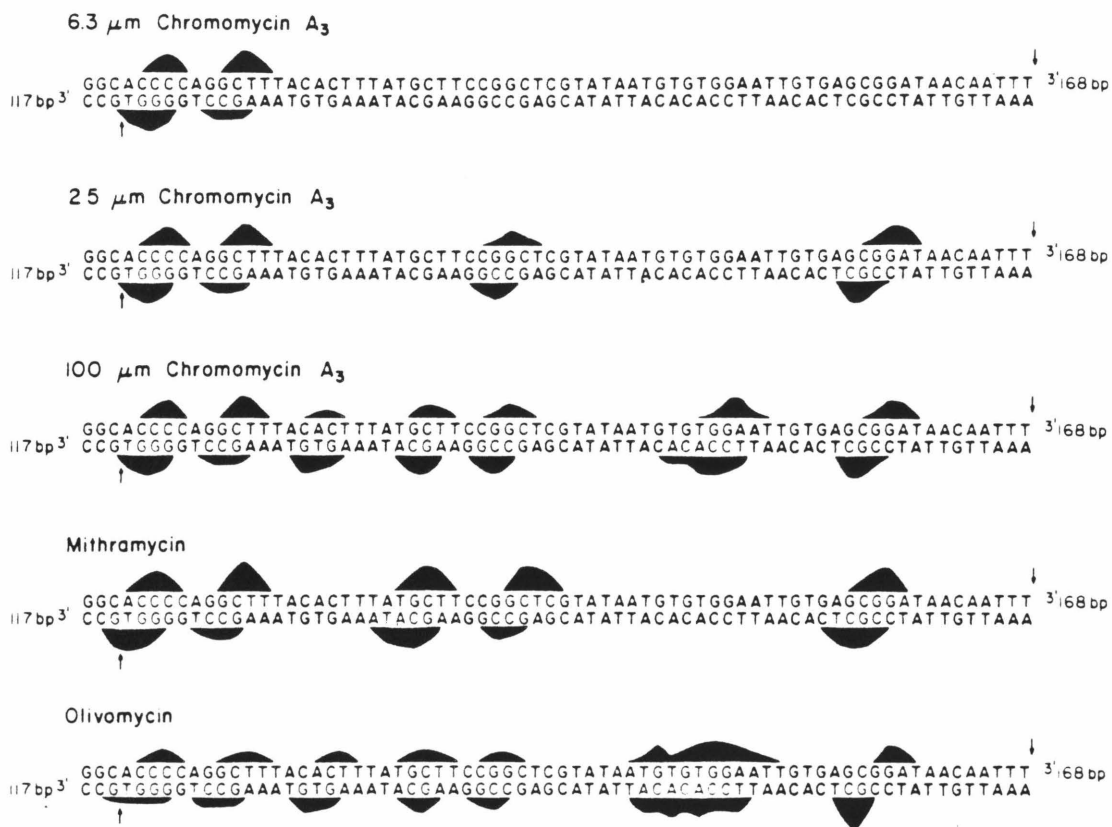


Figure 16

Illustrations of drug-protected regions (black areas) from MPE·Fe(II) cleavage on 70 base pairs of complementary strands of DNA, taken from Van Dyke and Dervan.<sup>8c</sup> Arrows indicate the bottom of the gel autoradiogram for each strand (Figure 14).

Since the binding constant of MPE·Fe(II) to DNA has been estimated, the footprinting technique can be used to quantitate the binding of small molecules to particular sites on native DNA. In order to do this, certain assumptions must be made: 1) we assume that MPE·Fe(II) binds to all sites on DNA equally, with a similar affinity as MPE·Ni(II) ( $1.5 \times 10^5 \text{ M}^{-1}$ ) or MPE·Mg(II) ( $1.2 \times 10^5 \text{ M}^{-1}$ ); 2) we assume that in the presence of an inhibiting drug, MPE binds to a particular site in a competitive binding mode based on the binding constants of MPE and the inhibiting drug to that site; and 3) the decreased concentration of MPE·Fe(II) on a particular site (due to the competition with the inhibiting drug) is directly related to the decrease in cleavage (footprint) at that site. For the competitive binding of two different dyes,  $D_1$  and  $D_2$ , at the same sites on a nucleic acid with binding constants,  $K_1$  and  $K_2$ , the following equation applies:<sup>65c</sup>

$$\frac{r_1}{D_1} = \frac{K_1}{(1 + K_2 D_2)} (n - r_1) \quad (1)$$

where  $r_1$  is the bound dye ( $D_1$ ) per base pair and  $n$  is the number of binding sites. This is a variation of the well known Scatchard equation:<sup>70</sup>

$$r/D = K(n-r) \quad (2)$$

where  $D$  is the concentration of free drug. Although these equations do not strictly apply to MPE·Fe(II) because of nearest neighbor exclusion they are reasonably close approximations.

We will use MPE·Fe(II) as  $D_1$  and the inhibiting drug as  $D_2$ . From assumption number 3, we can state that:

$$I_f/I = r_1/r$$

where  $I_f$  is the intensity of the band (extent of cleavage) within a

footprint and  $I$  is the intensity of the band outside the footprint (extent of cleavage when MPE has nothing to compete with);  $r_1$  is the bound MPE·Fe(II) when it has to compete for a site (defined by eq. 1) and  $r$  is the bound MPE·Fe(II) when it does not have to compete (defined by eq. 2). Solving for  $r_1/r$  and rearranging terms, we arrive at the following equation:

$$\frac{r_1}{r} = \frac{I_f}{I} = \frac{1 + K_1 D_1}{1 + K_1 D_1 + K_2 D_2}$$

An example of how this equation works when evaluating footprints follows. Since we are discussing the competition for a particular site, and there are many sites, we may assume that the concentrations of free drug ( $D_1$  and  $D_2$ ) are equal to the concentrations of drug added to the reaction. In the footprinting gel shown in Figure 14, the concentration of inhibiting drug is  $2.5 \times 10^{-5}$  M (in lanes 4,7,10,16,19 and 22) and the concentration of MPE·Fe(II) is  $10^{-5}$  M. The  $I_f/I$  ratio is  $\leq 0.2$  for most of the footprints in these lanes. Using a value of  $1 \times 10^5$  for  $K_1$ , we calculate a minimum value of  $3.2 \times 10^5$  for  $K_2$  to these sites. Now in lanes 3,6,9,15,18 and 21 in Figure 14, where the inhibiting drug concentration is only  $6.3 \times 10^{-6}$  M, there are no intense footprints. This is consistent with the calculated  $I_f/I$  ratio of 0.5 (using  $K_2 = 3.2 \times 10^5$ ). Finally, raising the concentration of inhibiting drug to  $10^{-4}$  M (as in lanes 5,8,11,17,20, and 23) lowers the  $I_f/I$  ratio to 0.06, giving rise to intense footprints.

MPE·Fe(II) footprinting is a rapid technique for assaying hundreds of potential DNA binding sites for antibiotics on one gel. This direct method should prove useful for identifying the relative affinities of multiple binding sites of other small molecules on the

native nucleic acid template which will be necessary for any understanding of the molecular basis of drug action for DNA binding molecules.

**Cleavage of Chromatin with MPE·Fe(II).** Chromatin is the complex of DNA and protein in the nucleus of cells. It consists of basic structural subunits called nucleosomes, which contain 200 base pairs of DNA and an octamer of histone proteins. It has been pertinent to ask whether or not specific nucleosome positioning on the eukaryotic genome is a functional requirement. Numerous studies arguing for a specific, or, conversely, for a random distribution of nucleosomes have been reported, and these have been reviewed.<sup>102</sup> Many of these experiments have utilized micrococcal nuclease for the generation of nucleosomal arrays. The DNA is purified subsequent to nuclear digestion and the cleavage sites are mapped by reference to well-characterized restriction sites. Unfortunately, micrococcal nuclease has a marked sequence preference and introduces cleavages into purified DNA at quite specific and reproducible positions.<sup>103</sup> In some cases these occur at exactly the same sites in chromatin, leading to uncertainty concerning which cleavages are chromatin specific and which are micrococcal nuclease specific.

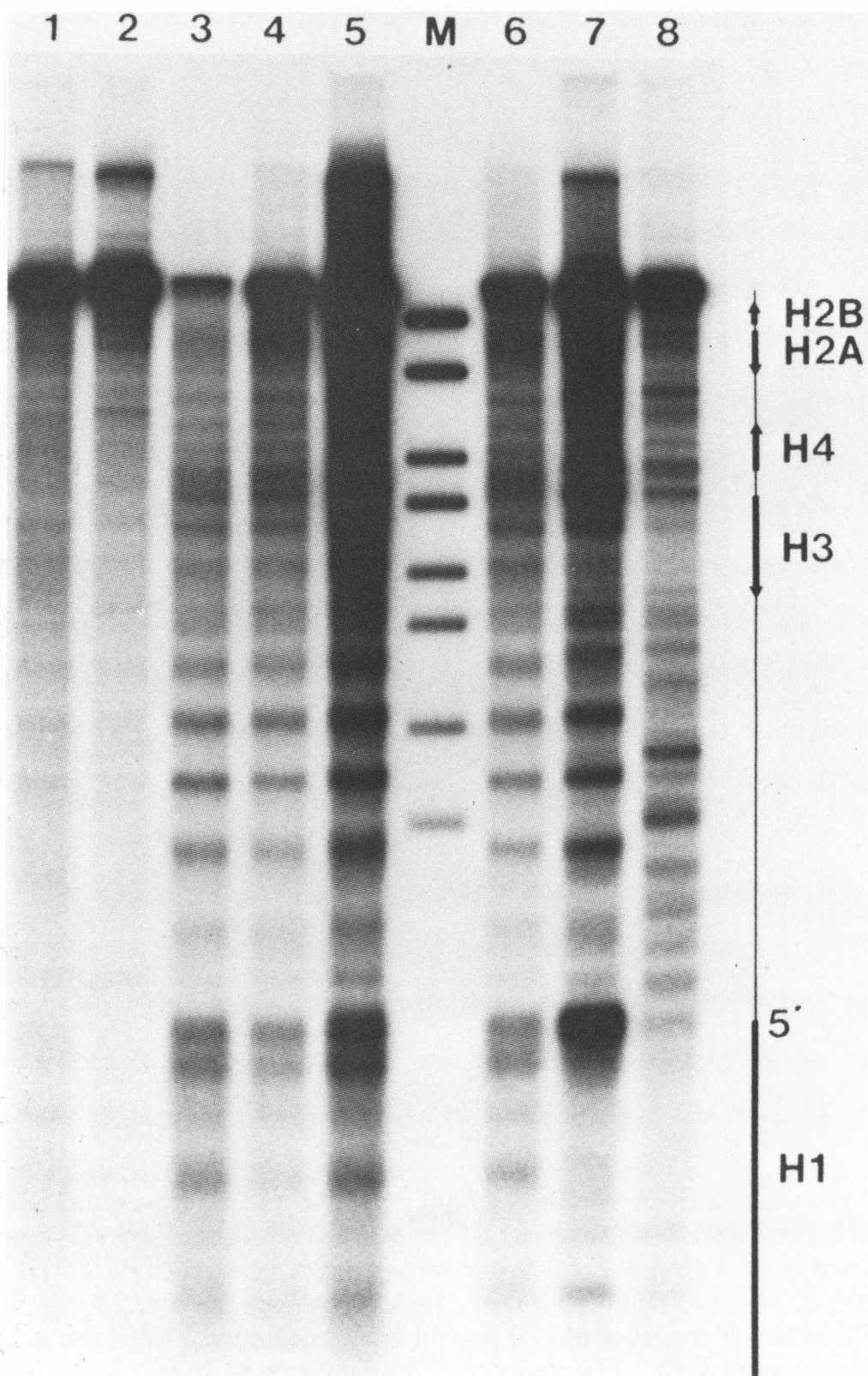
MPE·Fe(II) cleaves DNA with low sequence specificity, and will efficiently introduce a regular series of single-strand (and some double-strand) scissions in chromatin DNA.<sup>104</sup> The nucleosomal products generated are similar in size to those from micrococcal nuclease digestion and appear to be due to highly preferential cleavage in linker DNA. An example of chromatin structure analysis using MPE·Fe(II) is

**Figure 17**

A comparison of MPE·Fe(II) (lanes 1-6) and micrococcal nuclease (lanes 7 and 8) digestion of chromatin (lanes 3-7) and purified DNA (lanes 1,2, and 8).<sup>104</sup> Chromatin samples in lanes 3,4, and 5 were treated with S1 nuclease subsequent to MPE·Fe(II) cleavage.

- Lane 1)  $10^{-5}$  M MPE·Fe(II), 0.5 mM H<sub>2</sub>O<sub>2</sub>, 1 mM DTT, 4 min.  
2) Same as lane 1, 1 min.  
3)  $5 \times 10^{-6}$  M MPE·Fe(II), 0.5 mM H<sub>2</sub>O<sub>2</sub>, 5 min.  
4)  $5 \times 10^{-6}$  M MPE·Fe(II), 10 min.  
5)  $2 \times 10^{-5}$  M MPE·Fe(II), 0.5 mM H<sub>2</sub>O<sub>2</sub>, 1 mM EDTA,  
0.1 mM EGTA, 7.5 min.  
6)  $5 \times 10^{-6}$  M MPE·Fe(II), 0.5 mM H<sub>2</sub>O<sub>2</sub>, 5 min.  
7) 8.8 u/ml micrococcal nuclease, 3 min.  
8) 12 u/ml micrococcal nuclease, 1 min.

All DNA samples were completely digested with Bgl II, and 4 µg samples were subjected to electrophoresis on a 1.6% agarose gel, blotted to nitrocellulose, and hybridized to the small Bgl II/Bam HI fragment of B5, all as described.<sup>104</sup> M, pBR-322 size markers.



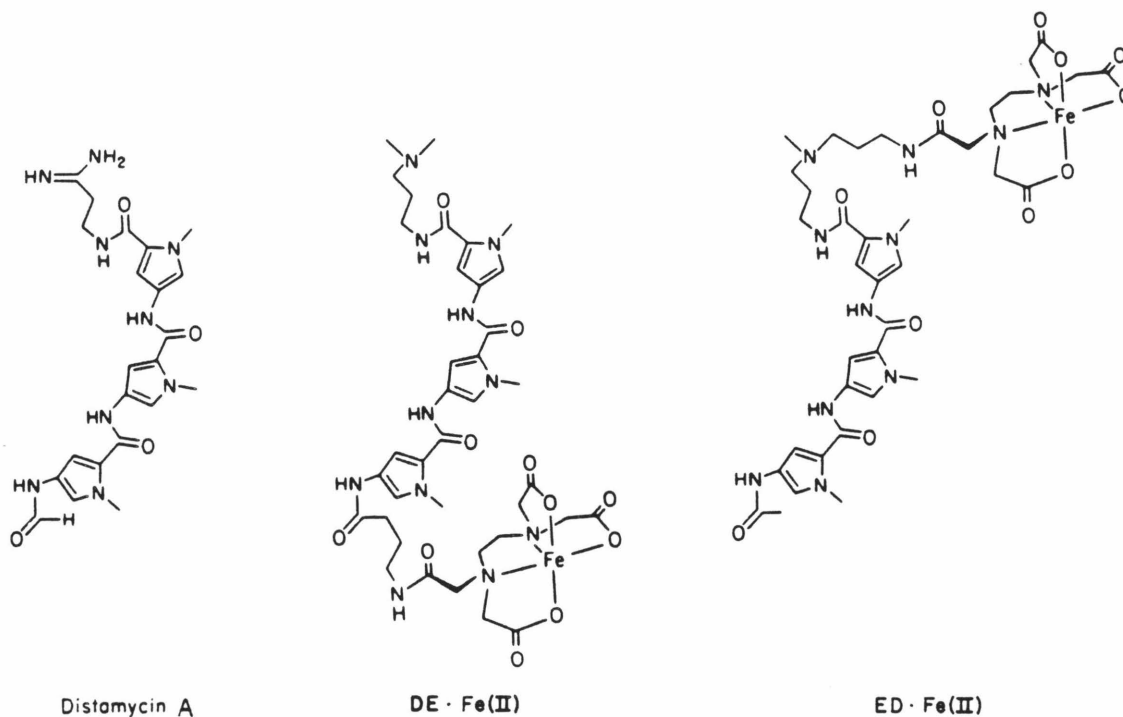
illustrated in Figure 17.

The histone gene sequences of Drosophila melanogaster chromatin were subjected to MPE·Fe(II) or micrococcal nuclease digestion, followed by cleavage with the restriction enzyme Bgl II and analysis by gel electrophoresis. The indirect labeling technique<sup>105</sup> using a probe from within the H1 gene allows the sites of cleavage to be mapped (mapping is shown from the Bgl II site; Figure 17). The data demonstrate an identical pattern of cleavage sites at approximately 190 bp intervals for chromatin in the H1-H3 spacer for both MPE·Fe(II) and micrococcal nuclease. In addition, MPE·Fe(II) responds to some features of the specific chromatin structure that are probably not related in a direct way to nucleosome placement - e.g., the hypersensitive sites at the 5' ends of the genes, previously detected with DNase I.<sup>106</sup> Finally, there are two regularly spaced (155-bp) sites in the H1 gene immediately distal to the 5' hypersensitive region, which may represent a compact nucleosome spacing or may be a manifestation of some other form of protein-DNA interactions.

The comparison between the protein-free DNA controls for the two reagents (Figure 17; lanes 1,2, and 8) reveals some interesting features. Both reagents exhibit specific patterns, but MPE·Fe(II) has much less distinct sequence preferences than micrococcal nuclease. In particular, in regions other than in the H1-H3 spacer, the nuclease cleavage sites are similar for chromatin and protein-free DNA, both in intensity and location. This is not true for MPE·Fe(II) cleavage sites.

It seems apparent that MPE·Fe(II) will be a very useful reagent for analysis of chromatin structure. In addition to the genetic locus described above, it has been used to probe the 1.688 g/cm<sup>3</sup> complex satellite and 5S ribosomal RNA gene sequences of Drosophila melanogaster chromatin.<sup>104</sup> At the present level of resolution MPE·Fe(II) appears to provide more definitive data than micrococcal nuclease on nucleosome distributions across the loci examined. Other features of the protein-DNA interaction are also revealed.

**DNA Affinity Cleaving.**<sup>111</sup> The cleavage efficiency of MPE·Fe(II) demonstrates that attachment of EDTA·Fe(II) to a DNA binding molecule creates a DNA cleaving molecule. The relative sequence neutrality of MPE·Fe(II) cleavage is most likely a reflection of the binding characteristics of methidium. These facts suggest that a sequence specific DNA cleaving molecule could be constructed by attachment of EDTA·Fe(II) to a sequence specific DNA binding molecule. Schultz, Taylor, and Dervan<sup>107,108</sup> confirmed the validity of this concept by synthesizing distamycin-EDTA·Fe(II) (DE·Fe(II)) and EDTA-distamycin·Fe(II) (ED·Fe(II)).



The antibiotic distamycin is an oligopeptide containing three N-methylpyrrolecarboxamides that binds in the minor groove of double helical DNA with a strong preference for A+T rich regions<sup>8a,b,d,109</sup> and a binding site size of five base pairs.<sup>108</sup> The sequence specificity of distamycin binding presumably results from hydrogen bonding between the amide N-H's of the antibiotic and the O(2) of thymine and the N(3) of adenine.<sup>110</sup> DE·Fe(II) and ED·Fe(II) are N-methylpyrrole tripeptides with EDTA attached to the amino and carboxy terminus, respectively. In the presence of O<sub>2</sub> and DTT, DE·Fe(II) and ED·Fe(II) cleave DNA sequence

specifically.<sup>107,108</sup>

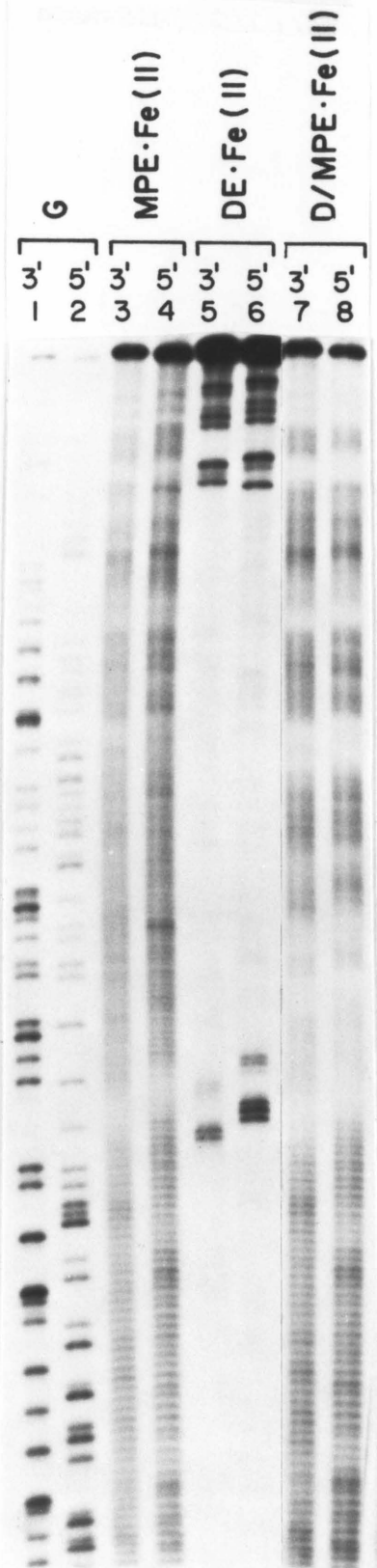
A high resolution gel autoradiogram demonstrating the sequence specificity of DE•Fe(II) is shown in Figure 18.<sup>111</sup> An end-labeled restriction fragment (381 bp) was allowed to react with MPE•Fe(II), DE•Fe(II), or for comparison, with distamycin and MPE•Fe(II) to generate footprints of distamycin binding sites. MPE•Fe(II) shows a relatively uniform pattern, with a slight bias against regions rich in AT base pairs. In contrast, the DNA cleavage patterns generated by DE•Fe(II) are confined to highly localized sites. They cover four base pairs and occur on both sides of a five base pair A+T binding site. MPE•Fe(II) footprinting of distamycin on this same DNA fragment reveals two asymmetric footprints, one of which is in the same location as the DE•Fe(II) cleavage site.

The appearance of common binding location and binding site sizes suggests that attachment of EDTA•Fe(II) to distamycin or the presence of bound MPE•Fe(II) for footprinting does not greatly alter the N-methylpyrrolecarboxamide binding specificity at those sites. However, MPE•Fe(II) footprinting does reveal additional binding sites for distamycin than affinity cleaving at similar binding densities. This result suggests that EDTA•Fe(II) attachment is not without influence; it may change the overall affinities of peptides for different sites on DNA due to increased steric or electrostatic interactions.

A histogram corresponding to the DE•Fe(II) cleavage pattern is shown in Figure 19. Arrows represent the extent of cleavage resulting from removal of the indicated base. There are three to five strand scissions flanking the DE•Fe(II) binding site. This may reflect

**Figure 18**

Autoradiogram of high resolution denaturing gel using a 381 bp DNA fragment, taken from Schultz and Dervan.<sup>111</sup> Lanes 1,3,5, and 7 are 3' end labeled DNA fragments; lanes 2,4,6, and 8 are 5' end labeled DNA fragments. Lanes 1,2: Maxam-Gilbert G reactions; Lanes 3,4: MPE·Fe(II),  $5 \times 10^{-6}$  M; Lanes 5,6: DE·Fe(II),  $1 \times 10^{-5}$  M; Lanes 7,8: distamycin  $1 \times 10^{-5}$  M, MPE·Fe(II)  $5 \times 10^{-6}$  M. All reactions are  $>10000$  cpm [ $^{32}$ P] DNA, made up to  $10^{-4}$  M bp DNA with sonicated calf thymus DNA in 40 mM Tris base, pH 7.9, 5 mM NaOAc; 1 mM DTT.



DE·Fe(II) 381



D/MPE·Fe(II) 381



Figure 19

Histograms of the DE·Fe(II) cleavage pattern and the distamycin footprinting pattern on the 381 bp DNA fragment, taken from Schultz and Dervan, 111

multiple overlapping binding modes of the oligopeptide, such as sliding one to two base pairs within the site. Data in the literature suggest that the formation of a long-lived distamycin-DNA complex follows the association and dissociation of short-lived low specificity complexes. In these experiments, the DE•Fe(II) was equilibrated with the DNA for one hr at 37°C prior to initiating cleavage with DTT. Therefore, it is likely that the drug-DNA complex which causes cleavage is stable and long-lived. If so, then the multiple strand scissions reflect the generation of a diffusible hydroxyl radical at some average position of the EDTA•Fe(II) complex. These radicals could diffuse as far as two base pairs in either direction before reacting with either a deoxyribose moiety, a component of the reaction mixture, or a drug molecule. The DNA termini produced by DE•Fe(II), MPE•Fe(II), or EDTA•Fe(II) cleavage are consistent with this interpretation, and will be discussed in more detail in the section on products of the cleavage reaction.

**Cleavage of RNA.** Ethidium bromide is capable of binding to double-helical RNA,<sup>112</sup> which raises the question of whether MPE•Fe(II) can cleave RNA. The antibiotic bleomycin is incapable of this reaction,<sup>113</sup> and in fact only degrades the DNA strand of an RNA-DNA hybrid.<sup>114</sup> This indicates that the secondary structural configuration is not responsible for the DNA-specificity of bleomycin. Rather, it seems that the deoxyribose moiety is a necessity for bleomycin cleavage.

We first investigated the ability of exogenous RNA to inhibit the DNA cleaving reaction by MPE•Fe(II).

Table XIII

RNA Added	% Form			S
	I	II	III	
None	0	95	5	5.2
10 <sup>-3</sup> M tRNA-Glu	0	95	5	5.2
10 <sup>-3</sup> M polyA·polyU	32	68	0	1.14
10 <sup>-3</sup> M 5S rRNA	0	98	2	3.3

Form I pBR-322 (10<sup>-5</sup> M bp), MPE (10<sup>-7</sup> M), Fe(II) (10<sup>-7</sup> M), RNA, DIT (10<sup>-3</sup> M) and buffer (40 mM Tris·HCl, 5 mM NaOAc, pH 7.8) were allowed to react at 37°C for 60 mins.

Of these three RNA's tested, only the synthetic homopolymer, polyA·polyU, was effective at inhibition. This indicates that polyA·polyU is capable of binding MPE·Fe(II), thereby diluting the effective drug concentration available for binding to and cleaving the plasmid DNA. The other types of RNA's, transfer RNA and 5S ribosomal RNA, did not appreciably inhibit the cleavage reaction indicating that they bind MPE·Fe(II) poorly.

The ability of MPE·Fe(II) to cleave polyA·polyU was tested using gel electrophoresis. PolyA RNA covering a narrow size range (200-240 bp) was annealed to high molecular weight polyU RNA, subjected to MPE·Fe(II)/DIT cleavage, and analyzed by 8% polyacrylamide denaturing gel electrophoresis. Both the starting material and reaction product streaked out on the gel. However, the MPE·Fe(II)-reacted RNA was of noticeably smaller molecular weight, moving further down the gel. The

drug:nucleotide ratio used was 1:25. Lowering the drug binding density to 1:250 resulted in very little cleavage. Single-stranded polyA RNA was also cleaved by MPE·Fe(II), with a slightly lower efficiency.

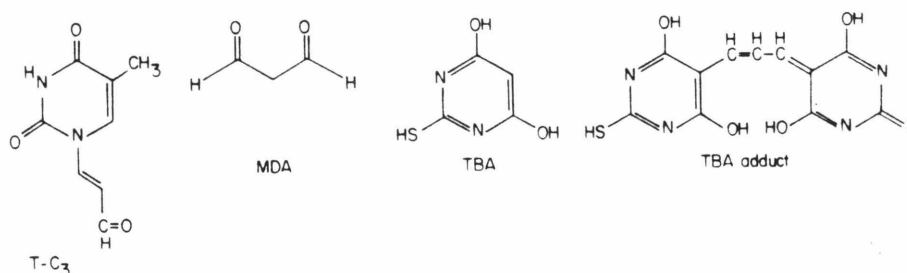
These experiments represent an initial study simply to determine if RNA is a substrate for MPE·Fe(II). More detailed experiments using end-labeled RNA would reveal additional characteristics of this cleavage reaction, including any sequence, conformational, or structural specificity. It is conceivable that MPE·Fe(II) could be used as a probe for RNA structure in various applications such as ribosomes, tRNA, and RNA splicing. In addition, the interaction between proteins and RNA could be probed in footprinting type experiments. Ribonucleases such as RNase H, RNase III, and RNase T1 have been used as probes for various structural interactions involving RNA, and MPE·Fe(II) could conceivably be added to this arsenal of molecular probes.

#### **Products of the Cleavage Reaction of MPE·Fe(II) with DNA**

**Base Release.** The production of UV absorbing, non-polymeric products from the cleavage reaction of DNA by MPE·Fe(II) was examined by using reverse-phase HPLC. Four prominent peaks are evident in the chromatogram (Figure 20a). The peaks which appear near the void volume are due to small oligonucleotides which were not removed by ethanol precipitation. The four compounds were identified as cytosine, guanine, thymine, and adenine (in order of elution) based on their retention times relative to authentic samples. These products were collected off of the HPLC and their identity was confirmed by co-migration with authentic standards on thin layer chromatography.

For comparison, a bleomycin·Fe(II) digest of DNA was analyzed in

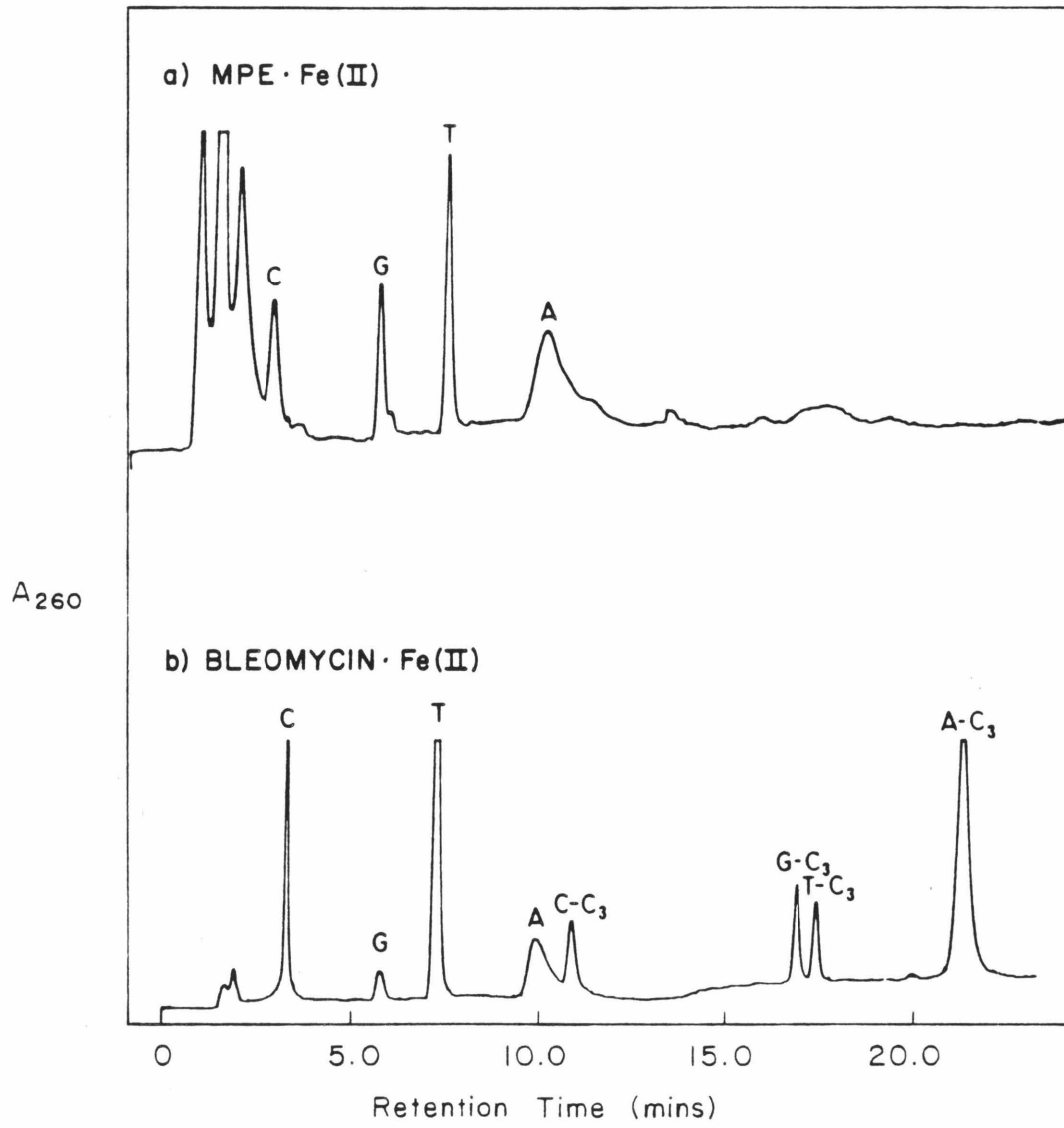
the same way (Figure 20b). Eight UV absorbing products were resolved, analogous to the eight products previously resolved by thin layer chromatography.<sup>49</sup> Compounds 1-4 were identified as the four nucleotide bases as before. Compounds 5-8 were collected off of the HPLC and each was reacted with thiobarbituric acid (TBA) to form a chromophore which displays an absorbance maximum of 532 nm. Thin layer chromatography analysis indicated that these compounds are the N-propenal derivatives of the four nucleotide bases as previously reported.<sup>48,49</sup>



The addition of DTT has been shown to enhance the cleavage efficiency MPE•Fe(II). Product analysis of an MPE•Fe(II)/DTT reaction showed that the same four bases were released, but in higher yield. No other products were seen, with the exception of a peak at 14 min which was shown by co-injection to be the cyclic disulfide product of DTT oxidation. Examination of a bleomycin•Fe(II)/DTT reaction revealed an increase in the yield of free bases, but an absence of base

**Figure 20**

HPLC analysis of cleavage reactions. Reaction mixtures contained 950  $\mu\text{M}$  (bp) sonicated calf thymus DNA, 50  $\mu\text{M}$  (bp) bacteriophage  $\lambda$  [ $^3\text{H}$ ] DNA and (a) 500  $\mu\text{M}$  MPE $\cdot\text{Fe(II)}$  or (b) 500  $\mu\text{M}$  bleomycin $\cdot\text{Fe(II)}$ . After 30 min at 22 $^{\circ}\text{C}$  the DNA was ethanol precipitated and the supernatant chromatographed as described in the Experimental Section.



propenals.  $\beta$ -Mercaptoethanol has been shown to react with base propenals<sup>49</sup> and this most likely occurs with DTT as well.

The MPE cleavage reaction can also be activated with Fe(III) and H<sub>2</sub>O<sub>2</sub>. Product analysis of an MPE·Fe(III)/H<sub>2</sub>O<sub>2</sub> reaction revealed that the four bases are released, in addition to five new products which were present in smaller amounts. Treatment of a 5 x 10<sup>-7</sup> M standard solution of the four nucleotide bases with MPE·Fe(III)/H<sub>2</sub>O<sub>2</sub> gave the same five products. Therefore, activation of MPE with Fe(III)/H<sub>2</sub>O<sub>2</sub> results in base release from DNA and subsequent partial degradation of the free bases.

**Stoichiometry of Base Release.** The HPLC analysis allowed precise quantitation of the amounts of the four bases released. The number of single strand scissions was simultaneously assayed by measuring the decrease in the single strand molecular weight of the DNA. After cleavage by MPE·Fe(II) or bleomycin·Fe(II), the DNA was ethanol precipitated, denatured with glyoxal and DMSO, and electrophoresed on 1.2% agarose gels next to oligonucleotide size standards. These denaturation conditions were shown not to introduce any additional strand scissions.

Figure 21 shows the single-stranded molecular weight distribution of bacteriophage  $\lambda$ [<sup>3</sup>H]DNA after cleavage with MPE·Fe(II). The curve matches the theoretical molecular weight distribution generated from the equations of Freifelder and Davison for the random degradation of a polymer.<sup>115</sup> These data were used to determine the weight average molecular weight of the degraded DNA, which leads to the mean number of single-strand scissions per strand (see Experimental for

equations).

The total number of nucleotide bases released from DNA by MPE·Fe(II) was shown to be stoichiometric with single strand scission (Table XIV). The adenine:thymine and guanine:cytosine ratios were approximately one to one. Since MPE has been shown to cleave DNA with low sequence specificity<sup>8</sup> there should be no preferential release of any given base. The A:T:G:C ratio found agrees favorably with literature values for calf thymus DNA.<sup>116</sup>

When bleomycin·Fe(II) reacts with DNA, both free bases and base propenals are released. The amounts of the four bases released are shown in Table XIV. As reported previously, thymine accounts for about half of the free bases.<sup>117</sup> The quantity of base propenal was simultaneously assayed by means of an intensely colored product formed after reaction with TBA. We have confirmed that bleomycin-induced DNA strand scission is stoichiometric with base propenal production,<sup>50b</sup> using our assay for strand scission and the TBA assay for base propenal (Table XIV).

The stoichiometry of base release by MPE·Fe(II) shows that thymine, adenine, cytosine, and guanine were produced in amounts which indicate that each strand scission event leads to the release of free base. Since these bases were not degraded under the normal cleavage conditions, we can conclude that strand scission results from attack on the deoxyribose ring and not on the base. Furthermore, the equivalent production of all four bases in contrast to the bleomycin reaction, supports the relatively low base composition specificity of MPE·Fe(II) as a cleaving reagent, previously determined using end-labeled DNA and

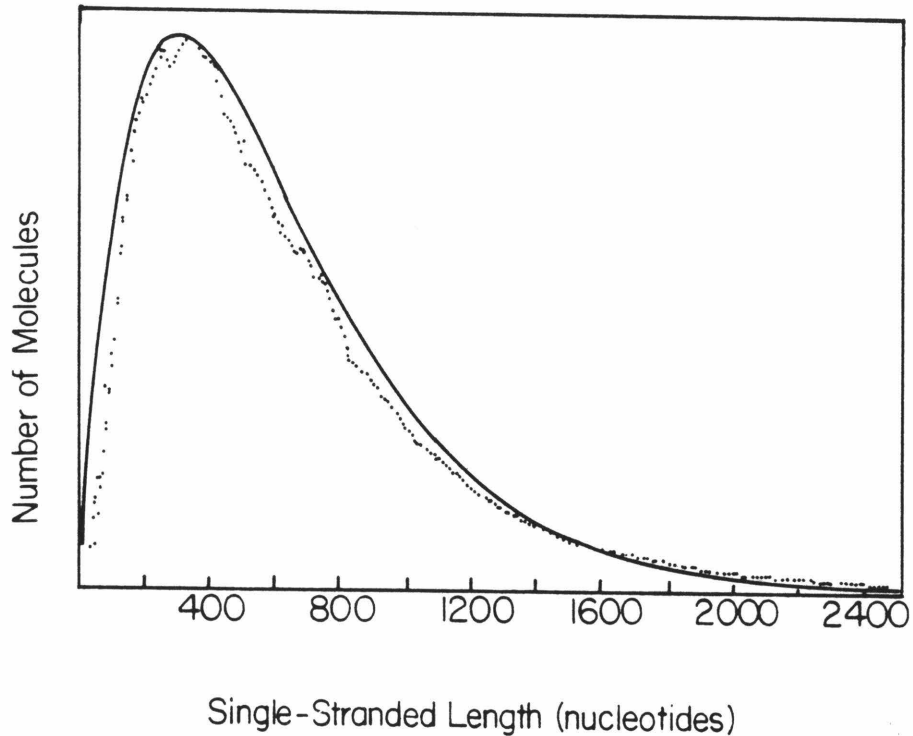


**Figure 21**

The reaction mixture from Figure 20a was ethanol precipitated; the DNA was denatured and electrophoresed on 1.2% agarose next to molecular weight size standards. The gel was cut into 1 mm slices, and the radioactivity of each slice was determined. The number of molecules in each slice is plotted against the molecular weight represented by that slice (determined by comparing its migration distance to the molecular weight standards). The experimental molecular weight distribution (.....) is compared to the theoretical molecular weight distribution (—) assuming a random degradation process.<sup>115</sup>

Conditions	$\mu\text{M}$ free bases					$\mu\text{M}$ single strand cleavage	$\frac{\text{A}+\text{T}}{\text{G}+\text{C}}$
	C	G	T	A	Total		
500 $\mu\text{M}$ MPE·Fe(II)	0.64	0.68	0.98	1.10	3.40	3.20	1.58
500 $\mu\text{M}$ MPE·Fe(II)	0.77	0.79	1.19	1.31	4.06	4.12	1.60
500 $\mu\text{M}$ BLM·Fe(II)	13.9	3.2	33.6	10.1	60.8	n.d.	2.56
	$\mu\text{M}$ TBA reactive species						
500 $\mu\text{M}$ MPE·Fe(II)	0.40					3.20	
25 $\mu\text{M}$ BLM·Fe(II)	3.18					3.49	

**Table XIV.** Stoichiometry of DNA strand scission, base release, and TBA reactive species. Reaction mixtures were as described in the legend to Figure 20. Aliquots were removed and assayed for TBA reactive species. The remaining mixture was ethanol precipitated and the DNA pellet was analyzed for single strand cleavage as described in the Experimental Section. Quantities of the four bases were determined by HPLC analysis of the supernatant.

sequencing gels.<sup>8</sup>

Although the HPLC analysis has shown that MPE·Fe(II) releases little or no base propenal from DNA, we tested for the presence of TBA reactive species. Since the optical absorbance of MPE overlaps that of the TBA adduct, it was necessary to remove the MPE from the reaction mixture using a cation exchange resin. Controls show that this treatment removes neither base propenals or malondialdehyde. Table XIV illustrates that MPE·Fe(II) treatment of DNA results in a small amount of some species which react with TBA to form the characteristic chromophore.

Since no base propenals were observed, it is likely that the TBA-adduct is a result of malondialdehyde production. Possibly some base propenals were initially formed and subsequently degraded to free bases and malondialdehyde. It has been shown that acidic or basic solutions<sup>48</sup> and thiol compounds<sup>49</sup> are capable of degrading base propenals, but these conditions were not present in the standard reaction. Since we were able to observe base propenals in the bleomycin·Fe(II) reaction, we can rule out the possibility that the work-up employed resulted in their destruction.

Another possibility is that the MPE·Fe(II) itself is responsible for the degradation of base propenals. We tested this by analyzing the products of a bleomycin·Fe(II) reaction for base propenals both in the presence and absence of MPE·Fe(II). The analyses were identical, illustrating that these compounds are stable to MPE·Fe(II). Therefore, we conclude that the reaction mechanism initiated by MPE·Fe(II) leading to cleavage is different than from of bleomycin, although both involve

the deoxyribose. It is not known where the small amount of TBA-reactive material from the MPE·Fe(II) reaction comes from; it is most likely a remnant of deoxyribose fragmentation produced by oxidative reactions. Other fragments of the deoxyribose could remain attached to the polynucleotide chain. In order to examine this possibility, we undertook an investigation of the end groups left on the DNA fragments after MPE·Fe(II) treatment.

**Analysis of Termini Produced by MPE·Fe(II).** Since the electrophoretic mobility of a DNA fragment depends on its size, shape, and charge, the nature of the termini of the fragment can be determined by using high resolution polyacrylamide gel electrophoresis. The presence of a terminal phosphoryl group increases the mobility of a DNA fragment relative to a fragment with a terminal hydroxyl group.<sup>45,118</sup> Similarly, other perturbations such as esterification of the terminal phosphoryl group can be resolved using this technique.

A 279 base pair long 3'-end labeled DNA fragment was treated with MPE·Fe(II) in the presence of DTT and analyzed by denaturing 20% polyacrylamide gel electrophoresis. The mobilities of the resulting DNA fragments were compared to those produced by the reaction of bleomycin·Fe(II) on the same DNA fragment, and to those produced by dimethyl sulfate treatment as in the Maxam-Gilbert sequencing protocol (Figure 22). Both bleomycin<sup>119</sup> and dimethyl sulfate<sup>99</sup> are known to produce 5' termini which are phosphorylated. Figure 22 (lanes 1-3) demonstrates that MPE·Fe(II) produces oligonucleotides which co-migrate with those from the bleomycin or dimethyl sulfate reactions, indicating the presence of phosphoryl groups on the 5' termini.

Further evidence for this is obtained by treatment of these oligonucleotides with calf intestinal alkaline phosphatase, which removes 5' phosphoryl groups from DNA substrates.<sup>120</sup> Figure 22 (lane 5) shows that phosphatase treatment of a dimethyl sulfate reaction results in a decrease of the electrophoretic mobility, because of the removal of the negatively charged groups. This effect has been previously demonstrated by Kross et al.<sup>45</sup> Phosphatase treatment of the oligonucleotides from an MPE reaction (Figure 22, lane 4) produces the same shift in electrophoretic mobility, confirming that MPE·Fe(II) cleavage results in 5' phosphoryl groups.

In order to investigate the nature of the 3' termini, a 381 base pair long 5'-end labeled DNA fragment was used. Dimethyl sulfate treatment is known to lead to phosphorylated 3' termini<sup>99</sup> while DNase leads to hydroxylated 3' termini. The bleomycin·Fe(II) reaction produces 3' ends which consist of glycolic acid esterified, though its hydroxyl group, to the phosphate termini.<sup>49</sup> The electrophoretic mobilities of these three types of ends can all be resolved and are illustrated in Figure 23 (lanes 1,4, and 5).

The reaction of MPE·Fe(II) with this 5' end labeled fragment resulted in a set of oligonucleotides which migrated as doublets on the gel (Figure 23, lane 2). Comparison of the mobilities of these fragments with those in lanes 1,4, and 5 reveals that the slower moving band of each doublet co-migrates with fragments produced by dimethyl sulfate reaction, while the faster moving band co-migrates with fragments produced by the bleomycin reaction. This suggests that both 3'-phosphate and 3'-phosphoglycolic acid groups are produced by

MPE•Fe(II) cleavage of DNA.

To verify the presence of 3'-phosphate groups, half of the sample obtained from MPE•Fe(II)/DTT cleavage was subsequently treated with T4 polynucleotide kinase in the absence of ATP or ADP. T4 polynucleotide kinase has been shown to be effective as a 3'-phosphatase under these conditions.<sup>121</sup> Comparison of lanes 2 and 3 in Figure 23 illustrates that one of the bands of each doublet produced by MPE•Fe(II) cleavage disappears upon kinase treatment, and a new band appears. The bands which disappear co-migrate with oligonucleotides produced in the dimethyl sulfate reaction (with 3'-phosphoryl termini) while the new bands which appear co-migrate with oligonucleotides produced in the DNase reaction (with 3'-hydroxyl termini). These results demonstrate that the slower moving band of each doublet is a DNA fragment with a 3'-phosphoryl group.

The faster moving band of each doublet in lane 2 is resistant to T4 polynucleotide kinase. This band appears to co-migrate with fragments produced by bleomycin•Fe(II). The 3'-terminus of the bleomycin-induced scission is also resistant to kinase treatment.<sup>45</sup> These results indicate MPE•Fe(II) scission produces some fragments with phosphoglycolic acid groups at their 3' termini. To verify this, DNA labeled with [<sup>3</sup>H] at the 5'-position was reacted with MPE•Fe(II)/DTT, ethanol precipitated, and then hydrolyzed in 6N HCl for 2 h at 150°C. The residual products were treated with alkaline phosphatase to release radioactive glycolic acid. This was analyzed by cellulose thin layer chromatography and a radioactive product was found which co-migrated with authentic glycolic acid. The product was eluted from the plate and

**Figure 22**

Analysis of 5' termini. The 279 base pair 3'-end labeled DNA fragment ( $\geq 10^4$  cpm) and sonicated calf thymus DNA (total DNA concentration was 100  $\mu$ M) was incubated with: Lane 1, 100  $\mu$ M bleomycin $\cdot$ Fe(II); 2, G reaction; 3, 10  $\mu$ M MPE $\cdot$ Fe(II) and 1 mM DTT; 4, 10  $\mu$ M MPE $\cdot$ Fe(II) and 1 mM DTT followed by calf intestinal alkaline phosphatase treatment; 5, G reaction followed by calf intestinal alkaline phosphatase treatment. The DNA was ethanol precipitated and analyzed by denaturing 20% polyacrylamide gel electrophoresis as described in the Experimental Section.

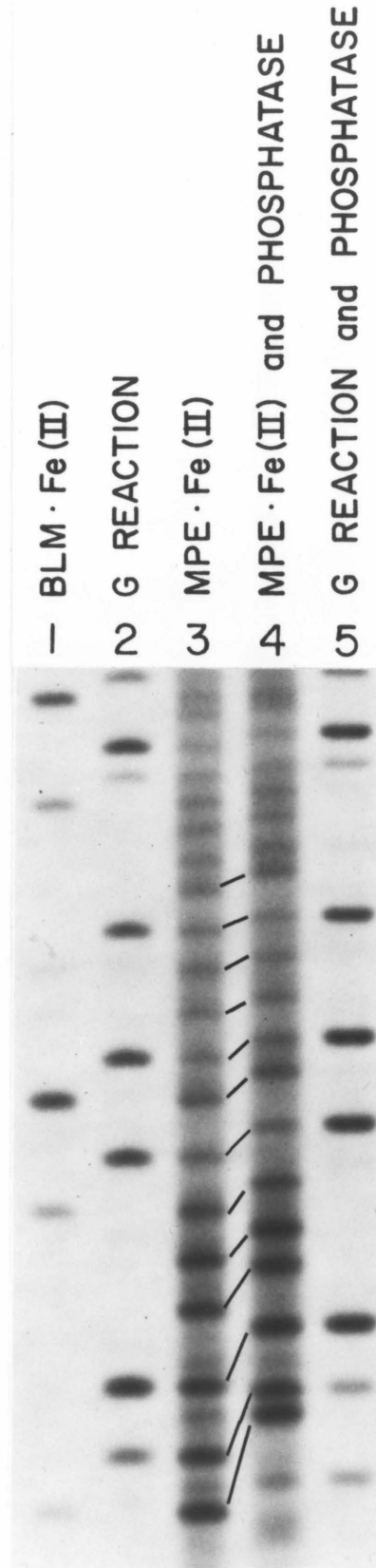


**Figure 23**

Analysis of 3' termini. The 381 base pair 5'-end labeled DNA fragment ( $\geq 10^4$  cpm) and sonicated calf thymus DNA (total DNA concentration was 100  $\mu$ M) was incubated with: Lane 1, G reaction; 2, 10  $\mu$ M MPE $\cdot$ Fe(II) and 1 mM DTT; 3, 10  $\mu$ M MPE $\cdot$ Fe(II) and 1 mM DTT followed by T4 polynucleotide kinase; 4, 100  $\mu$ M bleomycin $\cdot$ Fe(II); 5, DNase I reaction, 1 min.<sup>2</sup> The DNA was ethanol precipitated and analyzed by denaturing 20% polyacrylamide gel electrophoresis as described in the Experimental Section.

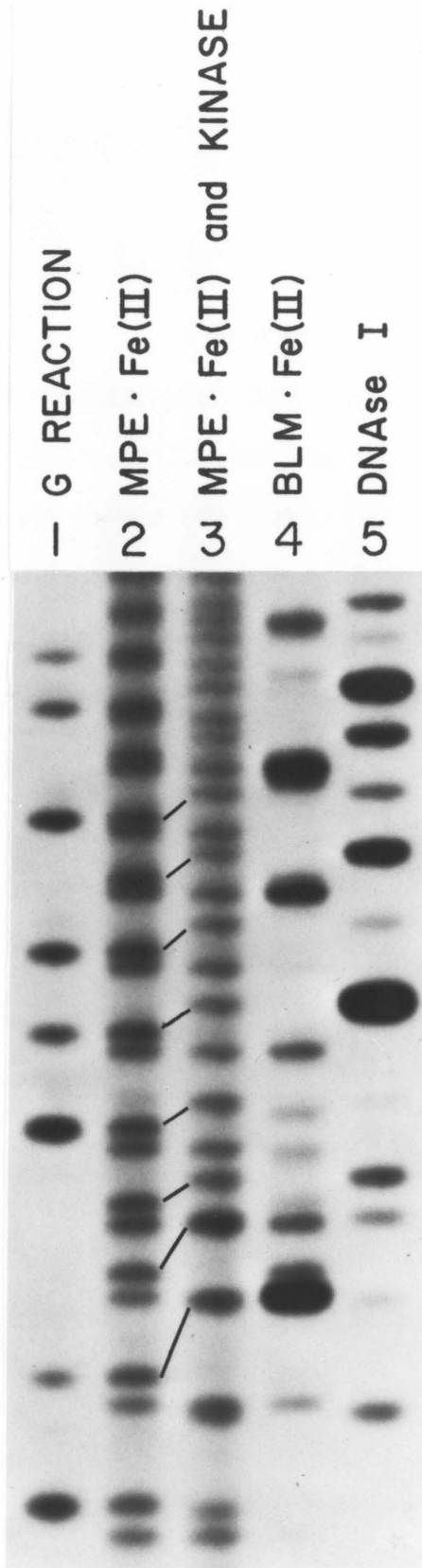
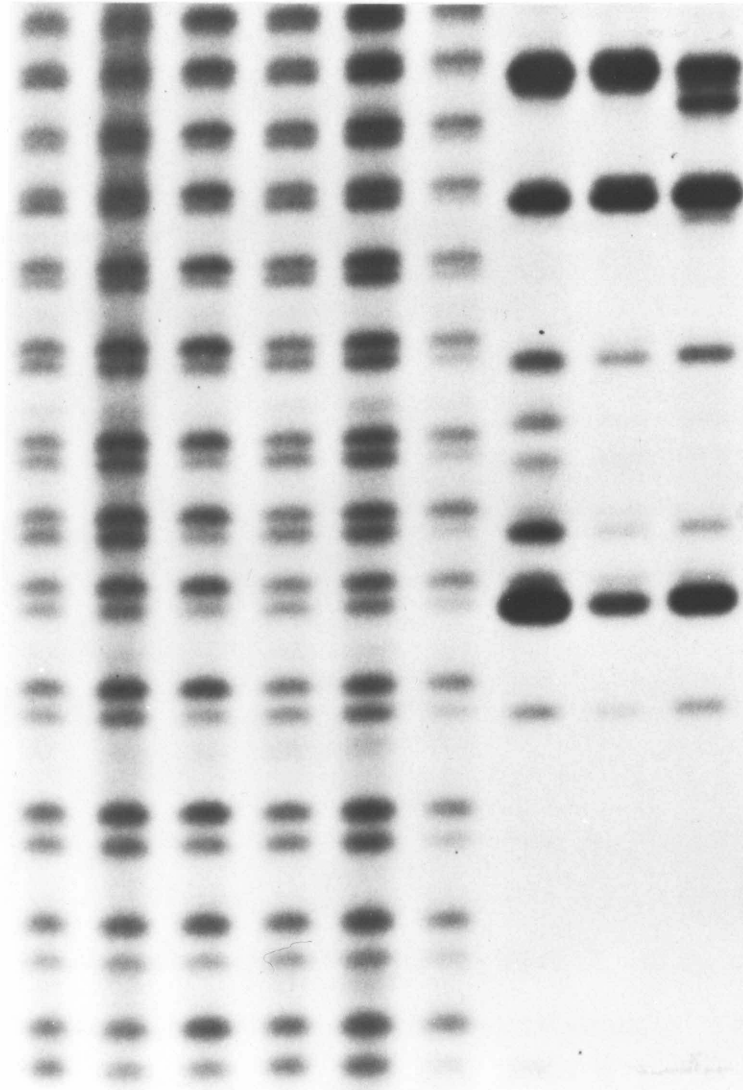


**Figure 24**

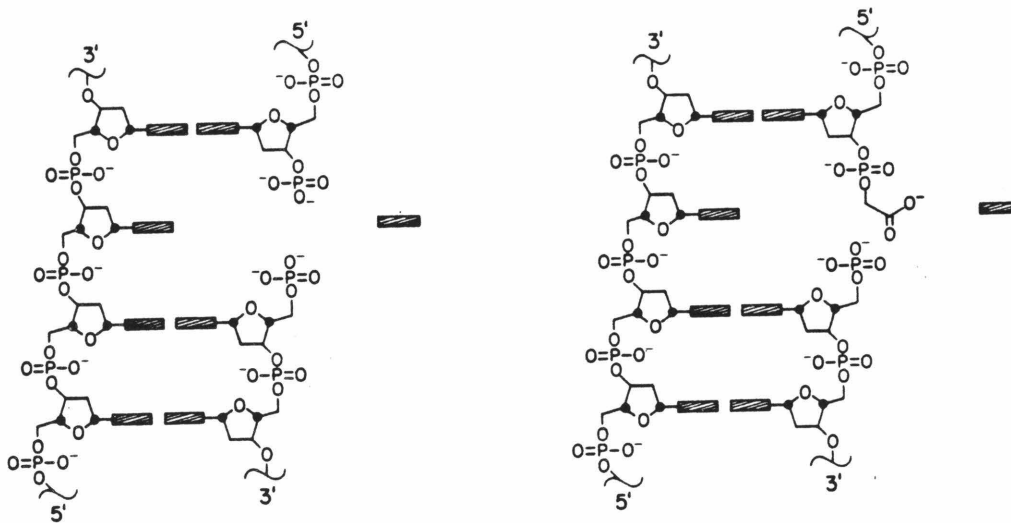
Comparison of 3' termini with different cleaving reagents. The 381 base pair 5'-end labeled DNA fragment ( $\geq 10^4$  cpm) and sonicated calf thymus DNA (total DNA concentration was 100  $\mu$ M) was incubated with: Lane 1, 1 mM MPE·Fe(II); 2, 10  $\mu$ M MPE·Fe(II) and 1 mM DTT; 3, 500  $\mu$ M MPE·Fe(III) and 10 mM H<sub>2</sub>O<sub>2</sub>; 4, 1 mM EDTA·Fe(II); 5, 1 mM EDTA·Fe(II) and 1 mM DTT; 6, 1 mM EDTA·Fe(III) and 10 mM H<sub>2</sub>O<sub>2</sub>; 7, 50  $\mu$ M bleomycin·Fe(II); 8, 5  $\mu$ M bleomycin·Fe(II) and 1 mM DTT; 9, 20  $\mu$ M bleomycin·Fe(III) and 10 mM H<sub>2</sub>O<sub>2</sub>. The DNA was ethanol precipitated and analyzed by denaturing 20% polyacrylamide gel electrophoresis as described in the Experimental Section.

- 1 MPE · Fe(II)
- 2 MPE · Fe(II) and DTT
- 3 MPE · Fe(III) and H<sub>2</sub>O<sub>2</sub>
- 4 EDTA · Fe(II)
- 5 EDTA · Fe(II) and DTT
- 6 EDTA · Fe(III) and H<sub>2</sub>O<sub>2</sub>
- 7 BLM · Fe(II)
- 8 BLM · Fe(II) and DTT
- 9 BLM · Fe(III) and H<sub>2</sub>O<sub>2</sub>



the TMS derivative was prepared with N-trimethylsilylimidazole (Pierce). GC-MS analysis confirmed the identity of glycolic acid. The amount of glycolic acid recovered represented 0.35 equivalents of the free thymine released from the original DNA, which was assayed by HPLC of the reaction mixture supernate.

These results demonstrate that each MPE•Fe(II) induced strand scission produces a 5' phosphoryl group, a mixture of 3' phosphoryl and phosphoglycolic acid groups, and a free base.



MPE can be activated with Fe(II), Fe(II)/DTT, or Fe(III)/H<sub>2</sub>O<sub>2</sub>. Figure 24 (lanes 1-3) illustrates that the two types of 3' termini occur

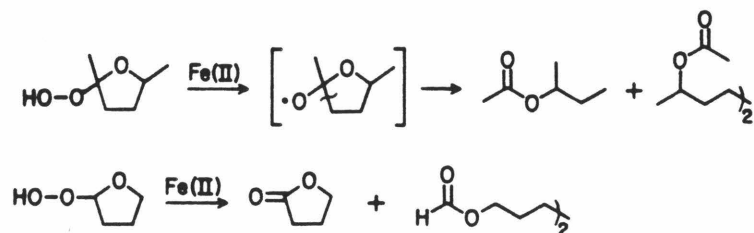
regardless of which of these methods is used. However, the relative amounts of the two bands appear to be different. Densitometry of the autoradiogram confirms that  $\text{MPE}\cdot\text{Fe(III)}/\text{H}_2\text{O}_2$  produces a greater percentage of 3'-phosphoryl groups than either  $\text{MPE}\cdot\text{Fe(II)}$  or  $\text{MPE}\cdot\text{Fe(II)}/\text{DTT}$ . To test the possibility that the phosphoglycolic acid 3'-end was degraded by  $\text{H}_2\text{O}_2$ , a set of oligonucleotides generated by  $\text{MPE}\cdot\text{Fe(II)}$  was purified on cation exchange resin and subsequently treated with  $\text{H}_2\text{O}_2$ . The intensity of the bleomycin-like band did not decrease, indicating that it is stable to  $\text{H}_2\text{O}_2$ .

High concentrations of  $\text{EDTA}\cdot\text{Fe(II)}$  can also produce some strand scissions in DNA. Since the cleavage efficiency is low, larger amounts of  $[^{32}\text{P}]$  DNA were needed to detect the few small oligonucleotides which moved down the gel. Figure 24 (lanes 4-5) illustrates that  $\text{EDTA}\cdot\text{Fe(II)}$ , with or without  $\text{DTT}$ , produces the same kinds of 3'-termini as  $\text{MPE}\cdot\text{Fe(II)}$ . Again, activation with  $\text{Fe(III)}/\text{H}_2\text{O}_2$  (lane 6) gives rise to a greater percentage of 3' phosphoryl groups than 3' phosphoglycolic acid groups.

The presence of two different kinds of 3' ends suggests a dual mechanism for cleavage. Since the same mixture of 3' ends were found when free  $\text{EDTA}\cdot\text{Fe(II)}$  degraded DNA, this duality in mechanisms is not a peculiarity of  $\text{MPE}\cdot\text{Fe(II)}$ . Possibly the active oxidizing species produced by these reagents attacks two different sites on the deoxyribose ring, and subsequent reactions lead to base release and strand scission in both cases. Alternatively, a unique site on the sugar is attacked and the reaction mechanism bifurcates at a point further along in the reaction scheme.

Bleomycin, when activated with Fe(II), Fe(II)/DTT, or Fe(III)/H<sub>2</sub>O<sub>2</sub>, produces only one type of 3' end on DNA, a phosphoglycolic acid (Figure 24, lanes 7-9). This suggests that it initiates strand-scission in a site-directed manner. In contrast, both MPE•Fe(II) and EDTA•Fe(II) generate two cleavage products and most likely initiate strand scission via a diffusible active species. Recently, Haseltine investigated the nature of the 3' termini produced by  $\gamma$ -radiolysis.<sup>60</sup> The gel migration of  $\gamma$ -irradiated DNA fragments were consistent with the presence of a mixture of phosphoryl and phosphoglycolic acid groups on the 3' ends. It is well established that the hydroxyl radical is primarily responsible for DNA damage induced by ionizing radiation.<sup>58,59,122</sup> The similarity of products from MPE•Fe(II) cleavage and hydroxyl radical mediated DNA cleavage further supports the intermediacy of •OH in the MPE•Fe(II) strand-scission reaction.

The first step of the reaction of •OH with deoxyribose is likely to be H-abstraction leading to a sugar radical.<sup>58,59</sup> In oxygenated solutions, this reaction is followed by a diffusion-controlled addition of O<sub>2</sub>.<sup>59b</sup> Schultz has proposed a plausible mechanism of deoxyribose fragmentation (Scheme II) which leads to the experimentally derived products.<sup>123,124</sup> This mechanism is based upon the products obtained from the reaction of 2,5-dimethyl-2-hydroperoxytetrahydrofuran,<sup>124a</sup> and 2-hydroperoxytetrahydrofuran<sup>124b</sup> with aqueous Fe(II).



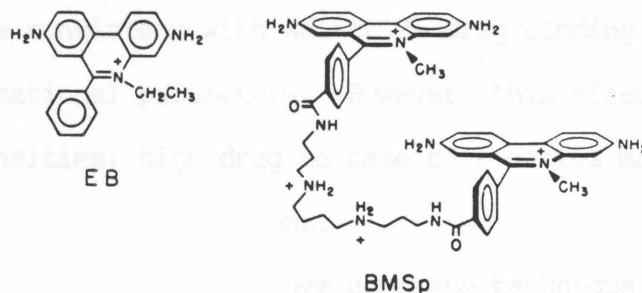


The confirmation of the mechanism outlined in Scheme II awaits identification of the remaining deoxyribose degradation products.

#### Design and Approach to the Synthesis of Bis(methidiumpropyl-EDTA).

The phenomenon of bisintercalation was originally discovered with an antibiotic, echinomycin.<sup>5</sup> Since then a number of dimeric derivatives of classic intercalating drugs have been synthesized, and their DNA binding characteristics have been determined.<sup>125</sup> The DNA affinity of these dimers is substantially higher than the DNA affinity of the respective monomers. In many cases the dimer binds to DNA so tightly that binding constants can only be estimated.

A dimer of methidium using a spermine linker has been synthesized, bis(methidium)spermine (BMSp).<sup>67</sup> The binding



of BMSp to DNA was found to be 1.6 times more energetically favorable than the binding of ethidium bromide (EB). In addition, BMSp was shown to have a substantially higher conformational specificity than the monomer. From the work of Bresloff and Crothers,<sup>126</sup> it is known that the binding of EB to the RNA-DNA hybrid rA·dT is favored over the

DNA-DNA duplex dA·dT by a factor of 100. Becker and Dervan found that this 100-fold specificity exhibited by EB increases to 1440 for BMSp.<sup>127</sup>

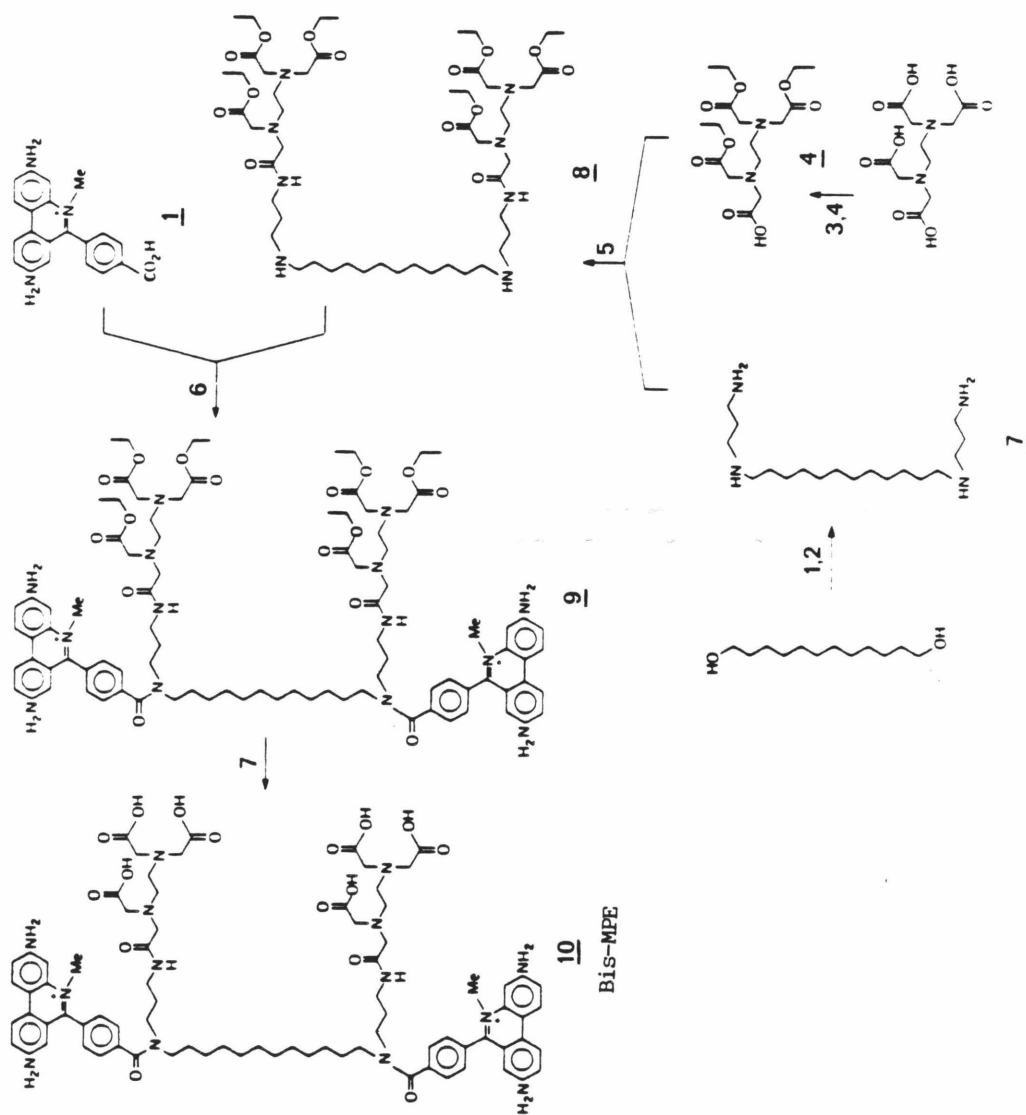
Further evidence for specific recognition of DNA binding sites by BMSp was found by Ikeda.<sup>128</sup> The dimer selectively inhibited restriction sites on heterogeneous DNA (pBR-322 plasmid) while the monomer, EB showed no selective action in competition with any of the restriction enzymes used. It is probable that this demonstrates the enhanced selectivity of a dimer (BMSp) over a monomer (EB).

Alternatively, both drugs may bind selectively, but only BMSp competes effectively with the restriction enzyme due to its higher binding affinity.

Yielding and coworkers<sup>100</sup> have investigated the selective inhibition of restriction sites using the ethidium analog, monoazido ethidium. This molecule covalently binds to DNA upon photoactivation. Their findings are consistent with selective drug binding dictated by long range conformational parameters. However, this effect only occurs at low binding densities; high drug to base pair ratios mask the consequences of specific interactions.

The experiment described above uses the technique of photoaffinity labeling to detect the locations of binding sites. We have seen that the attachment of EDTA to a DNA binding molecule allows the use of affinity cleaving to determine the locations of binding sites. Therefore, the attachment of EDTA to a dimer of methidium would create an efficient DNA cleaving molecule potentially capable of selective recognition of DNA.

Scheme III



The target molecule and its proposed synthesis is shown in Scheme III. The target is a simple dimer of MPE (Bis-MPE, 10) using a 12-carbon linker, which would allow both methidiums to intercalate. Steps 1-5 have been accomplished; the ditosylate of 1,12-dodecanediol was reacted with an excess of 1,3-diaminopropane affording the tetra-amine 7. The imidazole<sup>68</sup> of triethyl ester 4, available in two steps from EDTA,<sup>69</sup> was condensed with 7 affording 8. The final two steps (6 and 7) have not yet been accomplished. The imidazole of paracarboxymethidium, 1, will be condensed with 8 to afford 9. A model reaction using diethylamine as a substitute for 8 has been successfully carried out in high yield. Finally, the ester 9 will be hydrolyzed to yield Bis-MPE.

Bis-MPE is expected to have a very high binding affinity for DNA, on the order of  $10^8$  ( $K_{MPE}^{1.6}$ ). This would allow for efficient DNA cleavage at very low binding densities. The off-rate for Bis-MPE is expected to be slower than for MPE, possibly resulting in double-strand DNA cleavage in a single binding event. In addition, the presence of two EDTA moieties on the molecule raises the possibility of two simultaneous oxygen activation events. This is expected to raise cleavage efficiency, and possibly result in cleavage of opposite DNA strands.

The conformational specificity exhibited by BMSp may be reflected in Bis-MPE. This will be easy to determine using both synthetic polymers and pBR-322 plasmid DNA. One experiment could be a competitive experiment between rA·dT and dA·dT to see if the rA·dT selectivity of BMSp is conserved. In addition, the regiospecificity

demonstrated by BMSp using restriction enzyme inhibition analysis could be probed with Bis-MPE using affinity cleaving on pBR-322 plasmids. Any conformational hot-spots would be revealed by banding patterns on an agarose gel (either nondenaturing gels to examine double-strand scission or denaturing gels to examine single-strand scission). These hot-spots could be mapped by subsequent cleavage with restriction enzymes.

High resolution gel electrophoresis using end-labeled DNA fragments would reveal more about the potential specific recognition of base sequences or DNA conformations by Bis-MPE. We have already seen how MPE has a slight bias against AT base pairs. This bias is expected to increase for the dimer. Perturbations in the double-helix could be artificially induced using DNA binding drugs to see what effect they would have on the Bis-MPE cleavage patterns. In summary, this dimer of MPE is expected to be a conformational probe for DNA. Since it would have different properties than MPE, it may be able to answer different questions about the double helix.

### **Conclusion**

The design and synthesis of a bifunctional DNA cleaving reagent, methidiumpropyl-EDTA (MPE), has been described. This reagent demonstrates that judicious attachment of EDTA to a DNA binding molecule creates a DNA cleaving molecule. MPE cleaves DNA efficiently in the presence of Fe(II), oxygen, and reducing agents. A study of the DNA binding characteristics of MPE has shown that it binds with a high affinity and unwinds supercoiled DNA. The factors affecting the DNA cleavage efficiency by MPE have been determined, demonstrating that Fe(II) and O<sub>2</sub> are absolute requirements and that •OH is a probable

intermediate in the strand scission reaction. Analyses of the DNA cleavage products have led to insight regarding the strand scission reaction mechanism, and further support the intermediacy of  $\cdot\text{OH}$ .

$\text{MPE}\cdot\text{Fe}(\text{II})$  cleaves DNA in a relatively non-sequence specific manner. It is a useful tool for the determination of small molecule binding sites on naturally occurring heterogeneous DNA,<sup>8</sup> and in the study of chromatin structure.<sup>104</sup>  $\text{MPE}\cdot\text{Fe}(\text{II})$  and other related bifunctional cleaving reagents should be useful as probes for small molecule-DNA interactions, protein-DNA structure, and DNA conformation analysis.

## EXPERIMENTAL

**Materials and Methods.** Nuclear magnetic resonance (NMR) spectra were obtained on a Varian Associates EM-390, or a Bruker WM 500 spectrometer. Chemical shifts are given as parts per million (ppm) downfield from tetramethylsilane (TMS), and coupling constants in cycles per second (Hz). Infrared (IR) spectra were recorded on a Perkin-Elmer Model 257 or Shimadzu IR-435 spectrophotometer, and are reported in wavenumbers ( $\text{cm}^{-1}$ ). Ultraviolet-visible (UV-VIS) spectra were recorded on a Cary 219 spectrophotometer. Elemental analyses were performed by Galbraith Laboratories, Inc., Knoxville, Tennessee. Mass spectra (MS) were performed by the University of California, San Francisco (Kratos MS-50S spectrometer equipped with a SIMS ion source) or by the University of Nebraska (Fast Atom Bombardment). High pressure liquid chromatography (HPLC) was performed on an Altex system using an Ultrasphere octadecylsilane (ODS) reversed phase column. Radioactive samples were counted in a Beckman LS200B scintillation counter. Gels were photographed with Polaroid type 55 film and the negatives were scanned with a Cary 219 spectrophotometer interfaced to an Apple computer.

Most reagent grade chemicals were used without further purification. Dimethyl sulfoxide (DMSO) and N,N-dimethylformamide (DMF) were dried over 4A molecular sieves. All of the water used was double distilled. Bleomycin, a clinical bleomycin sulfate, was generously supplied by Bristol Laboratories. Ferrous ammonium sulfate was a Baker Analyzed Reagent. Dithiothreitol (DTT) was purchased from Calbiochem. Iodosylbenzene (PhIO) was from Pfaltz and Bauer. All solutions of Fe,

DTT, ascorbate,  $H_2O_2$ , and PhIO were prepared immediately before use. Thiobarbituric acid (TBA) and nucleotide bases were from Sigma. Desferrioxamine (desferal) was supplied by Ciba-Geigy. Calf intestinal alkaline phosphatase, superoxide dismutase, and catalase were purchased from Boehringer Mannheim. DNase was from Worthington, topoisomerase I from Bethesda Research Labs and all other enzymes from New England Biolabs. Amersham supplied [ $^{32}P$ ]ATP and [ $^3H$ ]thymidine.

**Methidiumpropylamine (2).** Paracarboxymethidium chloride (1) (1.0g, 2.6 mmol) and N-ethyl morpholine (0.3 ml) were combined in 40 ml dry DMSO under an argon atmosphere. Carbonyl diimidazole (470 mg, 2.9 mmol) in 6 ml DMSO was added at room temperature and the solution was stirred for one hour. The contents of the flask were transferred via syringe to a dropping funnel, and subsequently added dropwise to a solution of 1,3-diaminopropane (2.2 ml, 26 mmol) in 2 ml dry DMSO under argon. Stirring was maintained for 24 h, followed by concentration in vacuo to yield a purple solid. The solid was flash chromatographed on silica gel 60 with acidic methanol (0.1% (v/v) acetyl chloride in dry methanol). A dark orange band was collected, concentrated in vacuo, and dried for several days in vacuo at 50°C to yield 998 mg (89%) of the desired product as a maroon solid: NMR ( $D_2O$ )  $\delta$  7.19–8.07 (m, 10H, ar + phenyl), 4.19 (s, 3H,  $N^+-CH_3$ ), 3.63 (t,  $J=7Hz$ , 2H,  $-CH_2-$ ), 3.20 (t,  $J=7Hz$ , 2H,  $-CH_2-$ ), 2.13 (m, 2H,  $-CH_2-$ ). IR (KBr) 3300, 3200, 3100 to 2900, 1620, 1540, 1490, 1470, 1420, 1380, 1350, 1315, 1260, 1225, 1155, 820. Mass spec.:  $m/z = 400$  ( $M^+$ ).

**Methidiumpropyl-EDTA triethyl ester (5).** Triethyl ethylenediaminetetraacetate (4) was prepared by the method of Hay and

Nolan.<sup>69</sup> **4** (119 mg, 0.32 mmol) was combined with carbonyl diimidazole (57 mg, 0.35 mmol) in 3 ml dry DMF and stirred at room temperature for 30 minutes. **2** (138 mg, 0.32 mmol) was added and the solution was stirred at room temperature for 24 h. The mixture was concentrated in vacuo to a red solid and flash chromatographed on silica gel 60 with acidic methanol (0.2% (v/v) acetyl chloride in dry methanol) to yield 124 mg (49%) of the desired product. NMR (CD<sub>3</sub>OD)  $\delta$  7.3-8.7 (m, 9H, aromatic H's), 6.48 (d, J=3Hz, 1H, H-7), 4.12 (m, 9H, N<sup>+</sup>-CH<sub>3</sub> and -COOCH<sub>2</sub>CH<sub>3</sub>), 3.2-3.7 (m, 12H, -N-CH<sub>2</sub>-CO- and CO-NH-CH<sub>2</sub>-), 2.76 (s, 4H, -N-CH<sub>2</sub>), 1.86 (m, 2H, -CH<sub>2</sub>-), 1.25 (t, J=7Hz, 9H, -COOCH<sub>2</sub>CH<sub>3</sub>). IR (KBr) 3400, 3100, 1625, 1590, 1490, 1090, 1050, 820.

**Methidiumpropyl-EDTA (3). Method A.** 4.5g EDTA (15.4 mmol; free acid form) was dissolved in 600 ml dry DMF at 120°C under an argon atmosphere. Molecular sieves were added, and then **2** (435 mg, 1 mmol) in 150 ml DMF was added dropwise to the hot, stirring solution. The solution was stirred at 120°C one hour, cooled to room temperature and filtered. The filtrate was concentrated in vacuo to a red solid, which was taken up in warm water and passed over Amberlite IRA 45 to remove excess EDTA. The orange aqueous solution was concentrated in vacuo to yield a purple solid, which was flash chromatographed on a silica gel 60 with basic methanol (2% aq-NH<sub>3</sub> in methanol). A dark orange band was collected and concentrated in vacuo. The product was rendered metal-free by dissolving it in 100 ml of 5% aq. Na<sub>2</sub>EDTA, adding HCl to make the solution pH 2, and subsequent neutralization with aq. NH<sub>3</sub>. The solution was passed over a column of Amberlite XAD-2 polystyrene resin (Rohm and Haas) to effect adsorption of the product. This column was

washed with 200 ml of 5% aq. Na<sub>2</sub>EDTA, 200 ml of chelex treated metal free 5% aq. NaCl, and 200 ml of double distilled H<sub>2</sub>O. Subsequent elution with 50% aq. methanol yielded a red solution which was concentrated in vacuo to yield 475 mg (67%) of the desired product as a maroon solid: NMR (CD<sub>3</sub>OD)  $\delta$  7.33-8.62 (m, 9H, ar + phenyl), 6.54 (s, 1H, H-7), 4.12 (s, 3H, N<sup>+</sup>-CH<sub>3</sub>), 3.90 (s, 4H, -N-CH<sub>2</sub>-COOH), 3.05-3.55 (m, 12H, N-CH<sub>2</sub>- and CONH-CH<sub>2</sub>-), 1.92 (m, 2H, -CH<sub>2</sub>-). IR (KBr) 3400, 3200 (sh), 2900, 1630, 1580, 1490, 1410, 1315, 1260, 1110, 820. UV (H<sub>2</sub>O): 286 nm ( $\epsilon$  = 54725 M<sup>-1</sup> cm<sup>-1</sup>), 488 nm ( $\epsilon$  = 5994 M<sup>-1</sup> cm<sup>-1</sup>). MPE was isolated as the monopotassium salt, tetrahydrate. Anal: Calcd. for C<sub>34</sub>H<sub>47</sub>N<sub>7</sub>O<sub>12</sub>K: C, 52.03; H, 6.04; N, 12.49. Found: C, 52.24; H, 5.78; N, 12.46. Mass spec.: m/z 712 (monopotassium salt, M<sup>+</sup>).

**Method B.** **5** (124 mg, 0.16 mmol) was dissolved in 10 ml ethanol and 25 ml of 0.5M lithium hydroxide was added. The reaction was stirred at room temperature for 2 h, acidified to pH 4 with 1M HCl, and concentrated in vacuo to a red solid. The product was flash chromatographed on silica gel and further purified as described in method A to yield 101 mg (79%) of **3**. MPE prepared in this way identical to that produced in method A by NMR, IR, TLC and HPLC.

**EDTA-propane (6).** **4** (200 mg, 0.53 mmol) was combined with carbonyl diimidazole (95 mg, 0.58 mmol) in 5 ml dry DMF and stirred at room temperature for 30 minutes. Propylamine (0.052 ml, 0.64 mmol) was added and the solution was stirred at room temperature for 24 h. The mixture was concentrated in vacuo to a yellow oil, and taken up in 5 ml ethanol. 5 ml of 0.5M lithium hydroxide was added and the reaction was stirred at room temperature for 1 h, acidified to pH 7 with 1M HCl, and

concentrated in vacuo to a yellow oil. The product was flash chromatographed with basic methanol (20% aq-NH<sub>3</sub> in methanol) to yield 101 mg (56%) of VI. NMR (CD<sub>3</sub>OD):  $\delta$  3.28 (m, 2H, -CONH-CH<sub>2</sub>-), 3.18 (s, 2H, -N-CH<sub>2</sub>-CONH-), 3.08 (s, 6H, -N-CH<sub>2</sub>-COOH), 2.57 (s, 4H, -N-CH<sub>2</sub>-), 1.53 (m, 2H, -CH<sub>2</sub>-), 0.92 (t, J=7Hz, 3H, -CH<sub>3</sub>). IR (KBr) 3400, 3220, 2970, 1640, 1590, 1440, 1405, 1330, 1250, 1110, 850. Mass spec.: m/z 372 (M<sup>+</sup>).

**1,12-Dodecanediol bis(4-methylbenzene sulfonate).** 1,12-Dodecanediol (2.0g, 10 mmol) was suspended in 10 ml CCl<sub>4</sub>, p-toluenesulfonyl chloride (3.77g, 20 mmol) was added and the mixture was cooled to 0°C. Triethylamine (3.3 ml, 24 mmol) was slowly added and the mixture was stirred at room temperature for 40 h. The CCl<sub>4</sub> was removed in vacuo and the residue was washed thoroughly with hexane. The sample was dissolved in CH<sub>2</sub>Cl<sub>2</sub>, extracted with cold 5% HCl, H<sub>2</sub>O, and 5% K<sub>2</sub>CO<sub>3</sub>. The CH<sub>2</sub>Cl<sub>2</sub> solution was dried (NaSO<sub>4</sub>) and evaporated to a pale yellow solid in vacuo. Melting point (74°C) and NMR compared favorably to literature values.<sup>129</sup>

**N,N'-Bis(3-aminopropyl)-1,12-dodecanediamine (7).**

1,12-Dodecanediol bis(4-methylbenzene sulfonate) (510 mg, 1 mmol) was dissolved in 5 ml toluene and dropped slowly into 1,3-diaminopropane (8 ml, excess). The reaction mixture was stirred at room temperature for 16 h and evaporated to dryness. The white solid was recrystallized from hot water to yield 231 mg (73%) of white crystals. NMR (CDCl<sub>3</sub>)  $\delta$  2.58 (m, 12H, -N-CH<sub>2</sub>-), 1.1-1.8 (m, 30H, -CH<sub>2</sub>- and -NH<sub>2</sub>). 7 was isolated as the HCl salt. Anal: Calcd. for C<sub>18</sub>H<sub>42</sub>N<sub>4</sub>·HCl: C, 61.59; H, 12.35; N, 15.96. Found: C, 61.61; H, 12.65; N, 15.60.

**N,N'-Bis(triethyl-EDTA-propyl)-1,12-dodecanediamine (8).**

Triethyl EDTA (4) (295 mg, 0.79 mmol) was dissolved in 4 ml dry DMSO and carbonyl diimidazole (165 mg, 1 mmol) was added. After 30 min at room temperature, N,N'-bis(3-aminopropyl)-1,12-dodecanediamine (123 mg, 0.39 mmol, dissolved in 10 ml dry DMSO) was added and the reaction mixture was stirred at room temperature for 16 h. The DMSO was removed in vacuo and the residue was flash chromatographed on silica gel with  $\text{CH}_2\text{Cl}_2/\text{MeOH}/\text{aq. NH}_3$  (80:9:1) to yield 90 mg (18%) of a white solid. NMR ( $\text{CDCl}_3$ )  $\delta$  4.1 (q, 12H,  $J=7\text{Hz}$ ,  $-\text{COOCH}_2\text{CH}_3$ ), 3.05-3.7 (m, 20H,  $-\text{N-CH}_2\text{-CO-}$  and  $\text{CONH-CH}_2-$ ), 2.75 (m, 16H,  $-\text{N-CH}_2-$ ), 1.75 (m, 8H,  $-\text{N-CH}_2\text{-CH}_2-$ ), 1.15 (m, 34H,  $-\text{CH}_2-$  and  $-\text{CH}_3$ ).

**Para(diethylcarboxamide)methidium.** Paracarboxymethidium chloride 167 (68 mg, 0.18 mmol) was dried in vacuo at  $50^\circ\text{C}$  over  $\text{P}_2\text{O}_5$ . 1 was combined with N-ethyl morpholine (20  $\mu\text{L}$ ) in 2 ml dry DMF, acyl diimidazole (32 mg, 0.20 mmol) was added and the solution was stirred at room temperature for one hour. Diethylamine (20.5  $\mu\text{L}$ , 0.20 mmol) was added and stirring was maintained for 18 hr. TLC analysis (1000:1  $\text{MeOH}/\text{acetyl chloride}$ ) of an aliquot quenched with  $\text{H}_2\text{O}$  showed very little reaction, and so the mixture was heated at  $110^\circ\text{C}$  for 3 hrs. TLC showed complete reaction, and the reaction mixture was concentrated in vacuo to a purple solid. The solid was flash chromatographed on silica gel with acidic methanol (0.1% (v/v) acetyl chloride in dry methanol). Concentration in vacuo followed by further purification on Amberlite XAD-2 (200 ml  $\text{H}_2\text{O}$  wash followed by elution with 75% aq. methanol) yielded 40 mg (51%) of the desired product. NMR ( $\text{CD}_3\text{OD}$ )  $\delta$  7.2-8.6 (m, 9H, arom H's + phenyl), 6.5 (d,  $J=3\text{Hz}$ , 1H, H-7), 4.06 (s, 3H,  $\text{N}^+-\text{CH}_3$ ),

3.5 (m, 4H, -N-CH<sub>2</sub>-CH<sub>3</sub>), 1.25 (t, J=7Hz, 6H, -N-CH<sub>2</sub>-CH<sub>3</sub>). IR (KBr) 3400, 3200, 1620, 1490, 1400, 1380, 1315, 1260, 1090, 820. Mass spec.: m/z 399 (M<sup>+</sup>).

**DNA Substrates.** Calf thymus DNA, purchased from Sigma, was sonicated, phenol extracted, and extensively dialyzed. PM2 plasmid DNA was from Boehringer Mannheim. pBR-322 plasmid DNA was grown in Escherichia coli strain HB101, and isolated in supercoiled form by procedures similar to those of Tanaka and Weisblum.<sup>130</sup>

[<sup>32</sup>P] end-labeled DNA fragments of defined sequence were obtained from the bacterial plasmid pBR-322.<sup>76</sup> A 279 base pair long 3'-end labeled DNA fragment was prepared by cleavage of the plasmid with Bam HI and enzymatic extension of the 3'-end with the Klenow fragment of DNA polymerase I and [ $\alpha$ -<sup>32</sup>P] (3000 Ci/mmol).<sup>131</sup> After a second cleavage with Sal I, the fragment was isolated by gel electrophoresis on a 5% polyacrylamide, 1:30 crosslinked, 2 mm thick gel.<sup>99</sup>

A 381 base pair long 5' end labeled DNA fragment was prepared by cleavage of the plasmid with Bam HI followed by removal of the 3' and 5' phosphoryl groups with calf intestinal alkaline phosphatase. The 5'-ends were labeled with [ $\gamma$ -<sup>32</sup>P]ATP (5000 Ci/mmol) and T4 polynucleotide kinase. After a second digestion with Eco RI, the DNA fragment was isolated from a 5% polyacrylamide gel. Bacteriophage  $\lambda$  [<sup>3</sup>H] DNA labeled at the 5-methyl group of thymine was purchased from Bethesda Research Labs. [<sup>3</sup>H] DNA labeled at the 5' position of thymidine was extracted from purified bacteriophage  $\lambda$ , grown in a thy<sup>-</sup> host, Escherichia coli strain RS15, kindly provided by Richard Burger.<sup>48</sup> This heat-inducible, lysis-defective bacteriophage  $\lambda$  lysogen was grown

and isolated as described<sup>132</sup> with the addition of 5'-labeled thymidine and 85  $\mu\text{g/ml}$  uridine after induction. The DNase treatment and cesium chloride step gradient were omitted. DNA was extracted from phage using formamide dialysis<sup>133</sup> and extensively dialyzed with 10 mM Tris, pH 7.4, 50 mM NaCl. The specific activity was 9.5 mCi/mmol bp.

**Determination of Binding Affinities.** The absorbance titrations were performed with a Cary 219 spectrophotometer using 10 cm long cells (25 ml) at  $23 \pm 1^\circ$ . The buffer was 10 mM Tris-HCl, 50 mM NaCl, pH 7.4. Increasing amounts of drug were added to a known quantity of sonicated calf thymus DNA and the absorbance at 488 nm was recorded until equilibrium was attained (10 minutes). Absorbance measurements were reproducible to  $\pm 0.0003$  AU. The extinction coefficient at 488 nm of free drug is  $5994 \text{ M}^{-1} \text{ cm}^{-1}$ , and of bound drug is  $2685 \text{ M}^{-1} \text{ cm}^{-1}$ . These numbers were determined by performing absorbance titrations in the absence of DNA (free drug), or in the presence of excess (4 mM) calf thymus DNA (bound drug). Beer's law plots (absorbance vs. drug concentration) were constructed and the slopes determined to obtain these extinction coefficients. Binding affinities and binding site sizes were obtained by fitting theoretical Scatchard curves<sup>70,71</sup> to the experimentally derived curves from the absorbance titrations.

**Determination of Unwinding Angle.** Each experiment contained 500  $\mu\text{M}$  PM2 plasmid DNA in 10  $\mu\text{L}$  of buffer (50 mM Tris-HCl, 50 mM KCl, 10 mM  $\text{MgCl}_2$ , pH 7.5) and MPE·Mg(II) in the concentration indicated. 1  $\mu\text{L}$  of bovine serum albumin (0.5 mg/ml) was added followed by 10 units of topoisomerase I. The reaction was incubated at  $37^\circ\text{C}$  for 4 h, 10 more units of enzyme was added, and the reaction proceeded for four more

hours. 1  $\mu$ L of 10% sodium dodecyl sulfate was added and the mixture was phenol extracted twice, ether extracted twice, and then passed through a 1 mm x 5 mm column of DOWEX 50W-X4 to remove drug. The column was washed with 1M sodium acetate and the DNA was ethanol precipitated from the eluent. The pellet was washed with 95% ethanol, dried in vacuo, and taken up in gel loading solution (5% ficoll, 0.025% bromophenol blue, 0.025% xylene cyanol in electrophoresis buffer). The samples were loaded onto a 1% agarose slab gel and electrophoresed for 15 h at 60V (running buffer 40 mM Tris-HCl, 5 mM sodium acetate, 1 mM EDTA, pH 7.8). The gel was stained with 2  $\mu$ g/ml ethidium bromide and photographed with Polaroid type 55 film. Shifts in band position were evaluated by using densitometer tracings.

**Reaction Conditions for DNA Cleavage.** Reactions using supercoiled pBR-322 plasmid DNA as a substrate for MPE cleavage were performed in 10  $\mu$ L of 10 mM Tris-HCl, 50 mM NaCl, pH 7.4 (unless noted). The DNA concentration was  $10^{-5}$ M (bp). An MPE solution (5 mM) was pre-mixed with a metal ion solution (5 mM) in a 1:1 complex followed by dilution to the desired concentration. In some experiments (noted in the figure legends) the MPE and metal ion solutions were diluted prior to mixing. Addition of reducing agents was done last, in concentrations noted in the figure legends. Reactions proceeded for 60 mins at 22°C (unless noted), and were directly analyzed for cleavage by agarose gel electrophoresis.

Anaerobic reactions were performed in a four-chamber vessel. Each component of the reaction mixture was placed in a separate chamber, and the vessel was placed onto a vacuum line. The solutions were

degassed by four cycles of freeze-thawing, the vessel was filled with ultrapure argon (Linde), and the components were mixed via syringe. After the reaction degassed desferal was added to a concentration of 50 mM and the vessel was opened to the atmosphere. The reaction mixture was immediately analyzed by gel electrophoresis.

Reactions for HPLC analysis contained 20 mM sodium phosphate, pH 7.2; 950  $\mu$ M (bp) sonicated calf thymus DNA; 50  $\mu$ M (bp) bacteriophage  $\lambda$  [ $^3$ H]DNA; MPE or bleomycin,  $\text{Fe}(\text{NH}_4)_2(\text{SO}_4)_2$  or  $\text{Fe}(\text{NH}_4)(\text{SO}_4)_2$ , and when present, DTT or  $\text{H}_2\text{O}_2$  in the amounts noted in the figure legends. Bleomycin ( $\epsilon_{292} = 1.45 \times 10^4 \text{ M}^{-1} \text{ cm}^{-1}$ )<sup>134</sup> and MPE ( $\epsilon_{488} = 5994 \text{ M}^{-1} \text{ cm}^{-1}$ ) were standardized optically prior to use. The reaction mixture (0.2 ml) was incubated at 22°C for 30 mins and terminated by ethanol precipitation. The DNA pellet was assayed for strand scission by denaturing gel electrophoresis while the supernate was analyzed for products by HPLC or by reaction with TBA. This protocol removed less than 5% of the reaction products as shown by HPLC analyses before and after precipitation.

Reactions for end group analysis contained  $\geq 10^4$  cpm of [ $^{32}$ P] end-labeled DNA made up to a total DNA concentration of 100  $\mu$ M (bp) with sonicated calf thymus DNA. The buffer was 10 mM Tris-HCl, pH 7.4, 50 mM NaCl. MPE, bleomycin, or EDTA was included in the amounts indicated in the figure legends and  $\text{Fe}(\text{NH}_4)_2(\text{SO}_4)_2$  or  $\text{Fe}(\text{NH}_4)(\text{SO}_4)_2$  was added. The molar ratio of chelator to iron was one to one. When present, the reactions were initiated by the addition of DTT or  $\text{H}_2\text{O}_2$ . All of these reagents except Fe(III) were prepared in double-distilled water within a few minutes of use. Fe(III) solutions were freshly prepared in 1 mM

aqueous H<sub>2</sub>SO<sub>4</sub>. The reactions were incubated at 22°C for 30 mins and the DNA was ethanol precipitated for high resolution gel electrophoresis.

**Quantitation of DNA Cleavage.** When supercoiled (form I) pBR-322 plasmid DNA was used as a substrate for cleavage, the mean number of single-strand scissions per DNA molecule, S, was determined by monitoring the conversion to open-circular (form II) and linear (form III) forms. The Poisson distribution states that

$$P_n = \frac{S^n}{n!} e^{-S}$$

where P<sub>n</sub> is the fraction of molecules that have n nicks each.<sup>135</sup> This equation assumes that the nicks are distributed at random throughout the DNA population. Since by definition form I DNA has zero nicks, when only forms I and II are present the Poisson distribution simplifies to

$$S = -\ln[f_I]$$

where f<sub>I</sub> is the fraction of form I molecules left untouched.

In those cases where the cleavage reaction proceeded to form linear DNA molecules S was calculated from the following equation:

$$f_I + f_{III} = \left[ 1 - \frac{S(2h + 1)}{2L} \right]^{S/2}$$

where h is the distance between nicks on opposite strands needed to produce a linear molecule (16 bp)<sup>78</sup> and L is the total number of bp's in pBR-322 (4361).<sup>76</sup>

The relative amounts of forms I, II, and III DNA were analyzed by agarose gel electrophoresis (1% agarose; running buffer 40 mM Tris·HCl, 5 mM NaOAc, 1 mM EDTA, pH 7.8). Reaction mixtures (10 μL) were mixed with 2 μL of gel loading solution (32% ficoll, 0.15%

bromophenol blue in water) and loaded onto a vertical slab gel. The gel was electrophoresed at 32V for 13 h or at 80V for 4 h and stained with 2  $\mu\text{g}/\text{ml}$  ethidium bromide. After destaining, the gel was photographed with Polaroid type 55 film and scanned with a densitometer. The film was found to have a linear response in the range of DNA quantities used. In addition, since supercoiled DNA is topologically restricted with respect to its ability to bind to ethidium bromide it was necessary to multiply the values obtained for form I DNA by a correction factor. This factor was determined to be 1.22 by the method of Haidle.<sup>79</sup>

When bacteriophage  $\lambda$ [<sup>3</sup>H]DNA was used as a substrate for cleavage, the single-strand scissions were quantitated by monitoring the decrease in the single-strand molecular weight of the DNA. The mean number of single-strand scissions per strand, P, is related to the decrease in the single-strand molecular weight of the DNA by the relationship<sup>136</sup>

$$M_r/M_r(\text{initial}) = 2[e^{-P} + P - 1] / P^2$$

This relationship uses the weight average molecular weight

$$M_r = nM^2/nM$$

where n represents the number of molecules of molecular weight M.

The single strand molecular weight of the DNA after cleavage was determined by denaturation with glyoxal/DMSO<sup>137</sup> and electrophoresis on 1.2% agarose gel. [<sup>3</sup>H] DNA was ethanol precipitated from the reaction mixtures and dissolved in 10  $\mu\text{L}$  of 10 mM sodium phosphate buffer (pH 7.0). 14  $\mu\text{L}$  of DMSO was added, followed by 4  $\mu\text{L}$  of freshly deionized 7M glyoxal (glyoxal was deionized by passage through AG 501 X-8 mixed bed resin). The solution was incubated at 50°C for 1 h and then loaded onto

a 1.2% agarose vertical slab gel (running buffer was 10 mM sodium phosphate, pH 7.0). The gel was electrophoresed at 80V for 2.75 h with constant recirculation of the running buffer. Staining was with 30 µg/ml acridine orange for 30 mins, followed by destaining in buffer overnight at 4°C. The gel was photographed, cut into 1 mm slices using a Hoefer SL280 gel slicer, and each slice was soaked in 10 ml of Econofluor/Protosil, 95:5 (New England Nuclear) for 24 h prior to scintillation counting. The number of molecules contained in each slice is represented by the radioactivity divided by the molecular weight of the oligonucleotides in that slice ( $n = \text{cpm}/M$ ). The molecular weight represented by each slice was determined by comparing its migration distance to a calibration curve constructed using restriction fragments of known size (denatured as described). The  $\log(MW)$  vs. distance plot was linear through the entire range of molecular weights examined. The initial size of the bacteriophage DNA was taken to be 49000 bp. These data were analyzed by an Apple computer in order to determine P. In addition, the molecular weight distribution curves of the degraded DNA were compared to theoretical curves assuming a random degradation process.<sup>115</sup>

**HPLC of DNA Cleavage Products.** The supernatant from the reaction mixture was reduced to 20 µL in vacuo and the entire sample was injected onto an Altex Ultrasphere ODS column. The solvent system used was 10 mM potassium phosphate, pH 5.5/methanol; gradient elution (0 to 10% methanol over five mins); detection was UV absorption at 260 nm. Quantitation of the four nucleotide bases was by the internal standard method using adenosine, which was added to the reaction mixture prior to

the ethanol precipitation.

**Thin Layer Chromatography of Base Propenals.** A reaction mixture (0.6 ml) containing 50 mM sodium phosphate (pH 7.2), 1 mM calf thymus DNA, and 450  $\mu$ M bleomycin $\cdot$ Fe(II) was incubated at 22°C for 30 mins. The DNA was ethanol precipitated, and the supernate was concentrated to 0.5 ml and applied to a 10 cm x 20 cm x 2 mm silica gel TLC plate. The plate was developed with ethyl acetate/isopropanol/water, 74:17:9, and the areas corresponding to the base propenals were located by spraying one end of the plate with 0.6% TBA and heating to 90°C for 10 mins. The base propenals show up red, and the corresponding areas were scraped off the plate and eluted with 80% aq. MeOH. The eluent was concentrated in vacuo and analyzed by HPLC as described above.

In the converse experiment, the peaks corresponding to the base propenals were collected off of the HPLC and concentrated in vacuo. These were analyzed by TLC as described above and visualized by spraying with TBA and heating to 90°C.

**TBA Assay.** Aliquots from the reaction mixtures were passed through a 1 mm x 5 mm column of Dowex 50W-X4 to remove MPE. The solution was mixed with nine volumes of 0.6% TBA and heated at 90°C for 20 mins. The TBA adduct was quantitated at 532 nm ( $\epsilon = 1.6 \times 10^5 \text{ M}^{-1} \text{ cm}^{-1}$ ).<sup>48</sup>

**Analysis of Termini by Gel Electrophoresis** The DNA derived from the cleavage reactions was suspended in 4  $\mu$ L of a pH 8.3, 100 mM Tris-Borate, 50% formamide loading buffer and heat denatured at 90°C for one minute. The samples were loaded onto a 0.4 mm thick, 40 cm long, 20% polyacrylamide, 1:20 crosslinked, 50% urea gel and electrophoresed

at 1200V until the bromophenol blue tracking dye had moved 26 cm. Autoradiography was carried out at  $-50^{\circ}\text{C}$  on Kodak X-omat AR film.

The presence of phosphoryl groups on the 5' termini of DNA fragments was tested by using calf intestine alkaline phosphatase. Degraded DNA was passed through a 1 mm x 5 mm column of Dowex 50W-X4 cation exchange resin in order to remove the MPE. The [ $^{32}\text{P}$ ]DNA was recovered in the void volume while the MPE remained on the column. The DNA was ethanol precipitated, dissolved in 50  $\mu\text{L}$  of 40 mM Tris-HCl, pH 7.8, 5 mM NaOAc and heat denatured at  $90^{\circ}\text{C}$  for five mins. Calf intestinal alkaline phosphatase was added and the sample incubated at  $37^{\circ}\text{C}$  for 30 mins. The reaction was terminated by ethanol precipitation and taken up in loading buffer for gel electrophoresis. Similarly, DNA from a dimethyl sulfate G reaction<sup>99</sup> was subjected to the same process (except for the Dowex treatment) in order to remove the 5' phosphoryl groups.

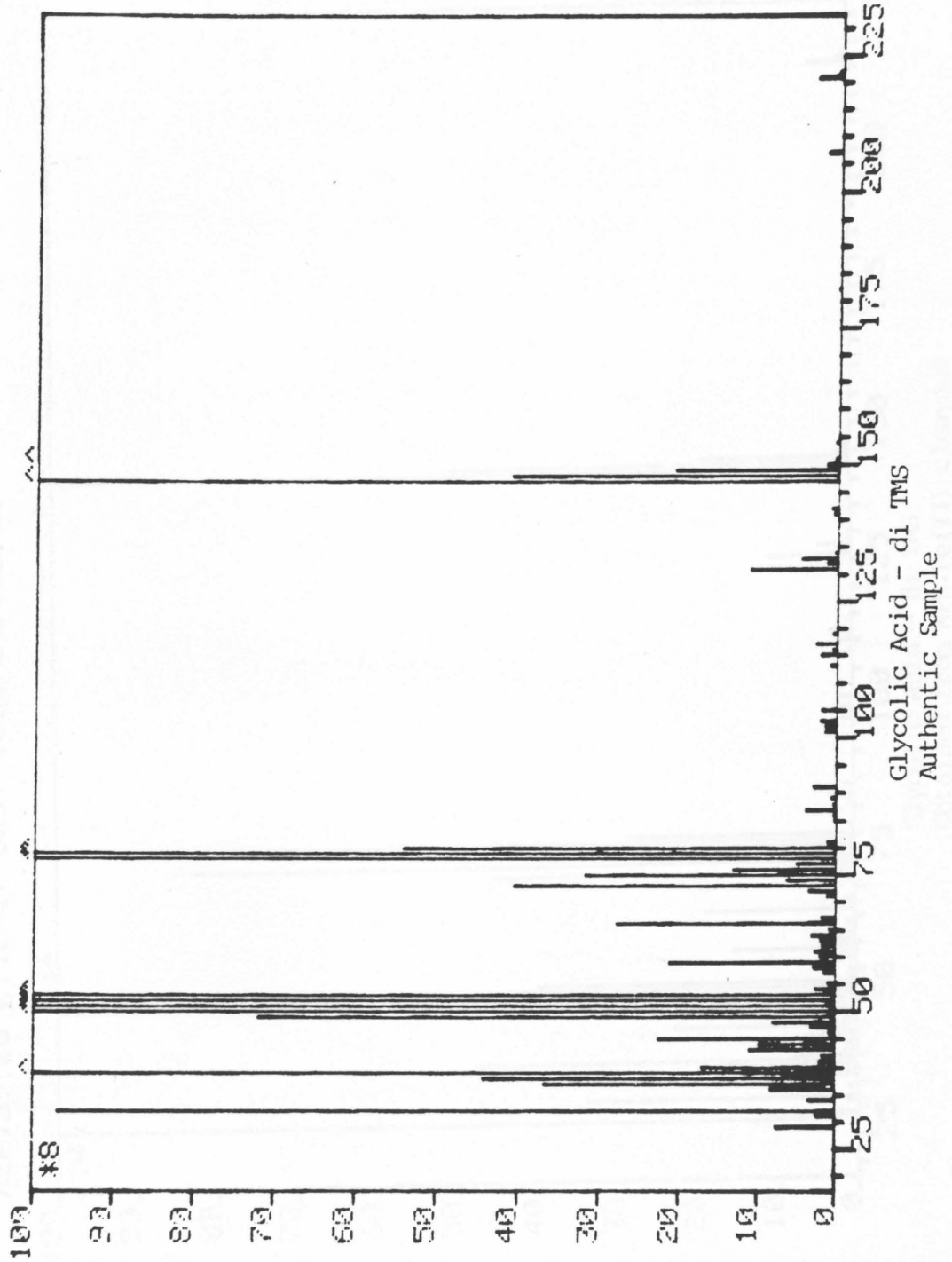
The nature of the 3' termini was examined by using T4 polynucleotide kinase to remove 3' phosphoryl groups.<sup>121</sup> DNA derived from the cleavage reactions was purified by Dowex as before to remove the MPE and then ethanol precipitated. The pellet was dissolved in 20  $\mu\text{L}$  of  $\text{H}_2\text{O}$ , heat denatured at  $90^{\circ}\text{C}$  for five mins and chilled on ice. 20  $\mu\text{L}$  of a buffer containing 20 mM Tris-HCl, pH 6.6, 20 mM magnesium chloride, and 10 mM  $\beta$ -mercaptoethanol was added followed by 4  $\mu\text{L}$  of T4 polynucleotide kinase (1.5 units/ $\mu\text{L}$ ). The reaction was incubated at  $37^{\circ}\text{C}$  for one hour and ethanol precipitated for polyacrylamide gel electrophoresis.

**Analysis of Glycolic Acid.** Bacteriophage  $\lambda$  DNA labeled with  $[^3\text{H}]$  at the 5'-position was reacted with MPE·Fe(II)/DTT. The reaction mixture contained 129  $\mu\text{M}$  bacteriophage  $\lambda$   $[^3\text{H}]$  DNA (9.51  $\mu\text{Ci}/\mu\text{mol}$  bp, 0.22  $\mu\text{Ci}$ ), 56  $\mu\text{M}$  MPE·Fe(II) and 1.4 mM DTT in 10 mM Tris·HCl, 50 mM NaCl, pH 7.4. After 1 hr at 22°C, the DNA was ethanol precipitated and the supernate was analyzed for thymine release by HPLC. The DNA pellet was dissolved in 60  $\mu\text{L}$  of 6M HCl and heated at 100°C for 2 h. The solution was frozen, lyophilized, and taken up in 20  $\mu\text{L}$  of 50 mM Tris base (final pH 8.5). 1  $\mu\text{L}$  of bacterial alkaline phosphatase was added and the mixture was incubated at 37°C for 13 h. The solution was applied to a cellulose TLC plate (Merck) next to authentic samples of glycolic acid, and the plate was developed with n-butanol/acetic acid/ether/water, 9:6:3:1. The plate was divided into 16 equal  $R_f$  zones, and each zone was scraped off and eluted with 0.5 ml of 0.01M HCl, to which was added 10 ml of Aquasol 2 (New England Nuclear). The samples were counted in a scintillation counter, and counting efficiency was determined using  $^3\text{H}_2\text{O}$  as an internal standard. In this way the  $R_f$  zone containing radioactivity could be located, and the amount of sample could be quantitated. Meanwhile the TLC plate containing authentic glycolic acid was stained with bromocresol purple to localize the  $R_f$  zone for glycolic acid.

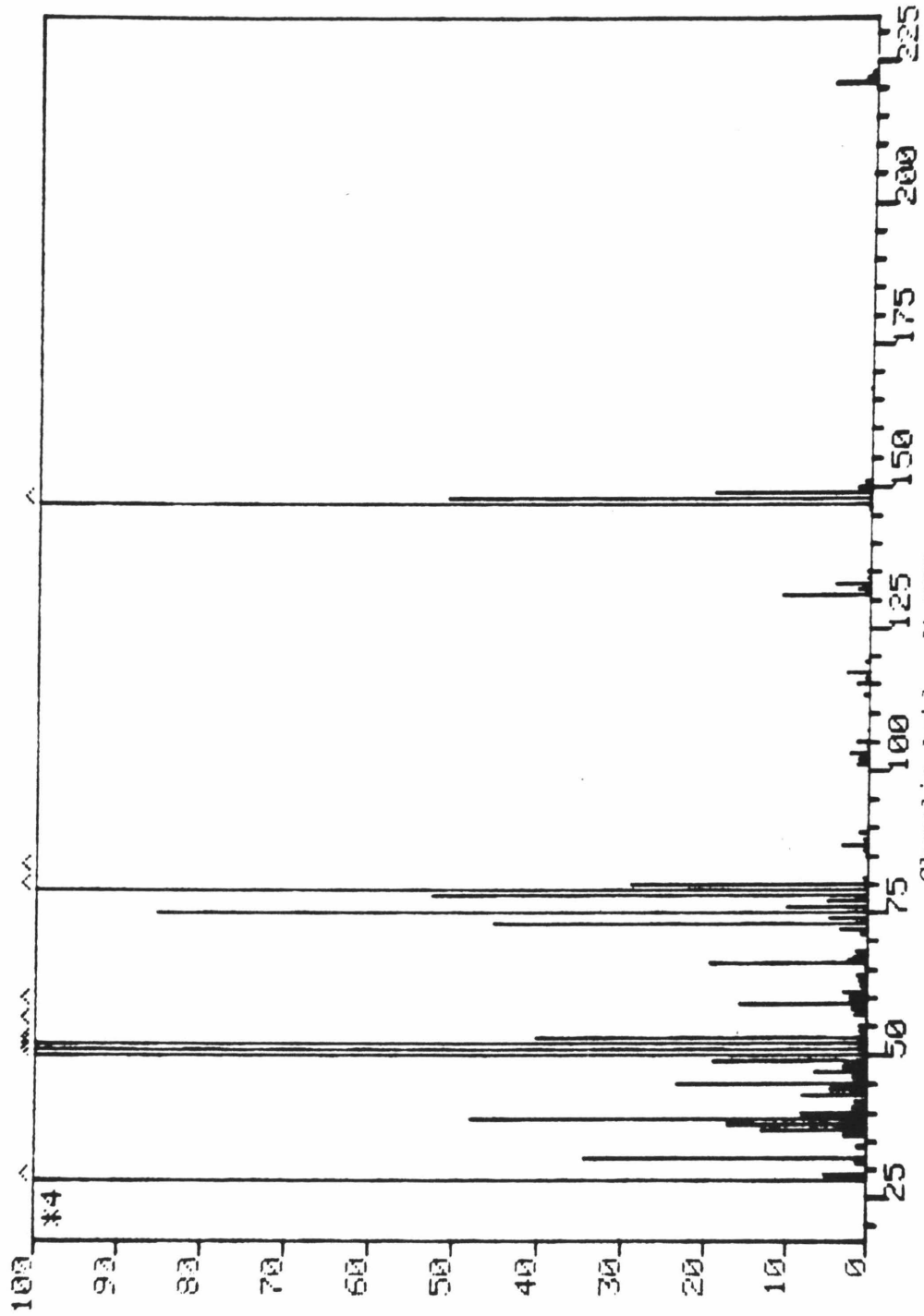
The experiment was repeated using cold calf thymus DNA and MPE·Fe(II)/DTT. The  $R_f$  zone corresponding to glycolic acid was scraped off the plate and eluted with 0.5 ml of 0.01M HCl. The eluent was lyophilized to dryness, and 7  $\mu\text{L}$  N-trimethylsilylimidazole (Tri-Sil Z, Pierce) was added. The mixture was heated at 60°C for 1 h and analyzed

by GC/MS. The di-TMS derivative of authentic glycolic acid was prepared in a similar manner and analyzed by GC/MS for comparison.

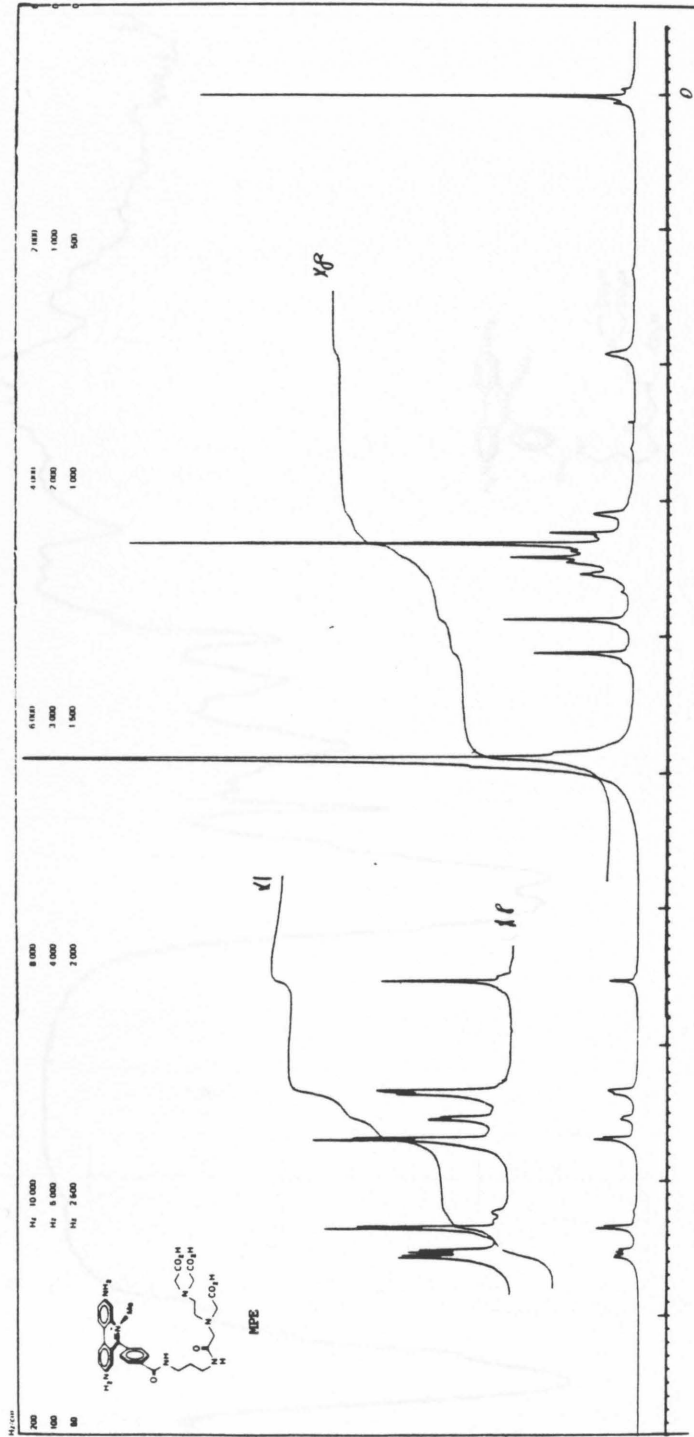
DS-50 MASS INTENSITY REPORT:  
HERTZ4.20 LTIC=178577, 100%=36065] EI

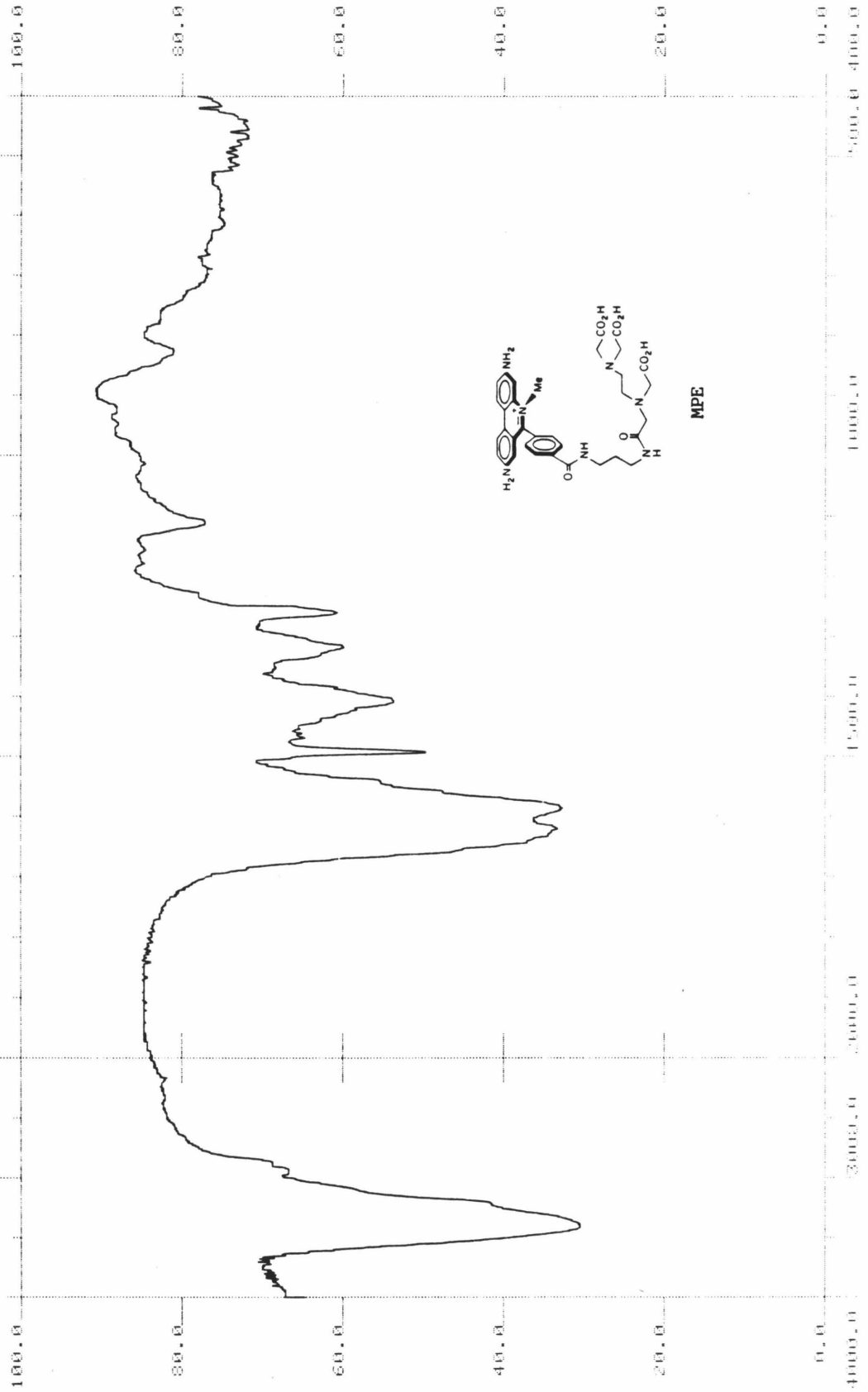


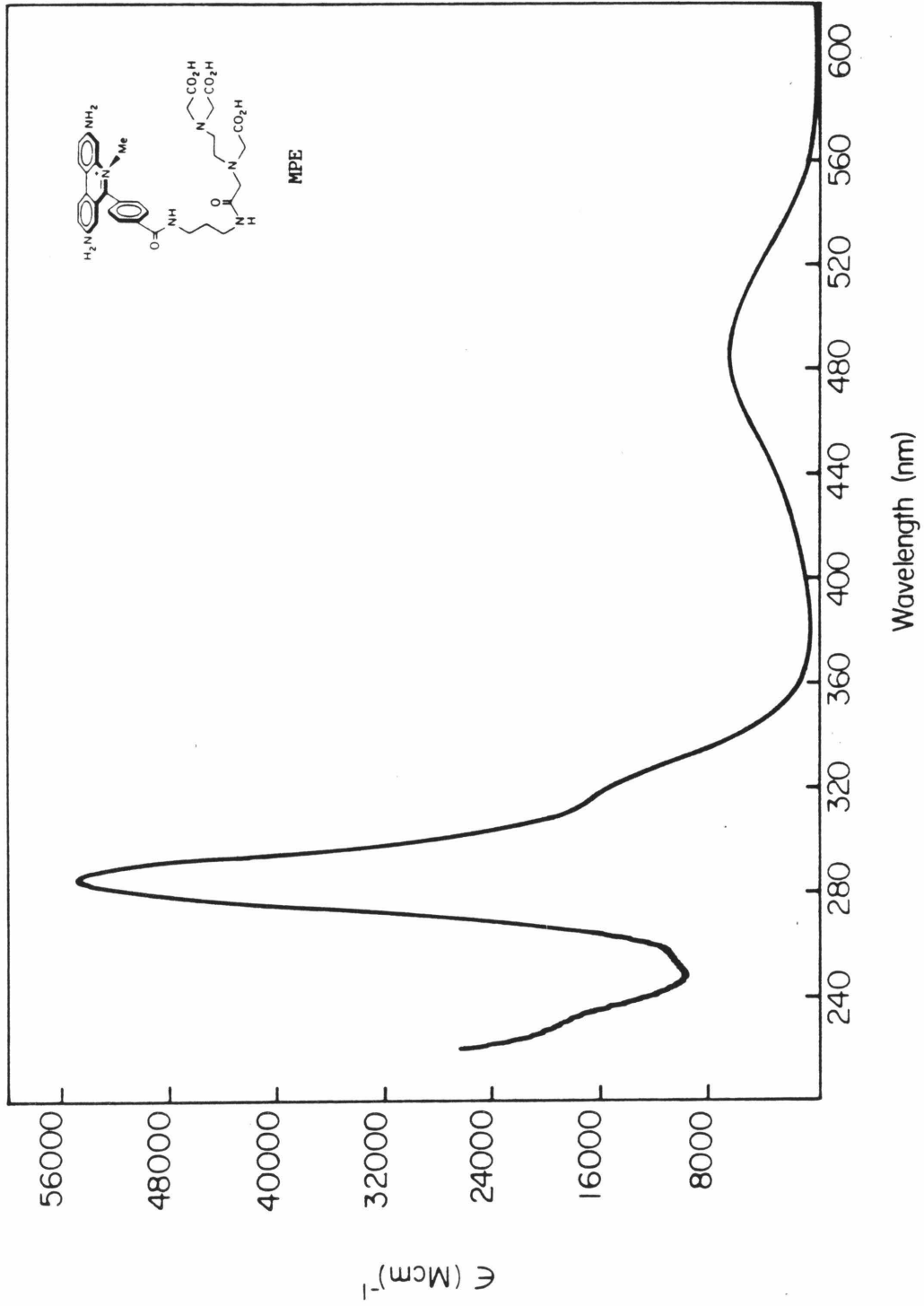
DS-50 MASS INTENSITY REPORT:  
HERTZ 29.26 [TIC=177529, 100%=34980] EI



Glycolic Acid - di TMS  
Obtained from MPE•Fe(II) cleavage







#### PROGRAMS FOR DATA ANALYSIS

**MW Dist.** This program calculates the "number average" and "weight average" molecular weight of a distribution, and the mean number of strand scissions per nucleotide. It generates plots of the experimentally derived molecular weight distribution compared to theoretical curves assuming a random degradation process according to the equations of Freifelder and Davison.<sup>115</sup> The user must input 1) the number of base pairs in the starting material; 2) the slope and y-intercept of the log (MW) versus distance plot for the gel being analyzed; 3) the size of each gel slice in mm; 4) the radioactivity of each gel slice (in cpm); and 5) the background radiation (in cpm). The slices are numbered from one (top of gel) to 150 (bottom of gel). The program determines the molecular weight represented by each gel slice and the amount of DNA contained in the slice. It stores the data on disk and generates molecular weight distribution plots.

**S Calc.** This program calculates the mean number of single-strand scissions per pBR-322 plasmid (S). The user must input the areas of the peaks representing form I and form II DNA, obtained from scanning densitometry. If there is no form I DNA, the program will ask for the percent of form II DNA and calculate S from the equation of Freifelder and Trumbo.<sup>78</sup> The program corrects for the decreased stainability of form I DNA (correction factor 1.22).

MM DIST

ILIST

```
110 DIM C(150)
120 DIM MK(150)
125 DIM P(600)
130 DIM NK(150)
135 D$ = CHR$(4)
137 F = .5
140 CO = 2
150 UOL = 200
160 INPUT "HOW MANY BASE PAIRS IN THE INITIAL DNA?";MI
165 INPUT "WHAT IS THE SIZE OF A GEL SLICE IN MM?";G
170 INPUT "WHAT IS THE BACKGROUND CPM?";B
172 INPUT "WHAT IS THE SLICE NUMBER OF THE FIRST HOT SLICE?";A
175 INPUT "WHAT IS THE SLOPE AND Y-INTERCEPT OF THE LOG(MM) VS DISTANCE P
    LOT?";SL,YI
180 IF SL = 0 THEN GOTO 300
185 INPUT "BETWEEN WHICH SLICE NUMBERS DOES THIS SLOPE APPLY?";J,K
186 INPUT "RECALL CPM DATA? ENTER NO OR NOTEBOOK NUMBER ";NB$
187 IF NB$ < > "NO" THEN GOSUB 1000: GOTO 260
190 FOR X = J TO K
200 PRINT "HOW MANY CPM IN SLICE NUMBER ";X;"?"
210 INPUT C(X)
230 NEXT X
340 INPUT "STORE CPM DATA? ENTER NO OR NOTEBOOK NUMBER ";NB$
250 IF NB$ < > "NO" THEN GOSUB 2000
260 FOR X = J TO K
270 MK(X) = 10 ^ (SL * G * (X - F) + YI)
280 NK(X) = (C(X) - B) / MK(X)
285 IF NK(X) > MAXN THEN MAXN = NK(X)
290 NEXT X
295 GOTO 175
300 HI = INT (MK(K)) + 1:W = HI
301 Y = 0
302 D = A + 1
304 FOR X = K TO D STEP - 1
306 M = (NK(X - 1) - NK(X)) / (MK(X - 1) - MK(X))
308 IF W >= MK(X - 1) THEN GOTO 322
310 P(Y) = (W - MK(X)) * M + NK(X)
312 SUMNM = SUMNM + P(Y) * W
314 SN = SN + P(Y)
316 SHMN = SHMN + P(Y) * W ^ 2
318 Y = Y + 1
319 W = HI + Y * 10
320 IF W < MK(X - 1) THEN GOTO 310
322 NEXT X
323 YL = Y - 1
325 HAMM = SHMN / SUMNM
330 MF = SUMNM / SN
340 R = 1 / MF - 1 / MI
350 N = R * CO * UOL
355 INPUT "DO YOU WANT A PRINTOUT OF THE DNA SIZE DISTRIBUTION?";A$
356 INPUT "DO YOU WANT TO PLOT THE DNA SIZE DISTRIBUTION?";B$
357 INPUT "ENTER NOTEBOOK NUMBER";NB$
358 PRINT D$;"PR#1"
359 PRINT NB$
360 IF A$ = "NO" THEN GOTO 430
370 PRINT "SLICE NO.", "LENGTH", "AMOUNT"
380 PRINT
390 FOR X = A TO K
400 PRINT X, INT (MK(X) + F), INT (1000 * NK(X) + F) / 1000
410 NEXT X
```

```
420 PRINT
430 PRINT "NUMBER AVERAGE LENGTH = "; INT (MF + F)
440 PRINT "NICKS PER NUCLEOTIDE = ";R;" (USING NAMM)"
450 PRINT "TOTAL NANOMOLES OF NICKS = ";N;" (USING NAMM)"
451 PRINT "WAMM = "; INT (WAMM + F)
452 PRINT "NICKS PER NUCLEOTIDE = ";2 / WAMM - 1 / MI;" (USING WAMM)"
453 PRINT "TOTAL NANOMOLES OF NICKS = ";(2 / WAMM - 1 / MI) * CO * VOL;"
      (USING WAMM)"
454 PRINT "BACKGROUND CPM = ";B
455 IF B$ = "NO" THEN END
460 Q = MK(A)
480 HGR2 : HCOLOR= 3
500 XFAC = 275 / Q
510 YFAC = 187 / MAXN
520 Z = INT (10 ^ - 3 * Q) * 100 * XFAC
525 HPLLOT 0,0 TO 0,189 TO 279,189
530 FOR X = Z TO 279 STEP Z
540 HPLLOT X,189 TO X,191
550 NEXT X
560 FOR X = A TO K
565 IF MK(X) > Q THEN GOTO 580
570 HPLLOT XFAC * MK(X),189 - YFAC * N(X)
580 NEXT X
585 PRINT D$;"PR#1"
590 PRINT "SCALE IS FROM 0 TO ";Q;" NUCLEOTIDES.  EACH DIVISION IS ";Z /
      XFAC
595 PRINT D$;"PR#0"
600 PRINT "DO YOU WANT TO RESCALE THE X-AXIS? ENTER 0 OR NEW MAXIMUM X-VA
      LUE"
605 INPUT QN
610 IF QN < > 0 THEN Q = QN: GOTO 480
612 GOSUB 5001
613 GET J$: IF J$ = "C" THEN GOSUB 4000
620 PRINT "DO YOU WANT A PRINTOUT OF THE GRAPHICS?"
625 INPUT A$
630 IF A$ = "NO" THEN END
632 POKE - 12524,0
633 POKE - 12525,64
635 PRINT D$;"PR#1"
640 PRINT CHR$(17)
700 END
1000 PRINT D$;"OPEN CPM ";NB$;", L10"
1010 FOR X = J TO K
1020 PRINT D$;"READ CPM ";NB$;", R";X
1030 INPUT C(X)
1040 NEXT X
1050 PRINT D$;"CLOSE CPM ";NB$
1060 RETURN
2000 PRINT D$;"OPEN CPM ";NB$;", L10"
2010 FOR X = J TO K
2020 PRINT D$;"WRITE CPM ";NB$;", R";X
2030 PRINT C(X)
2040 NEXT X
2050 PRINT D$;"CLOSE CPM ";NB$
2060 RETURN
```

```
3000 H PLOT 1,189 - 187 * F(1) / MXT
3010 FOR X = 2 TO 275
3020 Y = 189 - 187 * F(X) / MXT
3030 H PLOT TO X,Y
3040 NEXT X
3050 RETURN
4000 DIM F(276)
4010 MXT = 0
4012 R = 2 * (2 / WAMH - 1 / MI)
4013 POKE - 16304,0: POKE - 16299,0
4015 FOR T = 1 TO 275
4020 F(T) = R * 9 * T * (1 - R) ^ (9 * T - 1) * (2 + (MI - 9 * T) * R) / (
MI + 1)
4030 IF F(T) > MXT THEN MXT = F(T)
4040 NEXT T
4045 GOSUB 3000
4082 GET J$
4083 POKE - 16303,0: POKE - 16300,0
4084 INPUT "BLACK OUT LAST PLOT? ";C$
4085 IF C$ = "YES" THEN HCOLOR= 0: GOSUB 3000
4086 INPUT "CHANGE R-VALUE FOR CURVE-FIT PLOT? ";R$
4087 IF R$ = "NO" THEN GOTO 5000
4089 R = 2 * VAL (R$)
4090 MXT = 0
4092 HCOLOR= 3: GOTO 4013
5000 RETURN
5001 FOR Y = 0 TO YL
5010 W = WI + Y * 10
5015 IF W > 0 THEN GOTO 5024
5020 H PLOT XFAC * W,189 - YFAC * F(Y)
5022 NEXT Y
5024 RETURN
```

SAMPLE INPUT

```
IRUN
HOW MANY BASE PAIRS IN THE INITIAL DNA?49000
WHAT IS THE SIZE OF A GEL SLICE IN MM?1.176
WHAT IS THE BACKGROUND CPM?30
WHAT IS THE SLICE NUMBER OF THE FIRST HOT SLICE?31
WHAT IS THE SLOPE AND Y-INTERCEPT OF THE LOG(MM) VS DISTANCE PLOT?-.015015,4.126
0
BETWEEN WHICH SLICE NUMBERS DOES THIS SLOPE APPLY?31,67
RECALL CPM DATA? ENTER NO OR NOTEBOOK NUMBER UI-67 MPE
WHAT IS THE SLOPE AND Y-INTERCEPT OF THE LOG(MM) VS DISTANCE PLOT?-.025064,4.009
6
BETWEEN WHICH SLICE NUMBERS DOES THIS SLOPE APPLY?68,120
RECALL CPM DATA? ENTER NO OR NOTEBOOK NUMBER UI-67 MPE
WHAT IS THE SLOPE AND Y-INTERCEPT OF THE LOG(MM) VS DISTANCE PLOT?0,0
DO YOU WANT A PRINTOUT OF THE DNA SIZE DISTRIBUTION?YES
DO YOU WANT TO PLOT THE DNA SIZE DISTRIBUTION?YES
ENTER NOTEBOOK NUMBER UI-67 MPE
```

SAMPLE OUTPUT

SLICE NO.	LENGTH	AMOUNT
31	3868	.016
32	3714	.019
33	3566	.019
34	3423	.029
35	3297	.03
36	3156	.03
37	3030	.039
38	2910	.045
39	2794	.041
40	2682	.057
41	2576	.062
42	2473	.072
43	2374	.069
44	2280	.078
45	2189	.087
46	2102	.106
47	2018	.132
48	1939	.132
49	1860	.164
50	1786	.202
51	1715	.241
52	1647	.272
53	1581	.32
54	1518	.366
55	1458	.41
56	1400	.514
57	1344	.606
58	1290	.726
59	1239	.797
60	1190	.854
61	1142	1.039
62	1097	1.226
63	1053	1.3
64	1011	1.453
65	971	1.639
66	932	1.79
67	895	1.954
68	852	2.258
69	777	2.507
70	726	2.883
71	679	3.141
72	634	3.431
73	592	3.757
74	554	4.003
75	517	4.133
76	483	4.498
77	452	4.677
78	422	4.94
79	394	5.26700001
80	368	5.487
81	344	5.661
82	322	5.544
83	301	5.73
84	281	5.959
85	262	5.616
86	245	5.92
87	229	6.002

88	214	5.835
89	200	5.625
90	187	5.878
91	175	5.741
92	163	5.357
93	152	5.297
94	142	4.746
95	133	4.726
96	124	4.523
97	116	4.402
98	109	4.126
99	101	3.913
100	95	3.766
101	89	3.646
102	83	3.528
103	77	3.349
104	72	2.816
105	68	2.814
106	63	3.083
107	59	2.57
108	55	2.469
109	51	2.973
110	48	2.287
111	45	2.359
112	42	2.453
113	39	2.447
114	37	2.019
115	34	2.379
116	32	2.187
117	30	2.307
118	28	2.398
119	26	2.547
120	24	2.398

NUMBER AVERAGE LENGTH = 589

NICKS PER NUCLEOTIDE = 1.67843088E-03 (USING NAMM)

TOTAL NANOMOLES OF NICKS = .671372351 (USING NAMM)

NAMM = 991

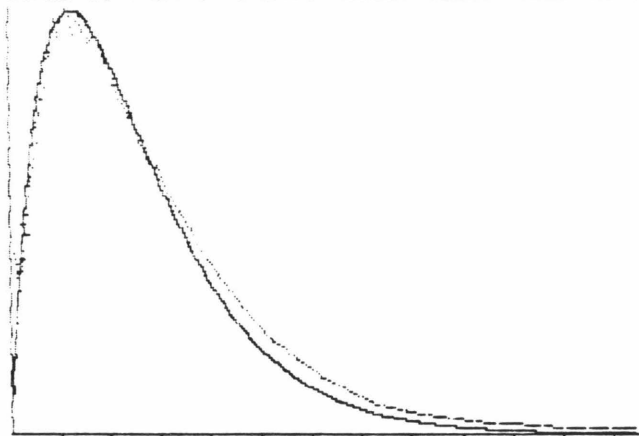
NICKS PER NUCLEOTIDE = 1.99829251E-03 (USING NAMM)

TOTAL NANOMOLES OF NICKS = .799317002 (USING NAMM)

BACKGROUND CPM = 30

SCALE IS FROM 0 TO 3967.60382 NUCLEOTIDES. EACH DIVISION IS 300

SCALE IS FROM 0 TO 2475 NUCLEOTIDES. EACH DIVISION IS 200



SCALC

ILIST

```
99 J = 1:K = 33:M = 8722:N = 2:P = .1:Q = 100
65 DIM C$(20)
70 DIM F1(20)
80 DIM F2(20)
90 DIM F3(20)
100 DIM S(20)
110 HOME : VTAB (3)
115 INPUT "NOTEBOOK NUMBER ";NB$: PRINT
117 INPUT "REACTION CONDITIONS HEADING ";C$: PRINT
120 INPUT "LANE NUMBER ";X: PRINT
130 IF X = 0 THEN GOTO 200
140 INPUT "REACTION CONDITIONS ";C$(X): PRINT
160 INPUT "AREA CTS. FORM I ";F1(X): PRINT
165 IF F1(X) < > 0 THEN GOSUB 1000
170 IF F1(X) = 0 THEN GOSUB 2000
190 GOTO 120
200 PRINT CHR$(4);"PR#1"
205 PRINT NB$: PRINT
210 PRINT "LANE I II III S"; SPC(4);C$
220 FOR X = 1 TO 20
230 IF S(X) = 0 THEN GOTO 250
235 S(X) = VAL ( LEFT$ ( STR$ (S(X)),5))
240 PRINT TAB(2);X;: HTAB(7): PRINT F1(X);: HTAB(14): PRINT F2(X);: HTAB
(22): PRINT F3(X);: HTAB(29): PRINT S(X);: HTAB(39): PRINT C$(X)
250 NEXT X
255 PRINT CHR$(12)
260 PRINT CHR$(4);"PR#0"
270 END
1000 INPUT "AREA CTS. FORM II ";F2(X): PRINT
1010 F1(X) = F1(X) * 1.22 / (F1(X) * 1.22 + F2(X))
1020 S(X) = - LOG (F1(X))
1030 F1(X) = INT (F1(X) * 10000 + .5) / 0
1040 F2(X) = INT ((100 - F1(X)) * Q + .5) / Q
1050 RETURN
2000 INPUT "PERCENT FORM II ";F2(X): PRINT
2005 F3(X) = INT ((Q - F2(X)) * Q + .5) / Q
2010 S = 2
2020 FA = (J - S * K / M) ^ (S / N) * 100
2030 S = S + P
2040 FB = (J - S * K / M) ^ (S / N) * 100
2050 IF FB < F2(X) THEN GOTO 2070
2060 FA = FB: GOTO 2030
2070 IF (FA - F2(X)) < (F2(X) - FB) THEN S(X) = INT ((S - P) * Q + .5) /
Q: GOTO 2090
2080 S(X) = INT (S * Q + .5) / Q
2090 RETURN
```

SAMPLE INPUT

IRUN  
NOTEBOOK NUMBER VII-68

REACTION CONDITIONS HEADING MILLIMOLAR DTT

LANE NUMBER 1

REACTION CONDITIONS 0.1

AREA CTS. FORM I .41788

AREA CTS. FORM II .21748

LANE NUMBER 2

REACTION CONDITIONS 1.0

AREA CTS. FORM I .17594

AREA CTS. FORM II .39752

LANE NUMBER 3

REACTION CONDITIONS 5.0

AREA CTS. FORM I 0

PERCENT FORM II 94

LANE NUMBER 0

SAMPLE OUTPUT

VII-68

LANE	I	II	III	S	MILLIMOLAR DTT
1	70.09	29.91	0	.3554	0.1
2	35.06	64.94	0	1.048	1.0
3	0	94	6	5.7	5.0

## References

- 1) Laskowski, M. In "The Enzymes"; Boyer, P.D.; Lardy, H.; Myrback, K., Eds.; Academic Press: New York, 1961; Vol. 5, pp. 123-147.
- 2) a) Galas, D.J.; Schmitz, A. Nucleic Acids Res. **1978**, 5, 3157-3170. b) Schmitz, A.; Galas, D.J. In "Methods in DNA and RNA Sequencing"; Weismann, S., Ed.; Plenum: New York, 1982.
- 3) Elgin, S.C.R. Cell **1981**, 27, 413-415.
- 4) a) Smith, H.O. Science **1979**, 205, 455-462. b) Malcolm, A.D.B. In "Genetic Engineering"; Williamson, R., Ed.; Academic Press: New York; p. 129. c) Roberts, R.J. Nucleic Acids Res. **1983**, 11, R135. d) Modrich, P. CRC Crit. Rev. Biochem. **1982**, 13, 287-323.
- 5) Gale, E.F.; Cundliffe, E.; Reynolds, P.E.; Richmond, M.H.; Waring, M.J. "The Molecular Basis of Antibiotic Action"; Wiley: New York, 1981; pp. 258-401.
- 6) Hertzberg, R.P.; Dervan, P.B. J. Amer. Chem. Soc. **1982**, 104, 313-315.
- 7) Hertzberg, R.P.; Dervan, P.B. Biochemistry submitted for publication.
- 8) a) Van Dyke, M.W.; Hertzberg, R.P.; Dervan, P.B. Proc. Natl. Acad. Sci. USA **1982**, 79, 5470-5474. b) Van Dyke, M.W.; Dervan, P.B. Cold Spring Harbor Symp. Quant. Biol., **1983**, 47, 347-353. c) Van Dyke, M.W.; Dervan, P.B. Biochemistry **1983**, 22, 2373-2377. d) Van Dyke, M.W.; Dervan, P.B. Nucleic Acids Res. **1983**, 11, 5555-5567.

- 9) Iyanagi, T.; Yamazaki, I. Biochim. Biophys. Acta **1969**, 172, 370-381.
- 10) Spiro, T.G., Ed. "Metal Ion Activation of Dioxygen"; Wiley: New York, 1980.
- 11) Ward, J.F.; Urist, M.M. Int. J. Radiat. Biol. **1967**, 12, 209-218.
- 12) Mizuno, N.S.; Gilboe, D.P. Biochim. Biophys. Acta **1970**, 224, 319-327.
- 13) Cone, R.; Hasan, S.K.; Lown, J.W.; Morgan, A.R. Can. J. Biochem. **1976**, 54, 219-223.
- 14) White, H.L.; White, J.R. Mol. Pharmacol. **1968**, 4, 549-565.
- 15) White, J.R.; Dearman, H.H. Proc. Natl. Acad. Sci. USA **1965**, 54, 887-891.
- 16) White, H.L.; White, J.R. Biochim. Biophys. Acta **1966**, 123, 648-651.
- 17) Weinstein, J.; Bielski, B.H.J. J. Amer. Chem. Soc. **1979**, 101, 58-62.
- 18) a) Lown, J.W.; Begleiter, A.; Johnson, D.; Morgan, A.R. Can. J. Biochem. **1976**, 54, 110-119. b) Lown, J.W. In "Mitomycin C: Current Status and New Developments"; Carter, S.K. and Crooke, S.T., Eds.; Academic Press: New York, 1979; pp. 5-26.
- 19) Szybalski, W.; Iyer, V.N. In "Antibiotics I. Mechanism of Action"; Gottlieb, D.; Shaw, P.D., Eds.; Springer-Verlag: Heidelberg, 1967; pp. 211-245.
- 20) Lown, J.W.; Sim, S.K.; Majumdar, K.C.; Chang, R. Biochem. Biophys. Res. Commun. **1977**, 76, 705-710.
- 21) Berlin, V.; Haseltine, W.A. J. Biol. Chem. **1981**, 256, 4747-4756.

- 22) Brox, L.; Gowans, B.; To, R.; Belch, A. Can. J. Biochem. **1982**, 60, 873-876.
- 23) Ross, W.E.; Glaubiger, D.; Kohn, K.W. Biochim. Biophys. Acta **1979**, 562, 41-50.
- 24) Goldberg, I.H.; Hatayama, T.; Kappen, L.S.; Napier, M.A.; Povirk, L.F. In "Bristol-Myers Cancer Symposia, Molecular Actions and Targets for Chemotherapeutic Agents"; Sartorelli, A.C.; Lazo, J.S.; Bertino, J.R., Eds.; Academic Press: New York, 1981; pp. 163-191.
- 25) Napier, M.A.; Holmquist, B.; Strydom, D.J.; Goldberg, I.H. Biochemistry **1981**, 20, 5602-5608.
- 26) a) Albers-Schonberg, G.; Dewey, R.S.; Hensens, O.D.; Liesch, J.M.; Napier, M.A.; Goldberg, I.H. Biochem. Biophys. Res. Commun. **1980**, 95, 1351-1356. b) Napier, M.A.; Goldberg, I.H. Biochem. Biophys. Res. Commun. **1981**, 100, 1703-1712.
- 27) a) Kappen, L.S.; Napier, M.A.; Goldberg, I.H. Proc. Natl. Acad. Sci. USA **1980**, 77, 1970-1974. b) Povirk, L.F.; Goldberg, I.H. Biochemistry **1980**, 19, 4773-4780.
- 28) Kappen, L.S.; Goldberg, I.H. Nucleic Acids Res. **1978**, 5, 2959-2967.
- 29) Sheridan, R.P.; Gupta, R.K. Biochem. Biophys. Res. Commun. **1981**, 99, 213-220.
- 30) a) D'Andrea, A.D.; Haseltine, W.A. Proc. Natl. Acad. Sci. USA **1978**, 75, 3608-3612. b) Hatayama, T.; Goldberg, I.H.; Takeshita, M.; Grollman, A.P. Proc. Natl. Acad. Sci. USA **1978**, 75, 3603-3607.

- 31) a) Poon, R.; Beerman, T.A.; Goldberg, I.H. Biochemistry **1977**, 16, 486-493. b) Hatayama, T.; Goldberg, I.H. Biochemistry **1980**, 19, 5890-5898.
- 32) Kappen, L.S.; Goldberg, I.H.; Liesch, J.M. Proc. Natl. Acad. Sci. USA **1982**, 79, 744-748.
- 33) Povirk, L.F.; Goldberg, I.H. Proc. Natl. Acad. Sci. USA **1982**, 79, 369-373.
- 34) For two recent reviews, see: a) Burger, R.M.; Peisach, J.; Horwitz, S.B. Life Sci. **1981**, 28, 715-727. b) "Bleomycin: Chemical, Biochemical, and Biological Aspects"; Hecht, S.M., Ed.; Springer-Verlag: New York, 1979.
- 35) Umezawa, H.; Maeda, K.; Takeuchi, T.; Okami, Y. J. Antibiot. (Tokyo) Ser. A. **1966** 19, 200-215.
- 36) Povirk, L.F.; Hogan, M.; Dattagupta, N. Biochemistry **1979**, 18, 96-101.
- 37) Chen, D.M.; Sakai, T.T.; Glickson, J.D.; Patel, D.J. Biochem. Biophys. Res. Commun. **1980**, 92, 197-205.
- 38) Kuroda, R.; Neidle, S.; Riordan, J.; Sakai, T.T. Nucleic Acids Res. **1982**, 10, 4753-4763.
- 39) Roy, S.N.; Orr, G.A.; Brewer, C.F.; Horwitz, S.B. Cancer Res. **1981**, 41, 4471-4477.
- 40) a) Sauseville, E.A.; Peisach, J.; Horwitz, S.B. Biochem. Biophys. Res. Commun. **1976**, 73, 814-822. b) Sauseville, E.A.; Peisach, J.; Horwitz, S.B. Biochemistry **1978**, 17, 2740-2746.

- 41) Burger, R.M.; Peisach, J.; Horwitz, S.B. J. Biol. Chem. **1981**, 256, 11636-11644.
- 42) Jones, P.; Wilson, I. In "Metal Ions in Biological Systems"; Sigel, H., Ed.; Marcel Dekkar: New York, 1978; Vol. 7, pp. 186-240.
- 43) Clore, G.M.; Lane, A.N.; Hollaway, M.R. Inorg. Chim. Acta **1980**, 46, 139-146.
- 44) Takeshita, M.; Grollman, A.P.; Ohtsubo, E.; Ohtsubo, H. Proc. Natl. Acad. Sci. USA **1975**, 75, 5983-5987.
- 45) Kross, J.; Henner, W.D.; Hecht, S.M.; Haseltine, W.A. Biochemistry **1982**, 21, 4310-4318.
- 46) Takeshita, M.; Kappen, L.S.; Grollman, A.P.; Eisenberg, M.; Goldberg, I.H. Biochemistry **1981**, 20, 7599-7606.
- 47) a) Muller, W.E.G.; Yamazaki, Z.; Breter, H.J.; Zahn, R.K. Eur. J. Biochem. **1972**, 31, 518-525. b) Suzuki, H.; Nagai, K.; Yamaki, H.; Tanaka, N.; Umezawa, H. J. Antibiot. **1970**, 23, 473-480.
- 48) Burger, R.M.; Berkowitz, A.R.; Peisach, J.; Horwitz, S.B. J. Biol. Chem. **1980**, 255, 11832-11838.
- 49) Giloni, L.; Takeshita, M.; Johnson, F.; Iden, C.; Grollman, A.P. J. Biol. Chem. **1981**, 256, 8608-8615.
- 50) a) Burger, R.M.; Peisach, J.; Horwitz, S.B. J. Biol. Chem. **1982**, 257, 3372-3375. b) Burger, R.M.; Peisach, J.; Horwitz, S.B. J. Biol. Chem. **1982**, 257, 8612-8614.
- 51) Wu, J.C.; Kozarich, J.W.; Stubbe, J. J. Biol. Chem. **1983**, 258, 4694-4697.

- 52) Takita, T.; Umezawa, Y.; Saito, S.; Morishima, H.; Naganawa, H.; Umezawa, H.; Tsuchiya, T.; Miyake, T.; Kageyama, S.; Umezawa, S.; Muraoka, Y.; Suzuki, M.; Otsuka, M.; Narita, M.; Kobayashi, S.; Ohno, M. Tetrahedron Lett. **1982**, 23, 521-524.
- 53) Aoyagi, Y.; Katano, K.; Suguna, H.; Primeau, J.; Chang, L.; Hecht, S.M. J. Amer. Chem. Soc. **1982**, 104, 5537-5538.
- 54) a) Sigman, D.S.; Graham, D.R.; D'Aurora, V.; Stern, A.M. J. Biol. Chem. **1979**, 254, 12269-12272. b) Graham, D.R.; Marshall, L.E.; Reich, K.A.; Sigman, D.S. J. Amer. Chem. Soc. **1980**, 102, 5421-5423.
- 55) a) Marshall, L.E.; Graham, D.R.; Reich, K.A.; Sigman, D.S. Biochemistry **1981**, 20, 244-250. b) Que, B.G.; Downey, K.M.; So, A.G. Biochemistry **1980**, 19, 5987-5991.
- 56) Jessee, B.; Gargiulo, G.; Razvi, F.; Worcel, A. Nucleic Acids Res. **1982**, 10, 5823-5833.
- 57) Scholes, G. In "Effects of Ionizing Radiation on DNA"; Hutterman, J.; Kohnlein, R.; Teoule, R., Eds.; Springer-Verlag: New York, 1978; p. 153.
- 58) a) Von Sonntag, C.; Schulte-Frohlinde, D. Ibid pp. 204-226. b) Scholes, G.; Willson, R.L.; Ebert, M. Chem. Comm. **1969**, 17-18.
- 59) a) Ward, J.F. Adv. Radiat. Biol. **1975**, 5, 181-239. b) Von Sonntag, C.; Hagen, U.; Schon-Bopp, A.; Schulte-Frohlinde, D. Adv. Radiat. Biol. **1981**, 9, 109-142.
- 60) Henner, W.D.; Grunberg, S.M.; Haseltine, W.A. J. Biol. Chem. **1982**, 257, 11750-11754.

- 61) The log K for binding Fe(II) to EDTA is 14.33. Bell, C.F. In "Metal Chelation, Principles and Applications"; Clarendon Press: Oxford, 1977; p. 78.
- 62) For a crystal structure of EDTA·Fe(III), see: Kennard, C.H. Inorg. Chim. Acta **1967**, 1, 347-354.
- 63) a) McCord, J.M.; Day, E.D. FEBS Lett. **1978**, 86, 139-142.  
b) Halliwell, B. FEBS Lett. **1978**, 92, 321-326.
- 64) Lerman, L.S. J. Mol. Biol. **1961**, 3, 18-30.
- 65) a) Bresloff, J.L.; Crothers, D.M. J. Mol. Biol. **1975**, 95, 103-123. b) Bauer, W.; Vinograd, J. J. Mol. Biol. **1968**, 33, 141-171. c) LePecq, J.B.; Paoletti, C. J. Mol. Biol. **1967**, 27, 87-106. d) Waring, M.J., in ref. 5, pp. 274-306.
- 66) a) Sobell, H.M.; Tsai, C.C.; Gilbert, S.G.; Jain, S.C.; Sakore, T.D. Proc. Natl. Acad. Sci. USA **1976**, 73, 3068-3072. b) Sobell, H.M.; Tsai, C.C.; Jain, S.C.; Gilbert, S.G. J. Mol. Biol. **1977**, 114, 333-365.
- 67) Dervan, P.B.; Becker, M.M. J. Amer. Chem. Soc. **1978**, 100, 1968-1970.
- 68) Paul, R.; Anderson, G.W. J. Org. Chem. **1962**, 27, 2094-2099.
- 69) Hay, R.W.; Nolan, K.B. J. Chem. Soc. Dalton **1975**, 1348-1351.
- 70) Scatchard, G. Ann. N.Y. Acad. Sci. **1949**, 51, 660-672.
- 71) McGhee, J.D.; von Hippel, P.H. J. Mol. Biol. **1974**, 86, 469-489.
- 72) Waring, M.J. in ref. 5, p. 286.

- 73) a) Keller, W.; Wendel, I. Cold Spring Harbor Symp. Quant. Biol. **1974**, 39, 199-208. b) Wieseahn, G.; Hearst, J.E. Proc. Natl. Acad. Sci. USA **1928**, 75, 2703-2707.
- 74) Wang, J.C. J. Mol. Biol. **1974**, 89, 783-801.
- 75) Miller, K.J.; Pycior, J.F. Biopolymers **1979**, 18, 2683-2719.
- 76) The sequence of pBR-322 plasmid DNA has been determined: Sutcliffe, J.G. Cold Spring Harbor Symp. Quant. Biol. **1979**, 43, 77-90.
- 77) Johnson, P.H.; Grossman, L.I. Biochemistry **1977**, 16, 4217-4225.
- 78) Freifelder, D.; Trumbo, B. Biopolymers **1969**, 7, 681-693.
- 79) Haidle, C.W.; Lloyd, R.S.; Robberson, D.L. In ref. 34b, pp. 222-243.
- 80) The log K for the binding of Fe(III) to Des is 30.60. Martell, A.E.; Smith, R.M. "Critical Stability Constants"; Plenum Press: New York, 1977; Vol. 3, p. 303.
- 81) Redpath, J.L. Radiat. Res. **1973**, 54, 364-374.
- 82) Adams, G.E.; Boag, J.W.; Curren, J.; Michael, B.D. "Pulse Radiolysis"; Ebert, M. et al., Eds.; Academic Press: New York, 1965; p. 137.
- 83) Taube, H. J. Gen. Physiol. **1965**, 49, Part 2, 29-52.
- 84) McCord, J.M.; Crapo, J.D.; Fridovich, I. In "Superoxide and Superoxide Dismutases"; Michelson, A.M. et al., Eds.; Academic Press: New York, 1977; p. 11.

- 85) a) Brawn, K.; Fridovich, I. Archs. Biochem. Biophys. **1981**, 206, 414-419. b) Lesko, S.A.; Lorentzen, R.J.; Ts'o, P.O.P. Biochemistry **1980**, 19, 3023-3028.
- 86) Nicholls, P.; Schonbaum, G.R. In "The Enzymes"; Boyer, P.D.; Lardy, H.; Myrback, K., Eds.; Academic Press: New York, 1963; Vol. 8, pp. 147-173.
- 87) Coon, M.J.; White, R.E. in ref. 10, pp. 73-123.
- 88) a) Moss, T-H.; Ehrenberg, A.; Bearden, A.J. Biochemistry **1969**, 8, 4159-4162. b) Dolphin, D.; Forman, A.; Borg, D.C.; Fajer, J.; Felton, R.H. Proc. Natl. Acad. Sci. USA **1971**, 68, 614-618.
- 89) a) Kurimura, Y.; Ochiai, R.; Matsuura, N. Bull. Chem. Soc. Japan **1968**, 41, 2234-2239. b) Bhattacharyya, S.N.; Kunda, K.P. Int. J. Radiat. Phys. Chem. **1974**, 4, 31-41. c) Ilan, Y.A.; Czapski, G. Biochim. Biophys. Acta **1977**, 498, 386-394. d) Fridovich, I. Ann. Rev. Biochem. **1975**, 44, 147-159. e) Borggaard, O.K.; Farver, O.; Anderson, V.S. Acta Chem. Scand. **1971**, 25, 3541-3543. f) Kachanova, Zh.P.; Kudryautseva, E.L.; Purmal, A.P. Russ. J. Phys. Chem. **1974**, 48, 849-852. g) Bull, C.; McClune, G.J.; Fee, J.A. J. Amer. Chem. Soc. **1983**, 105, 5290-5300. h) Cleland, W.W. Biochemistry **1964**, 3, 480-482.
- 90) a) Walling, C.H. Accts. Chem. Res. **1975**, 8, 125-131. b) Walling, C.; Partch, R.E.; Weil, T. Proc. Natl. Acad. Sci. USA **1975**, 72, 140-142. c) Walling, C.H.; Goosen, A. J. Amer. Chem. Soc. **1973**, 95, 2987-2991.

- 91) a) Groves, J.T.; Nemo, T.E.; Myers, R.S. J. Amer. Chem. Soc. **1979**, 101, 1032-1033. b) Groves, J.T. in ref. 10, pp. 157-158.
- 92) a) Record, M.T.; Anderson, C.F.; Lohman, T.M. Quart. Rev. Biophys. II **1978**, 2, 103-178. b) Record, M.T.; Lohman, T.M.; DeHaseth, P. J. Mol. Biol. **1976**, 107, 145-158.
- 93) a) Hecht, S.M. "Chemical Research Conference"; California Institute of Technology, 1983. b) Oppenheimer, N.J.; Chang, C.; Rodriguez, L.O.; Hecht, S.M. J. Biol. Chem. **1981**, 256, 1514-1517. c) Freedman, J.H.; Horwitz, S.B.; Peisach, J. Biochemistry **1982**, 21, 2203-2210.
- 94) Kochetkov, N.K.; Budowskii, E.I. In "Organic Chemistry of Nucleic Acids"; Plenum: New York, 1972; Part B, pp. 507-514.
- 95) Waring, M.J. J. Mol. Biol. **1965**, 13, 269-282. b) Muller, W.; Crothers, D.M. Eur. J. Biochim. **1975**, 54, 267-277.
- 96) Kastrup, R.V.; Young, M.A.; Krugh, T.R. Biochemistry **1978**, 17, 4855-4865.
- 97) Bresloff, J.L.; Crothers, D.M. Biochemistry **1981**, 20, 3547-3553.
- 98) Lomonossoff, G.P.; Butler, P.J.G.; Klug, A. J. Mol. Biol. **1981**, 149, 745-760.
- 99) a) Maxam, A.M.; Gilbert, W. Methods Enzymol **1980**, 65, 499-560. b) Maxam, A.M.; Gilbert, W. Proc. Natl. Acad. Sci. USA **1977**, 74, 560-564.
- 100) Coffman, G.L.; Gaubatz, J.W.; Yielding, K.L.; Yielding, L.W. J. Biol. Chem. **1982**, 257, 13205-13207.
- 101) MPE footprinting data were supplied by M.W. Van Dyke, from ref. 8c.

- 102) a) Kornberg, R.D. Nature (London) **1981**, 292, 579-580.  
b) Zachau, H.G.; Igo-Kemenes, T. Cell **1981**, 24, 597-598.  
c) Cartwright, I.L., et al., CRC Crit. Rev. Biochem. **1982**,  
13, 1-86.
- 103) a) Horz, W.; Altenburger, W. Nucleic Acids Res. **1981**, 9,  
2643-2658. b) Dingwall, C.; Lomonosoff, G.P.; Laskey, R.A.  
Nucleic Acids Res. **1981**, 9, 2659-2673.
- 104) Cartwright, I.L.; Hertzberg, R.P.; Dervan, P.B.; Elgin, S.R.  
Proc. Natl. Acad. Sci. USA **1983**, 80, 3213-3217.
- 105) Wu, C. Nature (London) **1980**, 286, 854-860.
- 106) Samal, B.; Worcel, A.; Louis, C.; Schedl, P. Cell **1981**, 23,  
401-409.
- 107) Schultz, P.G.; Taylor, J.S.; Dervan, P.B. J. Amer. Chem. Soc.  
**1982**, 104, 6861-6863.
- 108) Taylor, J.S.; Schultz, P.G.; Dervan, P.B. Tetrahedron Symposium on  
"Bioorganic Studies in Receptor Sites" 1983 in press.
- 109) a) Reinert, K.E. J. Mol. Biol. **1972**, 72, 592. b) Luck, G.;  
Zimmer, C.; Reinert, K.E.; Arcamoe, F. Nucleic Acids Res. **1977**,  
4, 2655. c) Nosikov, V.; Vain, B. Ibid. **1977**, 4, 2263.  
d) for reviews see: Zimmer, C. Prog. Nucleic Acids Res. Mol.  
Biol. **1975**, 15, 285. e) Gale, E.F. et al., in ref. 5, p. 345.
- 110) a) Luck, G.; Triebel, M.; Zimmer, C. Nucleic Acids Res. **1974**,  
1, 503. b) Zasedatelev, A.S.; Zhuze, A.L.; Zimmer, C.;  
Grokhovshy, S.L.; Tumaryan, V.G.; Gursky, G.V.; Gottikh, B.P.  
Dokl. Acad. Nauk. SSSR **1976**, 231, 1006. c) Krylov, A.S.;  
Grokhovsky, S.L.; Zasedatelev, A.S.; Zhuze, A.L.; Gursky, G.V.

- Gottikh, B.P. Nucleic Acids Res. **1979**, 6, 289. d) Marky, L.A.; Blumenfield, K.S.; Breslauer, K.J. Nucleic Acids Res. **1983**, 11, 2857.
- 111) DNA affinity cleaving data were supplied by P.G. Schultz from: Schultz, P.G.; Dervan, P.B. Biomolecular Structure and Dynamics in press.
- 112) a) Douthart, R.J.; Burnett, J.P.; Beasley, F.W.; Frank, B.H. Biochemistry **1973**, 12, 214-220. b) Waring, M.J. Biochem. J. **1974**, 143, 483-486.
- 113) Muller, W.E.G.; Yamazaki, Z.; Breter, H.J.; Zahn, R.K. Eur. J. Biochem. **1972**, 31, 518-525.
- 114) Haidle, C.W.; Bearden, J. Biochem. Biophys. Res. Commun. **1975**, 65, 815-821.
- 115) Freifelder, D.; Davison, P.F. Biophys. J. **1962**, 2, 235-247.
- 116) Marshak, A.; Vogel, H.J. J. Biol. Chem. **1951**, 189, 597-605.
- 117) Povirk, L.; Kohnlein, W.; Hutchinson, F. Biochim. Biophys. Acta **1978**, 521, 126-133.
- 118) Tapper, D.P.; Clayton, D.A. Nucleic Acids Res. **1981**, 9, 6787-6794.
- 119) Kuo, M.T.; Haidle, C.W. Biochim. Biophys. Acta **1974**, 335, 109-114.
- 120) Chaconas, G.; Van de Sande, J.H. Methods Enzymol. **1980**, 65, 75-85.
- 121) Cameron, V.; Uhlenbeck, O.C. Biochemistry **1977**, 16, 5120-5126.
- 122) Armel, P.R.; Strniste, G.F.; Wallace, S.S. Radiat. Res. **1977**,

- 69, 328-338.
- 123) Schultz, P.G., personal communication.
- 124) a) Murai, S.; Sonada, N.; Tsutsumi, S. Bull Chem. Soc. Japan **1963**, 36, 527-530. b) Digman, R.V.; Anderson, D.F. J. Org. Chem. **1963**, 28, 239-240.
- 125) a) Dervan, P.B.; Becker, M.M. in ref. 67. b) Wakelin, L.P.G.; Ramanos, M.; Canellakis, E.S.; Waring, M.J. Studia Biophysica **1976**, 60, 111-118. c) Gaugain, B.; Barbet, J.; Oberlin, R.; Roques, B.B.; LePecq, J.-B. Biochemistry **1978**, 17, 5071-5077. d) Kuhlmann, K.F.; Charbeneau, N.J.; Mosher, C.W. Nucleic Acids Res. **1978**, 5, 2629-2641.
- 126) Bresloff, J.L. Ph.D. Dissertation, Yale University, 1974.
- 127) Becker, M.M. Ph.D. Dissertation, California Institute of Technology, 1981.
- 128) Ikeda, R.A.; Dervan, P.B. J. Amer. Chem. Soc. **1982**, 104, 296-297.
- 129) Ribes, F.; Metzger, R.G.J. Bull. Soc. Chim. Fr. **1972**, 1, 143-147.
- 130) Tanaka, T.; Weisblum, B. J. Bacteriol. **1974**, 121, 354-362.
- 131) Sanger, F.; Coulson, A.R. J. Mol. Biol. **1975**, 94, 441-448.
- 132) Maniatis, T.; Fritsch, E.F.; Sambrook, J. In "Molecular Cloning, A Laboratory Manual"; Cold Spring Harbor Laboratories, 1982; pp. 78-84.
- 133) Thomas, M.; Davis, R.W. J. Mol. Biol. **1975**, 91, 314-328.
- 134) Dabrowiak, J.C.; Greenaway, F.T.; Longo, W.E.; Van Husen, M.; Crooke, S.T. Biochim. Biophys. Acta **1978**, 517, 517-526.

- 135) Stent, G.S.; Calender, R. In "Molecular Genetics"; W.H. Freeman and Co.: San Francisco, 1978; p. 163.
- 136) Charlesby, A. "Atomic Radiation and Polymers"; Pergamon Press Ltd: New York, 1960.
- 137) Carmichael, G.G.; McMaster, G.K. Methods Enzymol. **1980**, 65, 380-391.